The 15-aa Repeat Region of Adenomatous Polyposis Coli: Association with β-catenin and Interplay with Cell Cycle Regulator Topoisomerase IIα

By

Aaron James Rudeen

Submitted to the graduate degree program in Molecular Biosciences and the Graduate Faculty of the University of Kansas in partial fulfillment of the requirements for the degree of Doctor of Philosophy.

_____
Chair – Kristi Neufeld

_____
Audrey Lamb

_____
Yoshiaki Azuma

_____
Berl Oakley

_____
Michael Hageman

Date Defended: July 30, 2020

The dissertation committee for Aaron James Rudeen certifies that this is
the approved version of the following dissertation:

The 15-aa Repeat Region of Adenomatous Polyposis Coli: Association with β-catenin and Interplay with Cell Cycle Regulator Topoisomerase IIα

_____
Chair – Kristi Neufeld

Date Approved: July 30, 2020

Abstract

The tumor suppressor Adenomatous polyposis coli (APC) is a large, multi-domain protein with many identified cellular functions. The best characterized role of APC is to scaffold a protein complex that negatively regulates Wnt signaling via β-catenin destruction. This destruction is mediated by β-catenin binding to centrally located 15- and 20-amino acid (aa) repeat regions of APC. Greater than 80% of cancers of the colon and rectum present with an *APC* mutation. Most carcinomas with mutant *APC* express a truncated APC protein which retains the ~200-aa long 15-aa repeat region. Understanding why the presence of the 15-aa repeats in truncated APC is retained by cancer cells will help direct future therapeutic intervention strategies for *APC* mutant tumors. In this work, I show that the 15-aa repeat region of APC is intrinsically disordered. I characterize the binding of the 15-aa repeat region with binding partner β-catenin, the downstream transducer of Wnt signaling. I found that the 15-aa region of APC retains flexibility upon binding β-catenin and that APC does not have a single, observable "highest affinity" binding site for β-catenin. This flexibility has implications for the architecture and assembly of the β-catenin destruction complex. We hypothesize the disorder retained upon association allows β-catenin to be readily captured by APC and then remain accessible to other elements of the destruction complex for subsequent processing. In Chapter 4, I expand upon studies performed previously in our lab, which discovered a novel association between the tumor-suppressor APC and Topoisomerase IIα (TopoIIα). This association has implications in colon cancer progression and initiation. I show that tumors that harbor *APC* mutation are more resistant to chemotherapeutic compounds targeting topoisomerases than tumors with wild-type *APC*. I also show that APC does not appear to associate with the β-cat/TCF transcriptional complex, though it does associate with both β-catenin and TopoIIα in the

nucleus. I show that TopoIIα contained in the nuclear extract from cells with mutant or no APC has enhanced catalytic activity compared to TopoIIα from cells with wild type APC. This observed effect could explain why cells with altered *APC* status respond differently to TopoIIα-targeting compounds. Finally, I report generation of a new polyclonal antibody raised in chicken against the central region of APC. This new tool will be valuable for APC researchers worldwide. The work presented here expands our understanding of a critical binding region of APC, and will guide future studies aimed at defining precise molecular mechanisms of Wnt signaling.

This work is dedicated to my mentors, teachers, and coaches.

Acknowledgments

It is said that it takes a village to raise a child. While this body of work could hardly be compared to an actual child, the sentiment nevertheless rings true. Many people have contributed to this dissertation work either directly or indirectly, and I gratefully acknowledge that without all of the support, none of this would have been possible.

First and foremost, I would like to thank my graduate mentor, Dr. Kristi Neufeld. Kristi, you have been an inspiration for me since the first time I saw you give a lecture at the University of Kansas. Your zest for scientific inquiry and discovery is contagious, and every time I had a scientific discussion with you, I left more enthused and excited about my data than I was before we talked. Your willingness to pursue new challenges helped me to gain confidence in stepping into new areas myself. Your passion for teaching and mentoring is obvious, and I hope to be as effective and passionate of a mentor myself someday. I will carry lessons I learned in your lab, both scientific and otherwise, for the rest of my life. Thank you for everything!

I also would like to thank Dr. Audrey Lamb for the tremendous amount of support she has provided me as well. You generously shared your reagents, your lab space, and even your lab personnel to assist my project. Your diligence for conducting quality science has and will continue to shape who I am as a scientist. You also set a prime example of what it means to be a mentor who cares deeply about the development of your mentees. I hope to model those qualities someday myself. Audrey and Kristi, I almost certainly would not have been able to complete graduate school without you both after initial setbacks, and I cannot thank you enough for going above and beyond to make sure I found myself in an environment in which I could be successful.

I was privileged to work with excellent lab mates, both in the labs of Dr. Neufeld and Dr. Lamb. You all were patient with me when teaching new techniques or when I required assistance

for an experiment. Your discussion and feedback on presentations or written works was invaluable, and much appreciated. Aside from technical assistance, it was simply a joy to work with you all. I consider myself lucky to have been surrounded by such talented scientists that I could laugh with, talk current events with, or let off steam with. I specifically would like to thank Trey Ronnebaum for being a huge support during a switch of labs early in my career, and Taybor Parker for countless discussions, experimental assistance, and lots of rides to campus!

I would also like to thank the members of my graduate committee; Dr. Yoshiaki Azuma, Dr. Berl Oakley, Dr. Michael Hageman, and Dr. Eric Deeds for your feedback and advice. You consistently challenged me to ask good research questions and determine the best methods to answer my questions. Ultimately, you helped to shape me into a better scientist. I would especially like to thank Dr. Azuma for sharing many reagents and equipment, and for all the extra discussions about my project. I must also thank Dr. Justin Douglas and Dr. Minli Xing for all of you support, discussion, and data generation for Chapters 2 and 3. You were very patient with me explaining techniques that I was unfamiliar with and were absolutely essential to much of the work presented here. I am extremely grateful for your contributions, and assistance these past few years. I also would like to thank Dr. Roberto De Guzman, Dr. Hayes McDonald, and Dr. Jian Xiong for discussion and assistance with data analysis.

Outside of KU, I was supported by a network of friends and family that were constantly encouraging me, keeping tabs on my progress, and asking questions about my research. To my closest friends, and especially my mod-mates, thank you for always being understanding, patient, and encouraging throughout this process. To my friends here in Lawrence, thank you for all of the memories, the support and the comradery. You all made my time here in Lawrence so enjoyable, and I will cherish this time period for the rest of my life.

To my family and in-laws, I cannot thank you enough for everything you have done for my wife Rachel and I. Graduate school was made much easier knowing such an amazing family was so close by, and that I could escape the stresses for a meal or a coffee or an overnight stay. You all have made an immeasurable impact on me, helping navigate not only school but life as well. You have all challenged me to grow personally, and discussion about life and the world have made me into a more critical thinker. To Rachel's parents Jeff and Kareen, thank you for your constant words of encouragement and your unconditional support and love. It is comforting to know I can always count on you to have an excellent perspective and offer sage advice. To my parents, Jim and Margo, I cannot thank you enough for all of the opportunities you have made possible for me throughout my life to get to this point. You have been so supportive of the path I have taken and have wholeheartedly thrown your support behind Rachel in I in every way imaginable. I hope to live up to the standard you both and Jeff and Kareen have set as parents. I love you all very much! I must also acknowledge my grandparents, Clyde and Felice, who were in attendance for almost every event I had from when I was a toddler up until today. Your support was and continues to be so appreciated.

Finally, I would like to thank my incredible wife Rachel. I simply cannot put into words how big of an impact you have had on me, and how much your support has meant to me. You were exceedingly patient with the long hours and late nights in lab, sacrificing your own time day after day. You are such a hard worker, and consistently motivate me to get things accomplished and to move forward. You exemplify patience, grace, persistence, compassion, kindness, and maturity, and inspire me to be a better version of myself daily. I will be forever grateful for your continued support, your love, and your friendship.

Table of Contents

Abstract **iii**

Acknowledgments **vi**

Table of Contents **ix**

List of Abbreviations **xii**

Chapter 1: INTRODUCTION **1**

I. Colorectal Cancer and APC 2
The Burden of Colorectal Cancer 2
APC Discovery 2
Binding Domains of APC 3
Structure of APC 5

II. APC and the β-catenin Destruction Complex 6
APC in Wnt Signaling 6
Mutation of APC 8
Dynamics of the β-catenin Destruction Complex 9

III. Intrinsic Disorder in Cellular Signaling 11
Disorder and the structure-function paradigm 11
Characteristics of Disordered Proteins 13
Classification of Disordered Proteins 14
IDPs as Central Interaction Hubs 16

IV. Topoisomerase IIα and APC 18
TopoIIα Structure and Function 18
TopoIIα Role in Cancer 20
APC and TopoIIα 21

Summary 22

References 23

Chapter 2: STRUCTURAL ANALYSIS OF THE 15-AA REPEATS REGION OF APC **34**

Abstract 35

Introduction 35

Results
Expression and purification of human APC fragments 38
NMR analysis of APC15R 39
NMR analysis and backbone assignment of APC15R-BCD 42
Predictions of structure based on NMR backbone resonance assignments 45
Structural analysis of APC15R-BCD by circular dichroism 51
The central binding region of APC is susceptible to rapid proteolysis 53

Discussion 55

Materials and Methods 56

References 59

Chapter 3: THE ASSOCIATION OF β-CATENIN AND THE 15-AA REPEAT REGION OF APC 62

Abstract 63

Introduction 63

Results
Expression and purification of human β-catenin 64
The 15-aa repeat region of APC forms a complex with β-catenin in solution 67
Native association of APC and β-catenin 71
Titration of APC15R-BCD with β-catenin 73
Backbone dynamics of APC15R-BCD 79

Discussion 79

Materials and Methods 82

Collaborations and Workload Allocations 86

Supporting Materials 87

References 90

Chapter 4: TOPOISOMERASEIIα, APC, AND CANCER 92

Abstract 93

Introduction 93

Results
TopoIIα-targeted therapeutics are less effective in APC mutant tumors 96

Generation of a novel anti-APC IgY antibody 99
APC Associates with TopoIIα and β-catenin in the nucleus, but not TCF4 101
Cellular TopoIIα levels correlate with APC levels 101
TopoIIα shows higher catalytic activity in APC mutant or null cells 105

Discussion 108

Materials and Methods 110

Supporting Materials 115

References 125

Chapter 5: DISCUSSION, CONCLUSIONS, AND FUTURE DIRECTIONS 128

Disrupting what is "just-right" to kill mutant cells 129

TopIIα-targeting therapeutics in APC mutant tumors 131

Conclusions and Significance 132

Future Directions 133

References 134

List of Abbreviations

aa	amino acid
APC	Adenomatous polyposis coli
APCL	Adenomatous polyposis coli like
ATP	Adenosine triphosphate
AUC	Analytical ultracentrifugation
β-TrCP	β-transducin repeats-containing protein
BMRB	Biological magnetic resonance data bank
BSA	Bovine serum albumin
CD	Circular dichroism
CK1	Casein kinase 1
CRC	Colorectal cancer
CTD	C-terminal domain
C.V.	Column volume
DLG1	Disks large homolog 1
DMP	dimethyl pimelimidate
Dvl	Dishevelled
EB1	End binding 1
FAP	Familial adenomatous polyposis
FL	full-length
GDSC	Genomics of Drug Sensitivity in Cancer
GSK3β	Glycogen synthase kinase 3β
IC50	Half maximal inhibitory concentration

IDP	Intrinsically disordered protein
IDR	Intrinsically disordered region
IgG	Immunoglobulin G
IgY	Immunoglobulin Y
IPTG	Isopropyl-β-D-thiogalactopyranoside
HSQC	Heteronuclear single quantum coherence
JNK	c-Jun N-terminal kinase
kDa	kilodalton
KO	Knock out
LEF	Lymphoid enhancer factor
LRP5/6	Low-density lipoprotein receptor-related protein 5/6
mAb	Monoclonal antibody
MALDI-TOF	Matrix-assisted laser desorption/ionization time of flight
MCR	Mutation cluster region
mDeg	millidegree
ncSPC	Neighbor corrected structural propensity calculator
NMR	Nuclear magnetic resonance
NOE	Nuclear Overhauser effect
OD	Optical density
PBS	Phosphate-buffered saline
PP2A	Protein phosphatase 2
ppm	parts per million
PTM	Post-translational modification

RGS	Regulator of G protein signaling
RMSD	Root-mean-square deviation
RT	Room temperature
SAXS	small-angle X-ray scattering
SEC	Size-exclusion chromatography
SDS-PAGE	Sodium dodecyl sulfate polyacrylamide gel electrophoresis
siRNA	Small interfering RNA
TCF	T-cell factor
TOCSY	Total correlation spectroscopy
TopoIIα	Topoisomerase IIα
TFE	2,2,2-trifluoroethanol
TROSY	Transverse relaxation-optimized spectroscopy
TSP	Trimethylsilyl propanoic acid

CHAPTER 1

INTRODUCTION

I. Colorectal Cancer and APC

The Burden of Colorectal Cancer

Cancers of the colon and rectum remain a heavy burden on the United States healthcare system, as an estimated 150,000 new cases will be diagnosed in 2020, with over 50,000 deaths[1]. In 2017, the U.S. Multi-Society Task Force of Colorectal Cancer, which is made up of expert gastroenterologists, updated the colorectal cancer (CRC) screening recommendations to include colonoscopy every 10 years and annual fecal immunochemical tests[2]. Localized tumors detected early can be resected surgically, and initiatives to boost public awareness and improvements to screening technologies has contributed to raising the 5-year survival rate for stage I and II colorectal cancers to ~90%[3]. However, for later stage and metastatic disease the prognosis is significantly more severe, with the 5-year survival rate of metastatic disease dropping to ~14%[3]. Chemotherapeutic agents are frequently prescribed for inoperable and metastatic lesions, though these carry toxic side-effects and their own inherent risks such as development of secondary malignancies. Recently, there has been a strong push to develop targeted molecular therapies to limit the dangers of traditional chemotherapy and increase treatment effectiveness[4]. As such, there is an urgent need to increase our understanding of the molecular pathways that drive the initiation and progression of colorectal cancers. By understanding how cellular pathways become disrupted in colorectal cancer, specific targeted therapeutics can be developed to increase the arsenal of tools oncologists have to treat later stage patients.

APC Discovery

While the vast majority of colon cancers are sporadic[5], several hereditary cancers of the colon have been identified and characterized. Familial adenomatous polyposis (FAP) is the second

most common hereditary colon malignancy, and necessitates resection of the colon by age 35 or younger[6]. In the late 1980s, several groups studying families afflicted by FAP identified a common gene alteration on chromosome 5q21[7–9]. This gene was named *Adenomatous polyposis coli* (*APC*) and has since received considerable attention. It has been revealed that *APC* is not only causatively linked to FAP, but is mutated in greater than 80% of sporadic cancers of the colon and rectum[10,11]. Despite identification of *APC* as a tumor-suppressor over 30 years ago and thousands of publications on the gene since, there remains to this day not a single therapeutic treatment or drug that takes advantage of mutant *APC* expression to treat colorectal cancers.

Binding domains of APC

APC is a large protein, made up of 2,843 amino acids and migrating at a size of roughly 310 kDa by SDS-PAGE[9,12]. Figure 1.1.1 shows the many different domains that make up APC, and allow APC to interact with numerous cellular substrates. The N-terminus includes a stretch of ~55 amino acids which facilitates homodimerization[13]. Residues 453 – 767 make up an armadillo repeat domain, named for its close sequence homology to the *Drosophila* protein Armadillo, a homolog of human β-catenin[14]. This region can bind PP2A[15], the guanine nucleotide exchange factor Asef[16], and APC's own centrally-located β-catenin binding repeats[17]. Following the armadillo repeat region are the 15- and 20-amino acid (aa) repeat regions. These regions consist of conserved 15- or 20- (respectively) amino acid long repeats that have been shown to directly bind with β-catenin[18–20]. Phosphorylation of the 20-aa repeats greatly increases binding affinity to β-catenin, while the 15-aa remain unphosphorylated[18,21]. Interspersed among the 20-aa repeats are three Axin binding motifs. These motifs are approximately 20-aa long, and are referred to as

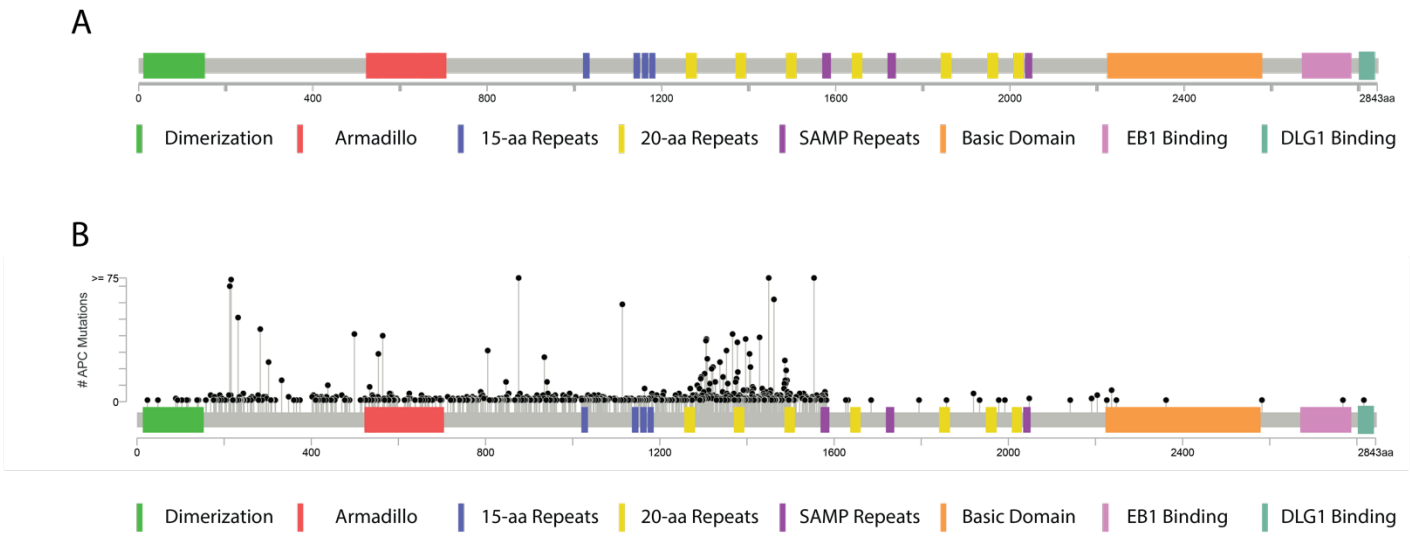

Figure 1.1.1 Linear schematic of APC domains. A) APC protein (grey) with binding domains in respective colors, in approximate locations. B) Black lollipops indicate location and number of truncating *APC* mutations in colorectal tumors of 8 compiled studies of 3,504 colorectal tumors[22,23]

SAMP repeats due to a conserved Ser-Ala-Met-Pro (S-A-M-P) sequence[24,25]. C-terminal to the β-catenin and Axin binding repeats is a stretch of residues (~aa's 2150-2600) referred to as the basic domain. This domain can bind tubulin and microtubules directly, and has been shown to have a positive effect on tubulin assembly *in vitro*[26,27]. On the C-terminal tail, a stretch of ~170 aa's binds the microtubule plus-end tracking protein End binding 1 (EB1)[28]. In addition to microtubules, APC binds and nucleates actin, and associates with intermediate filaments[29–31]. While outside the scope of this body of work, the association of APC with cytoskeletal components has interesting implications for the role of APC in cell migration, polarization, and cell division, especially considering this region is lost in all truncated APC mutants. Finally, the C-terminus of APC is able to bind DLG1, a human homolog of *Drosophila* discs large, which also links APC to cell cycle progression, migration, and polarization[32,33].

Structure of APC

While the importance of APC to the initiation of colorectal cancer has been known since the late 1980's, relatively few detailed structural analyses have been performed. Crystal structures reveal that the first N-terminal 250 residues constitute alpha helical coiled-coil elements[34,35]. The crystal structure of the armadillo region has also been solved, revealing that this region is largely homologous to canonical armadillo folds, barring one deviation between arm 2 and 5[36,37]. For the remaining domains of APC, little structural information is available aside from predictions. Three structures have been solved with short peptides of APC co-crystallized with β-catenin, and for each of these structures, only the residues of APC nestled into the armadillo binding groove of β-catenin are visible[19,21,38]. Many algorithms have been designed to calculate degrees of order versus disorder in a protein based on primary sequence. Servers running these algorithms predict that the C-terminal ~2000 residues of APC are generally disordered, with short regions of

predicted order that vary depending on the specific algorithm used[39,40]. Circular dichroism measurements of APC peptides consisting of amino acids 1202-1551[41] and 1362-1745[18] of the β-catenin binding and down-regulating region indicate a random coil conformation, reinforcing models predicting intrinsic disorder. How this large predicted area of disorder of APC contributes to regulation of the β-catenin destruction complex in tandem with the well-folded N-terminus remains to be determined.

II. APC and the β-catenin Destruction Complex

APC in Wnt Signaling

There is evidence that APC has roles in many cellular mechanisms and pathways, including chromosome segregation[42], microtubule regulation[43,44], adhesion[45], and more[46]. The best-characterized role for APC is its function as a scaffold in canonical Wnt signaling, illustrated in Figure 1.2.1. In the absence of an extracellular Wnt ligand, APC forms a complex along with APC-L, Axin 1/2, the protein kinases glycogen synthase kinase 3 beta (GSK3β) and casein kinase 1 (CK1), and protein phosphatase 2A (PP2A) to bind and phosphorylate β-catenin, the ultimate signal transducer of the Wnt signaling pathway. This phosphorylation is recognized by β-TRCP1, an E3 ubiquitin ligase, which results in the ubiquitination and subsequent proteasomal degradation of β-catenin (thoroughly reviewed here[47,48]). This so called "β-catenin destruction complex" prevents β-catenin from accumulating and translocating to the nucleus, where it functions as a pro-proliferation transcription factor by binding with the TCF/LEF family of transcription factors[49,50]. Wnt ligands activate the Wnt pathway when cells require proliferative signals, such as in development or stem cell self-renewal[51]. Extracellular Wnt ligands bind to

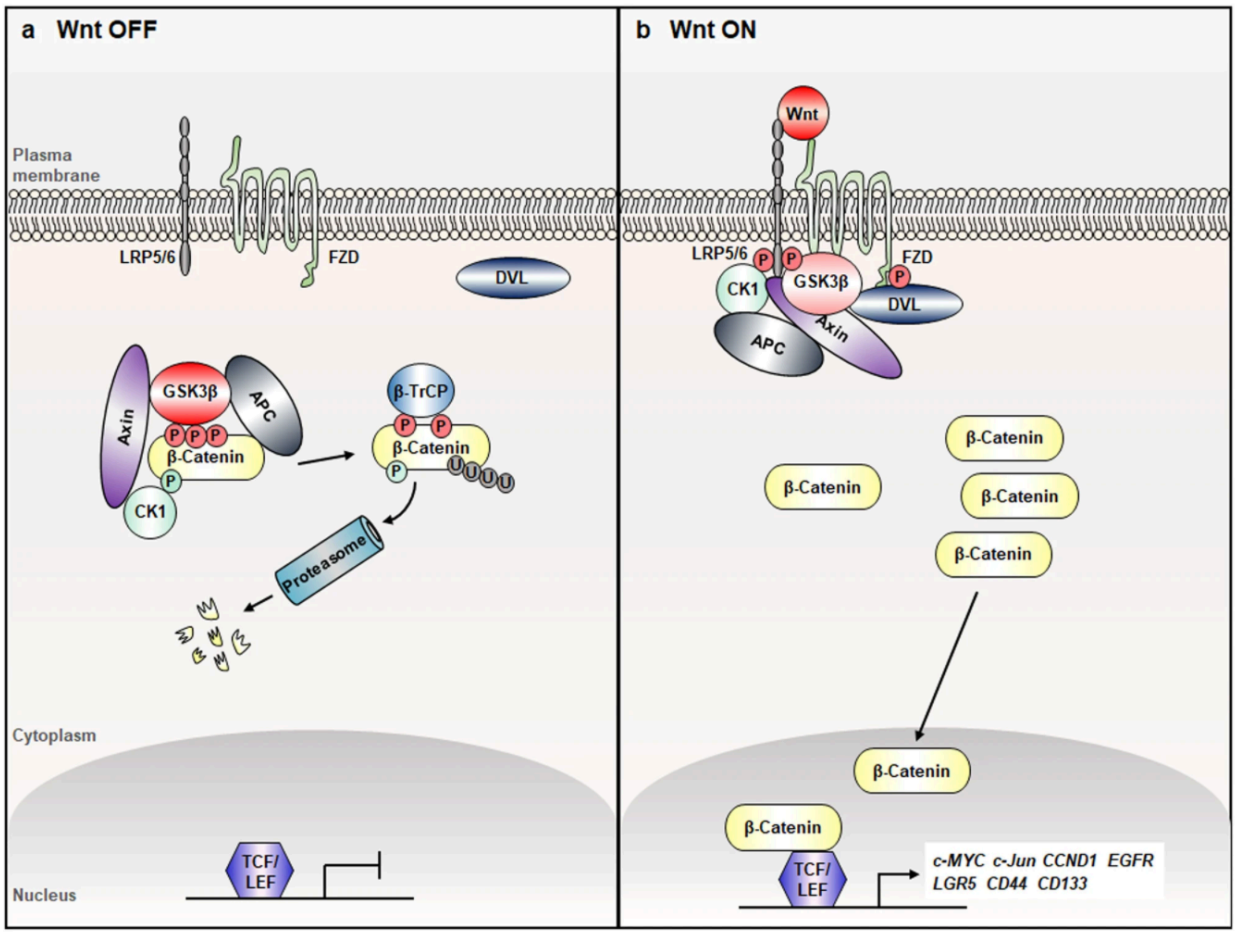

Figure 1.2.1 The Wnt Pathway Left 'Wnt Off' situation, with no extracellular Wnt ligand and an active β-catenin destruction complex. Right 'Wnt On', with inactivation of β-catenin destruction complex and accumulation of cytoplasmic β-catenin, which translocates to the nucleus and activates pro-proliferation genes (some examples listed). Figure from Jeong et al.[52] reproduced with permission.

surface receptors Frizzled and LRP5/6, initiating a signaling cascade that inactivates the destruction complex. This process is not well-understood, though evidence has shown that the destruction complex as a whole is recruited to the membrane at the site of bound Wnt ligand, and that the adaptor protein Dvl is involved[53–55]. Inactivation of the β-catenin destruction complex results in accumulation of β-catenin in the cytoplasm, which subsequently translocates to the nucleus and drives expression of pro-proliferation factors.

Outside of an extracellular Wnt ligand, the β-catenin destruction complex can be inactivated by genetic mutations to individual components. Nonsense and frame-shift *APC* mutations result in the expression of a truncated APC protein, which has a reduced capacity to bind Axin and β-catenin. Loss of binding domains to truncation results in disrupted β-catenin destruction complex activity.

Mutation of APC

As mentioned previously, mutation to *APC* is seen in upwards of 80% of colorectal tumors. Mutations lead to a premature stop codon, resulting in the expression of a truncated protein product. Eukaryotic cells employ a surveillance mechanism known as nonsense-mediated decay that eliminates mRNA containing premature stop codons[56]. However, in the unique case of APC, the final exon encodes more than 75% of the protein sequence[9]. Therefore, premature stop codons in this region evade nonsense-mediated decay mechanisms, resulting in expression of a truncated protein product.

While truncating *APC* mutations have been observed all along the 2,843 amino acid sequence, a central region between residues 1200-1600 harbors a significantly disproportionate number of mutations observed in colorectal tumors. This region has therefore been named the

"mutation cluster region (MCR)" (Figure 1.1.1)[57]. The MCR lies C-terminal to the 15-aa repeats of APC, indicating a selective preference for retention of the 15-aa repeat region by tumors.

In keeping with Alfred Knudson's "two-hit hypothesis"[58] for tumor-suppressors, both *APC* alleles must be inactivated to drive tumorigenesis[11,57,59]. Interestingly, it appears that initial location of somatic or germline mutation of one *APC* allele has an impact on the location of the mutation of the second allele[60]. For example, if the first "hit" or truncating mutation happens near or at codon 1,300, then complete loss of the second *APC* allele, a phenomenon known as loss of heterozygosity, is the most common second hit[60]. However, if the first allelic mutation to *APC* happens away from this codon, then a truncating mutation tends to be the second allelic hit, resulting in expression of two mutant forms of APC[60]. This suggests that cells that are mutated to alter wildtype APC binding and scaffolding ability are more prone to initiate tumorigenesis.

Dynamics of the β-catenin Destruction Complex

The β-destruction complex is — complex. Axin1, like APC, is highly flexible and contains multiple binding domains[25,61]. Kinases GSK3-β and CK1 bind to Axin, yet studies have shown this to be a purely scaffolding event, as binding sites are far from the kinases' catalytic sites, and binding does not increase catalytic activity[48,62,63]. Axin also contains β-catenin binding regions, which compete directly with the APC binding sites of β-catenin[19,21,48]. Axin also interacts with the SAMP repeats of APC via an N-terminally located RGS domain[24]. In addition to the multiple sites of protein-protein interactions, phosphorylation plays a key role in modulating the turnover of β-catenin. Phosphorylation of the 20-aa repeats of APC by GSK3β and CK1 significantly increases the affinity for β-catenin, while the 15-aa repeats of APC remain unphosphorylated[18,21]. β-catenin itself must be phosphorylated in order to be recognized by the E3 ubiquitin ligase β-TrCP. A detailed analysis of the phosphorylation events leading to this recognition revealed that

CK1-α first phosphorylates S45 of β-catenin, thereby enabling recognition by GSK3β for three subsequent phosphorylation events[64]. Kimelman and Xu[65] propose a model in which 1) β-catenin is captured by Axin and the 15-aa repeats of APC; 2) Axin associates with APC; 3) Axin-bound kinases phosphorylate the 20-aa repeats of APC; 4) β-catenin is transferred to the phospho-20-aa repeats; 5) β-catenin is phosphorylated by the kinases, marking it for degradation. However, confounding data complicates this basic model. Perhaps most notably, cells expressing a truncated APC that has lost the Axin-binding SAMP repeats are still able to exert some regulatory control over β-catenin[66–68]. This observation has led to a 'just-right' signaling hypothesis, which argues that in order for *APC* mutations to become oncogenic, APC must not lose *all* β-catenin binding domains[66]. The 15-aa repeats, therefore, appear to be essential to imparting oncogenesis in a mutated *APC* setting, and understanding the precise function of this region is of utmost importance.

When considering all components of the β-catenin destruction complex, the contributions of APC homolog APC-like (APCL) and Axin homolog Axin2/Conductin must not be overlooked. APCL lacks the 15-aa repeats but possesses some 20-aa repeats, two SAMP motifs, and a conserved N-terminal oligomerization domain. APCL was immunoprecipitated by APC, indicating presence in the complex, possibly via heterodimerization[69]. While the affinity of β-catenin to APCL is much weaker[70], and even though Axin2 is implicated in the *negative* feedback of Wnt signaling[71], compensatory contributions of these homologs may be key to driving oncogenic cell survival.

Finally, one must also consider that proteins of the β-catenin destruction complex are involved in many other cellular processes. Aside from Wnt signaling, β-catenin is involved in cell-cell junctions and has been detected at the centrosome playing an unknown role[72,73]. GSK3β

is a promiscuous kinase involved in multiple signaling pathways and has over 40 identified substrates[74]. As discussed above, APC is associated with many other cellular pathways as well, and Axin acts a scaffold in the JNK and TGF-β pathways[75]. Considering the heavy involvement of proteins of Wnt signaling in other cellular pathways, it may be that only a small proportion of the total cellular protein of each member is participating in active β-catenin destruction. The redundancy of binding sites and high amounts of structural flexibility within the β-catenin destruction complex may be a means to increase the rate of β-catenin control without needing high concentrations of assembled complex.

III. Intrinsic Disorder in Cellular Signaling

Disorder and the structure-function paradigm

The first three-dimensional model of a protein was obtained in 1958, when Kendrew and colleagues solved the X-ray crystal structure of sperm whale myoglobin[76]. For the next roughly forty years, the prevailing assumption of protein architecture was that a well-folded and globular tertiary structure was required to impart specific function. Perhaps the most well-known illustration of this theory is the "lock-and-key" model, in which a highly structured protein's function is determinant on forming a tight and specific interaction with its substrate(s) (as a key fits into only one unique lock)[77]. Significant and meaningful information can indeed be attained about unknown protein function by analyzing structural folds in tandem with sequence-based analysis, and programs such as the Protein Structure Initiative were established to expand those databases and efforts[78]. However, recognition of the prevalence and importance of proteins lacking well-defined globular structure has grown rapidly in the past few decades (Figure 1.3.1), primarily as a result of the genomics era unlocking sequence-based analysis.

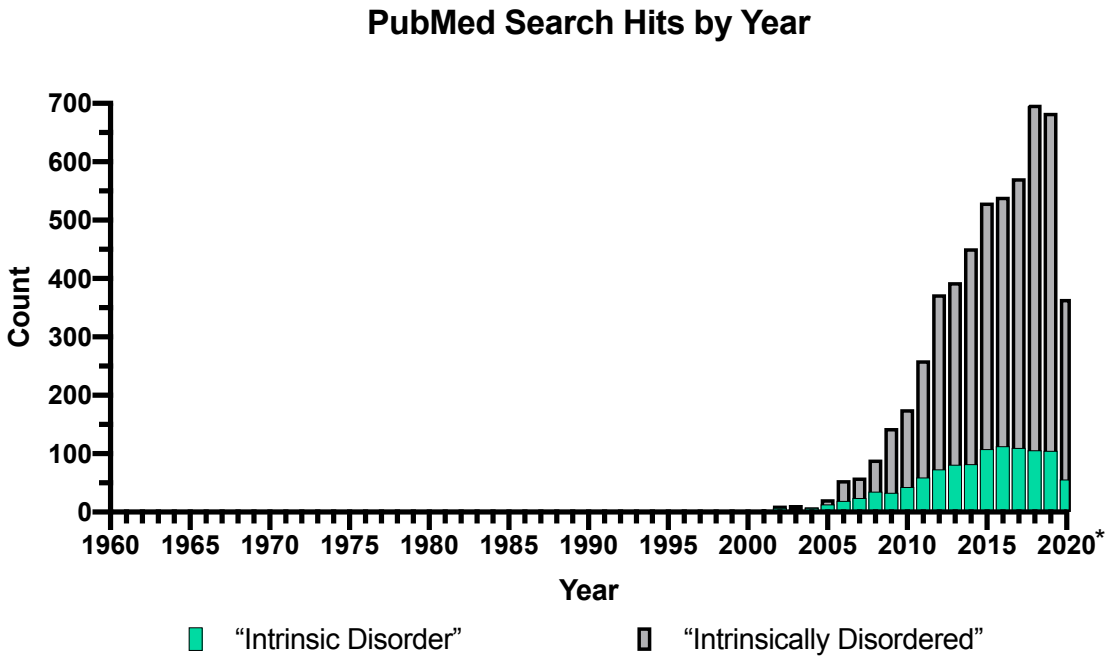

Figure 1.3.1 Intrinsic Disorder as a 21st Century Discovery Pubmed search results per year, queried for "intrinsic disorder" (green) and "intrinsically disordered" (grey)[84]. *As of June 2020.

Many computational models have been developed to predict intrinsically disordered regions (IDRs) or entire intrinsically disordered proteins (IDPs)[79], and studies have shown that 44% of human protein-coding genes contain IDR's longer than 30 residues[80,81]. Interestingly, bioinformatic studies have revealed a proportionate increase in the number of IDRs/IDPs as organisms become more complex[82,83]. This intriguing observation suggests that protein disorder plays crucial roles in orchestrating highly complex signaling systems. The very name of "disorder" itself conveys a sense of chaos, randomness, or uncontrollability of IDP function. Yet research continues to reveal that IDRs/IDPs are far from random, and their non-globular structure allows for specific, tunable control of complex cellular pathways.

Characteristics of Disordered Proteins

The failure to form stable secondary and/or tertiary structure is a defining feature shared by IDPs. IDPs are highly dynamic and exist in an ensemble of structurally heterogeneous conformations[82,85,86]. Figure 1.3.2 illustrates the various levels of order than can be present in proteins classified as IDPs, ranging from fully extended with no observable structural propensity or structural features to proteins that are largely well-folded with partial regions of disorder. Increasingly, multiple experimental approaches such as NMR techniques, small-angle X-ray scattering (SAXS), and molecular dynamics simulations are being combined to more accurately describe and investigate the average of the conformational ensemble within which an IDP exists [82,87]. IDPs tend to have a low percentage of hydrophobic residues (which helps to explain the lack of ability to spontaneously fold), as well as high net charges at neutral pH[79,88]. A subset of IDPs demonstrate "fold upon binding" or "coupled folding and binding" behavior, in which secondary structure develops upon association with a binding partner[89,90]. The mechanisms of this phenomenon is a matter of scrutiny, and how these folding events impact the kinetics of

associations in protein complexes will be important for generation and analysis of future therapeutic targets[91]. On the other end of the spectrum, disorder-to-disorder associations have been described, in which no observable dynamic or structural changes occur upon binding[85]. This behavior has been seen in IDP/IDP[92] as well as IDP/Globular[93] interactions. The term "fuzzy" association or "fuzziness" was first used in 2008 by Fuxreiter and colleagues to describe these types of interactions which remain highly heterogenous and dynamic[93]. A database called FuzDB (Fuzzy Complexes Database) has been established to compile growing experimental evidence of fuzziness in molecular mechanisms and signaling complexes[94].

Classification of Disordered Proteins

Obradović and colleagues proposed that IDRs/IDPs fall into four broad categories: molecular recognition, molecular assembly, protein modification, and entropic chains[95]. Later, classifications were expanded by van der Lee et al. and refined to include chaperones, effectors, and scavengers[80]. Entropic chains are typically regions of proteins such as linkers or spacers that are not observed to bind or have other roles aside from spacing. Molecular or entropic springs such as the elastic titin protein which functions in muscle cell contraction also fall into this category[96]. Protein modification sites (also defined as display sites) are places of a protein where extended flexibility allows for easy access to post-translational modifications (PTMs) like phosphorylation, PTM recognition, or access to binding motifs. Intrinsically disordered C-terminal tails are often sites of phosphorylation or other PTM, and are a prime example of this classification[97–99]. IDPs functioning as molecular chaperones to assist in the folding or prevent mis-folding/aggregation of other proteins have been observed, and are reviewed here[100]. In a similar way, some IDPs function as scavengers by binding to and storing small ligands or even other proteins. First identified as a disordered scavenger back in 1978, Chromogranin A binds

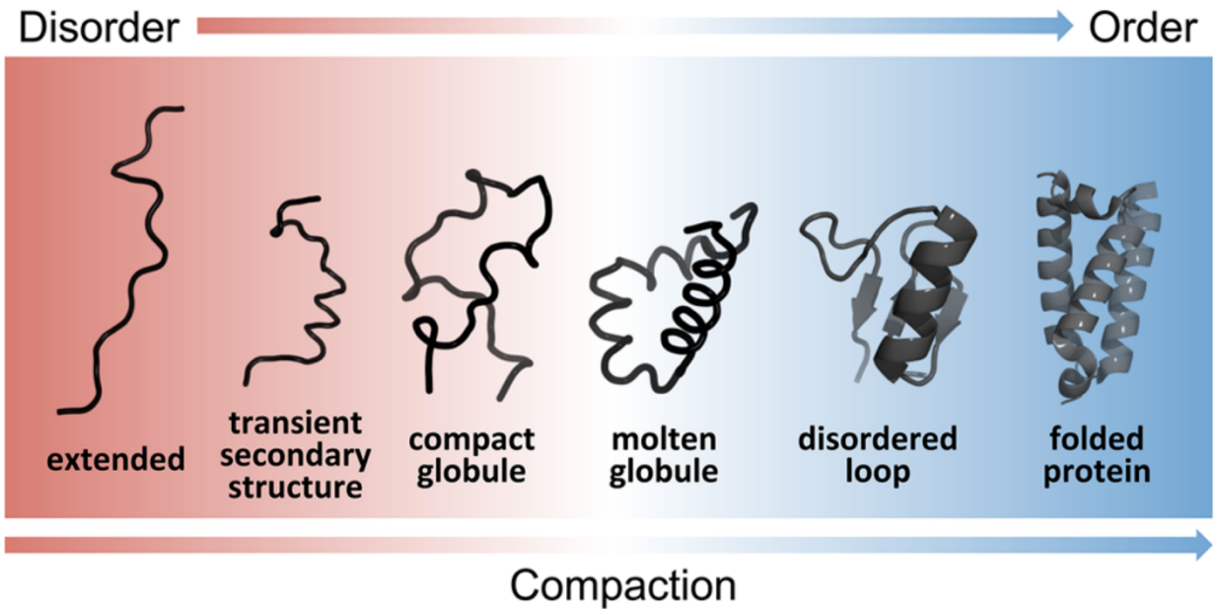

Figure 1.3.2 Protein Order Continuum

Model of the scale of protein structure from order to disorder. Compactness increases as secondary and tertiary structural features become more energetically favorable. Figure reproduced from from van der Lee et al.[80] with permission under the Standard ACS Author Choice permitted agreement.

and stores epinephrine and ATP in cells of the adrenal gland[101]. IDPs have also been observed to modify the enzymatic activity or binding affinity of partner protein, which places them into the effector category. These effectors often undergo fold-upon-binding behavior, which aids in these mechanisms[89,102]. Finally, molecular assemblers constitute a class of IDPs that contain multiple binding motifs and interfaces, are able to bind multiple different partners, and can act as scaffolds in molecular complexes[80]. APC falls squarely into the classification of a molecular assembler, with its many binding domains and key role in the β-catenin destruction complex. APC also contain regions that link well-folded N-terminal armadillo and oligomerization domains which could be classified as entropic chains. Additionally, because APC is phosphorylated, APC falls into the display site category as well[18,19,21,103].

IDPs as Central Interaction Hubs

IDPs are often found playing significant roles in signaling complexes[104–108]. Indeed, proteins that can interact with multiple different partners have been observed to have a higher proportion of disordered residues[106,107,109]. The presence of multiple binding motifs combined with inherent flexibility allows IDPs to facilitate rapid formation of higher order complexes at a sufficiently low entropic cost[110]. In some cases, the binding repeats as a whole interact weakly, with certain hotspots responsible for the majority of the binding affinity[111,112]. Two interesting theories have been put forward to explain why certain protein complexes contain disorder. The first is that the extended nature of an IDP increases the association rate (k_{on}) by increasing its capture radius. This so-called "fly-casting" effect, was named as an analogy to fishermen casting their lure (disguised to look like a fly) far from where they stand to reel in their catches[113]. The second is that disorder permits IDPs to bind with high specificity without a requirement of high affinity[114].

Mollica and colleagues note that the fly-casting theory is quite difficult to prove or disprove experimentally for a number of reasons[90]. For one, altering the level of disorder present in a protein of study inevitably changes many other aspects of the experimental conditions, making the capture radius effects difficult to uncouple. Secondly, a broad range of association rate constants has been observed for IDPs across relatively few kinetic studies, so more work is needed in this regard before informed assumptions of association rates between IDPs and globular proteins in complexes can be made. The range of association rates and observations that IDPs occasionally contain identical binding sites for different partners muddies the water of how disorder could contribute to specificity. Any binding site could be considered specific, provided concentrations of competing interactors are sufficiently low or are of sufficiently weaker affinity. While it makes sense that signaling pathways would benefit from weaker overall interactions to ensure reversibility of signal, it is unclear how disorder precisely imparts advantages to the kinetics and specificity of molecular complexes.

Finally, PTMs are extremely important to modulating signaling cascades, especially phosphorylation. Phosphorylation primarily occurs in regions of disorder[115], enabling the fine-tuning of complexes that at first glance might seem stochastic in nature. Phosphorylation is so frequent, that it has been estimated that when all PTMs are taken into account, the total number of interaction motifs within disordered regions in the human proteome may surpass one million[116]! This astonishing estimation speaks to the level of significance of IDPs/IDRs in cellular signaling and regulation.

IV. Topoisomerase IIα and APC

As mentioned previously, APC has many different binding partners. Studies in the Neufeld lab have revealed a novel association between Topoisomerase IIα (TopoIIα) and APC[117,118]. The central region of APC that is known to bind directly to β-catenin is implicated in this association and appears to be able to directly influence the catalytic activity of TopoIIα. These observations add another dimension to why the 15-aa repeat region of APC might be retained by tumors. The following section introduces the topoisomerase IIα enzyme, and how it relates to cancer and APC.

TopoIIα Structure and Function

While the genetic code embedded in DNA ultimately governs who we are and what makes us human, it is the topology of DNA that dictates how that code is deciphered, copied, and kept safe from harm[119–121]. Over 2 meters of DNA is packaged tightly into the ~6 micrometer diameter nucleus of each human cell, a remarkable feat that requires many proteins and enzymes to accomplish[122]. Inevitably, DNA becomes tangled and knotted in the process of recombination, chromatin compaction, and cellular division[119]. Topoisomerases are a family of enzymes responsible for relieving topological pressure such as knots, supercoils, and catenanes, and have roles in DNA transcription, replication, and chromosome segregation[123]. While there are six types of human topoisomerases (TopoI, TopoImt, TopoIIα, TopoIIβ, TopoIIIα and TopoIIIβ), this work focuses on TopoIIα.

TopoIIα is comprised of three domains: an N-terminal ATPase domain spanning the first ~450 residues, an internal DNA binding/cleavage/ligation domain spanning residues ~450-1200, and an intrinsically disordered C-terminal tail of ~300 residues[124,125]. While the ATPase and cleavage/binding domains of TopoIIα are well conserved across eukaryotes, the C-terminal

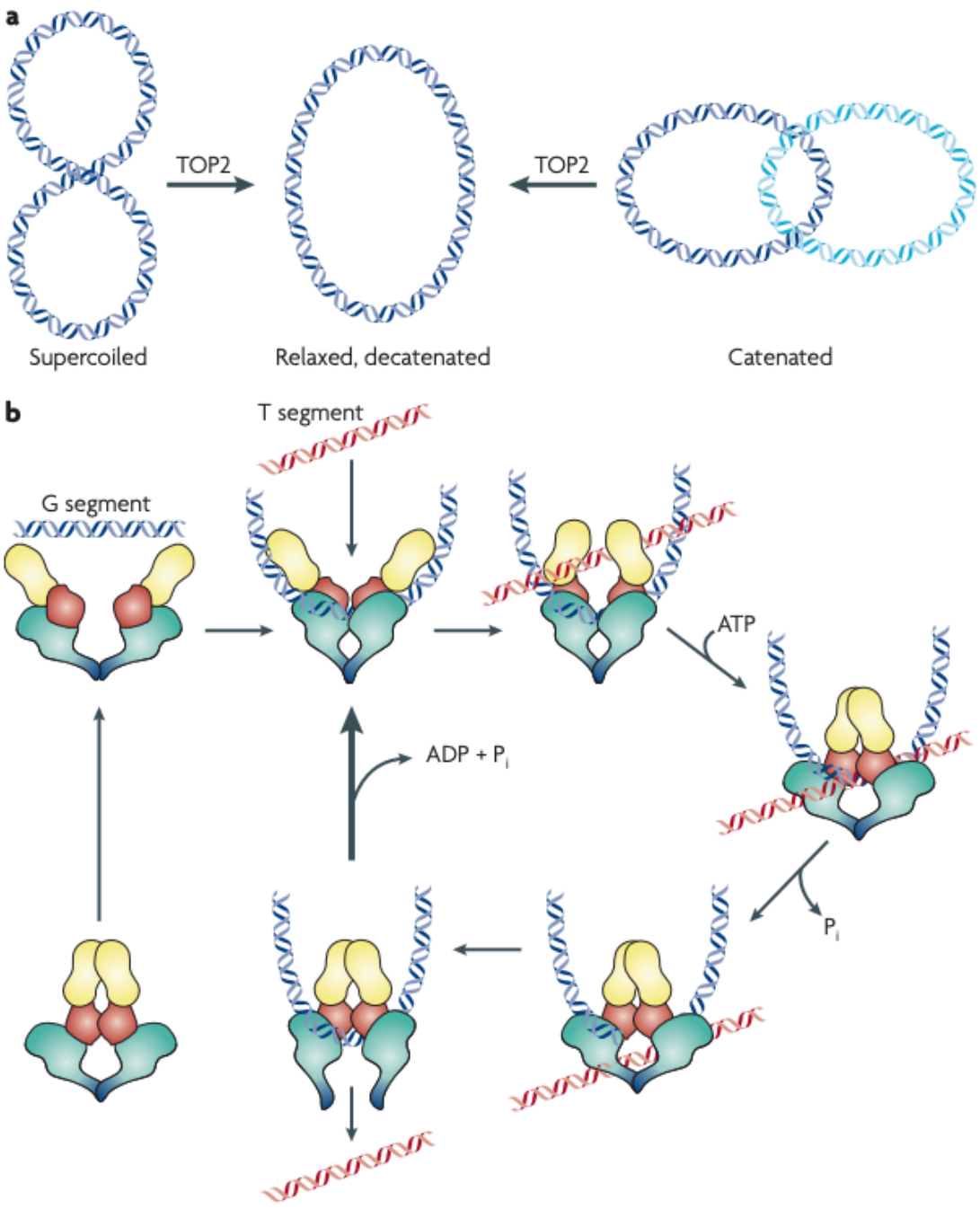

Figure 1.4.1 Strand Passage Reaction of TopoIIα a) Topology of DNA substrates for TopoIIα. b) Artistic depiction of the strand passage reaction. 1) Binding of G segment 2) Approach and binding of T segment 3) ATP-dependent cleavage of G segment 3) Pass-through of T segment 4) Re-ligation of G segment 5) Release of G segment OR binding of next T segment. Figure reproduced with permission from John Nitiss[132].

domain (CTD) is not, and contains many sites for phosphorylation, localization, and association[126]. Many crystal structures exist for the N-terminal and central domains of TopoIIα, however the high degree of disorder present in the CTD has prevented detailed structural analysis. While the CTD appears to be required for biochemical activity[127,128], it has been shown that the removal of the CTD alters cell sensitivity to compounds that target TopoIIα and influences regulation of the decatenation checkpoint during cell division[129].

TopoIIα catalyzes strand passage reactions, in which DNA double-strand breaks are transiently formed and re-ligated via transesterification reactions[123,130,131]. Figure 1.4.1 shows the ATP-dependent mechanism of a TopoIIα, which begins by binding two segments of DNA at once. The first strand to bind, termed the "G" strand is cleaved following binding of ATP. Conformational changes then permit the passage of the second strand, termed the "T" strand, through the G strand where it was cleaved. At this point, TopoIIα can either initiate a second phase of strand passage with another T strand, or it can ligate the G strand back together and release it to complete the catalytic cycle.

TopoIIα Role in Cancer

TopoIIα is overexpressed in many cancers, including colorectal cancers[133–135], and has been shown to be indispensable for cell cycle progression and cell survival[132,136–138]. These observations have made TopoIIα an attractive target for chemotherapeutics[139,140]. There are two classes of drugs that target TopoIIα. The first is a class of compounds that locks TopoIIα in a covalent complex with DNA and prevents the release or re-ligation of bound G strands. This block results in the generation of high amounts of DNA double strand breaks, triggering cell death. Compounds that have this activity have been termed Topo 'poisons'[139]. The second class consists of drugs that inhibit the catalytic activity of TopoIIα without generating locked covalent

complexes. These compounds are termed Topo 'inhibitors'[139]. Drugs targeting TopoIIα are currently used in treatment of cancer from many different tissues, including breast, esophageal, gastric, colorectal, prostate, ovarian, and even leukemias[141].

A major drawback of topoisomerase-targeting drugs is the risk of development of secondary malignancies. As an example, use of etoposide (VP-16), a commonly prescribed TopoIIα poison, has been associated with secondary leukemia[142]. Cells are also able to develop resistance to topoisomerase poisons such as etoposide, and this resistance has been correlated to a significant reduction in the levels of TopoIIα[143]. Interestingly, etoposide is not considered an effective treatment for cancers of the colon, even though expression levels of TopoIIα are elevated[144]. This observation raises the question of what other mechanisms are at play in cancers of the colon and rectum that limit the effectiveness of certain TopoIIα drugs.

APC and TopoIIα

As a reminder, APC is mutated in >80% of colorectal cancers. With this information, and the knowledge that TopoIIα levels are increased in colorectal cancers, yet they are resistant to etoposide, it is sensible to ask whether mutant APC is contributing to TopoIIα chemotherapeutic resistance in colorectal cancers. Previous work in the Neufeld lab has established that full-length APC, as well as segments of APC spanning the 15- and 20-aa repeats can be immunoprecipitated with TopoIIα[117,118]. Of even greater interest, *in vitro* experiments designed to assay the catalytic efficiency of TopoIIα revealed that recombinant fragments of APC spanning the 15-aa repeats (aa 959-1338) and the 20-aa repeats (aa 1211-2075) were each able to decrease the enzymatic activity of TopoIIα[117,118]. This observation suggests that APC could physically interact with TopoIIα, thereby lowering catalytic efficiency. Truncating APC mutations retain the 15-aa repeats in a majority of cases. In addition to the impact such mutation have on β-catenin

regulation, it is possible that truncating mutations allow APC to act on TopoIIα in a dominant negative fashion. A similar dominant negative behavior of APC has been observed in microtubule assembly and the spindle checkpoint[145,146]. One study showed that TopoIIα could be immunoprecipitated with the β-catenin/TCF-4 transcriptional complex, that β-catenin increases TopoIIα catalytic activity *in vitro*, and that TopoIIα inhibitors reduced the transcriptional activity of TCF/LEF[147]. While APC's contribution was not considered in that study, APC's presence in the nucleus has been established and should not be overlooked. Determining the contribution of APC (specifically the cancer-retained 15-aa repeat region) will be an important step in understanding the mechanisms of resistance of colorectal cancers to TopoIIα chemotherapeutics.

V. Summary

Even though APC was established as an important tumor suppressor and a major contributor to the initiation of colorectal cancer nearly 30 years ago, mechanistic insight into its roles in the β-catenin destruction complex remain poorly understood. Additionally, there are no treatments available for colorectal cancer patients that specifically take advantage of mutant APC. Understanding the precise molecular mechanisms underlying APC's role in the β-catenin destruction complex and other roles in the cell will be of utmost importance in developing more effective treatment options.

In Chapters 2 and 3 of this dissertation, I establish the 15-aa repeat region of APC as an intrinsically disordered protein that retains disorder upon binding to β-catenin. I analyze the 15-aa repeat region on an individual residue level and predict regions that may be contributing to transient secondary structure. I observe that the 15-aa repeat region is able to bind multiple β-catenin molecules at one time, and that this binding appears to be heterogenous in nature. In

Chapter 4, I show that truncating *APC* mutations impart resistance to cancer chemotherapeutic compounds, as well as a reduction of enzymatic activity of TopoIIα. I also show that APC is in a complex with TopoIIα and β-catenin when immunoprecipitated from a nuclear extract. In total, this work provides structural and backbone dynamic insights into of a region of APC that is retained by most tumors, and will aid in elucidating detailed mechanisms which may assist in development of future therapeutics.

References

(1) Siegel, R. L.; Miller, K. D.; Jemal, A. Cancer Statistics, 2020. *CA. Cancer J. Clin.* **2020**, *70* (1), 7–30. https://doi.org/10.3322/caac.21590.

(2) Rex, D. K.; Boland, C. R.; Dominitz, J. A.; Giardiello, F. M.; Johnson, D. A.; Kaltenbach, T.; Levin, T. R.; Lieberman, D.; Robertson, D. J. Colorectal Cancer Screening: Recommendations for Physicians and Patients from the U.S. Multi-Society Task Force on Colorectal Cancer. *Gastrointest. Endosc.* **2017**, *86* (1), 18–33. https://doi.org/10.1016/j.gie.2017.04.003.

(3) Howlander, N.; Noone, A.; Krapcho, M.; Miller, D.; Brest, A.; Yu, M.; Ruhl, J.; Tatalovich, Z.; Mariotta, A.; Lewis, D.; Chen, H.; Feuer, E.; Cronin, K. SEER Cancer Statistics Review, 1975-2017 https://seer.cancer.gov/csr/1975_2017 (accessed May 19, 2020).

(4) Xie, Y.-H.; Chen, Y.-X.; Fang, J.-Y. Comprehensive Review of Targeted Therapy for Colorectal Cancer. *Signal Transduct. Target. Ther.* **2020**, *5*. https://doi.org/10.1038/s41392-020-0116-z.

(5) Jasperson, K. W.; Tuohy, T. M.; Neklason, D. W.; Burt, R. W. Hereditary and Familial Colon Cancer. *Gastroenterology* **2010**, *138* (6), 2044–2058. https://doi.org/10.1053/j.gastro.2010.01.054.

(6) Familial Adenomatous Polyposis http://www.cancer.net/cancer-types/familial-adenomatous-polyposis (accessed Feb 25, 2017).

(7) Bodmer, W. F.; Bailey, C. J.; Bodmer, J.; Bussey, H. J.; Ellis, A.; Gorman, P.; Lucibello, F. C.; Murday, V. A.; Rider, S. H.; Scambler, P. Localization of the Gene for Familial Adenomatous Polyposis on Chromosome 5. *Nature* **1987**, *328* (6131), 614–616. https://doi.org/10.1038/328614a0.

(8) Herrera, L.; Kakati, S.; Gibas, L.; Pietrzak, E.; Sandberg, A. A. Gardner Syndrome in a Man with an Interstitial Deletion of 5q. *Am. J. Med. Genet.* **1986**, *25* (3), 473–476. https://doi.org/10.1002/ajmg.1320250309.

(9) Groden, J.; Thliveris, A.; Samowitz, W.; Carlson, M.; Gelbert, L.; Albertsen, H.; Joslyn, G.; Stevens, J.; Spirio, L.; Robertson, M. Identification and Characterization of the Familial Adenomatous Polyposis Coli Gene. *Cell* **1991**, *66* (3), 589–600.

(10) Kwong, L. N.; Dove, W. F. APC and Its Modifiers in Colon Cancer. *Adv. Exp. Med. Biol.* **2009**, *656*, 85–106.

(11) Rowan, A. J.; Lamlum, H.; Ilyas, M.; Wheeler, J.; Straub, J.; Papadopoulou, A.; Bicknell, D.; Bodmer, W. F.; Tomlinson, I. P. M. APC Mutations in Sporadic Colorectal Tumors: A Mutational "Hotspot" and Interdependence of the "Two Hits." *Proc. Natl. Acad. Sci. U. S. A.* **2000**, *97* (7), 3352–3357.
(12) Smith, K. J.; Johnson, K. A.; Bryan, T. M.; Hill, D. E.; Markowitz, S.; Willson, J. K.; Paraskeva, C.; Petersen, G. M.; Hamilton, S. R.; Vogelstein, B. The APC Gene Product in Normal and Tumor Cells. *Proc. Natl. Acad. Sci. U. S. A.* **1993**, *90* (7), 2846–2850. https://doi.org/10.1073/pnas.90.7.2846.
(13) Joslyn, G.; Richardson, D. S.; White, R.; Alber, T. Dimer Formation by an N-Terminal Coiled Coil in the APC Protein. *Proc. Natl. Acad. Sci. U. S. A.* **1993**, *90* (23), 11109–11113. https://doi.org/10.1073/pnas.90.23.11109.
(14) Peifer, M.; Berg, S.; Reynolds, A. B. A Repeating Amino Acid Motif Shared by Proteins with Diverse Cellular Roles. *Cell* **1994**, *76* (5), 789–791. https://doi.org/10.1016/0092-8674(94)90353-0.
(15) Seeling, J. M.; Miller, J. R.; Gil, R.; Moon, R. T.; White, R.; Virshup, D. M. Regulation of Beta-Catenin Signaling by the B56 Subunit of Protein Phosphatase 2A. *Science* **1999**, *283* (5410), 2089–2091. https://doi.org/10.1126/science.283.5410.2089.
(16) Kawasaki, Y.; Senda, T.; Ishidate, T.; Koyama, R.; Morishita, T.; Iwayama, Y.; Higuchi, O.; Akiyama, T. Asef, a Link Between the Tumor Suppressor APC and G-Protein Signaling. *Science* **2000**, *289* (5482), 1194–1197. https://doi.org/10.1126/science.289.5482.1194.
(17) Kim, S. B.; Zhang, L.; Yoon, J.; Lee, J.; Min, J.; Li, W.; Grishin, N. V.; Moon, Y.-A.; Wright, W. E.; Shay, J. W. Truncated Adenomatous Polyposis Coli Mutation Induces Asef-Activated Golgi Fragmentation. *Mol. Cell. Biol.* **2018**, *38* (17). https://doi.org/10.1128/MCB.00135-18.
(18) Liu, J.; Xing, Y.; Hinds, T. R.; Zheng, J.; Xu, W. The Third 20 Amino Acid Repeat Is the Tightest Binding Site of APC for Beta-Catenin. *J. Mol. Biol.* **2006**, *360* (1), 133–144. https://doi.org/10.1016/j.jmb.2006.04.064.
(19) Xing, Y.; Clements, W. K.; Le Trong, I.; Hinds, T. R.; Stenkamp, R.; Kimelman, D.; Xu, W. Crystal Structure of a β-Catenin/APC Complex Reveals a Critical Role for APC Phosphorylation in APC Function. *Mol. Cell* **2004**, *15* (4), 523–533. https://doi.org/10.1016/j.molcel.2004.08.001.
(20) Xu, W.; Kimelman, D. Mechanistic Insights from Structural Studies of β-Catenin and Its Binding Partners. *J. Cell Sci.* **2007**, *120* (19), 3337–3344. https://doi.org/10.1242/jcs.013771.
(21) Ha, N.-C.; Tonozuka, T.; Stamos, J. L.; Choi, H.-J.; Weis, W. I. Mechanism of Phosphorylation-Dependent Binding of APC to Beta-Catenin and Its Role in Beta-Catenin Degradation. *Mol. Cell* **2004**, *15* (4), 511–521. https://doi.org/10.1016/j.molcel.2004.08.010.
(22) Gao, J.; Aksoy, B. A.; Dogrusoz, U.; Dresdner, G.; Gross, B.; Sumer, S. O.; Sun, Y.; Jacobsen, A.; Sinha, R.; Larsson, E.; Cerami, E.; Sander, C.; Schultz, N. Integrative Analysis of Complex Cancer Genomics and Clinical Profiles Using the CBioPortal. *Sci. Signal.* **2013**, *6* (269), pl1. https://doi.org/10.1126/scisignal.2004088.
(23) Cerami, E.; Gao, J.; Dogrusoz, U.; Gross, B. E.; Sumer, S. O.; Aksoy, B. A.; Jacobsen, A.; Byrne, C. J.; Heuer, M. L.; Larsson, E.; Antipin, Y.; Reva, B.; Goldberg, A. P.; Sander, C.; Schultz, N. The CBio Cancer Genomics Portal: An Open Platform for Exploring Multidimensional Cancer Genomics Data. *Cancer Discov.* **2012**, *2* (5), 401–404. https://doi.org/10.1158/2159-8290.CD-12-0095.

(24) Behrens, J.; Jerchow, B.-A.; Würtele, M.; Grimm, J.; Asbrand, C.; Wirtz, R.; Kühl, M.; Wedlich, D.; Birchmeier, W. Functional Interaction of an Axin Homolog, Conductin, with β-Catenin, APC, and GSK3β. *Science* **1998**, *280* (5363), 596–599. https://doi.org/10.1126/science.280.5363.596.
(25) Spink, K. E.; Polakis, P.; Weis, W. I. Structural Basis of the Axin–Adenomatous Polyposis Coli Interaction. *EMBO J.* **2000**, *19* (10), 2270–2279. https://doi.org/10.1093/emboj/19.10.2270.
(26) Deka, J.; Kuhlmann, J.; Müller, O. A Domain within the Tumor Suppressor Protein APC Shows Very Similar Biochemical Properties as the Microtubule-Associated Protein Tau. *Eur. J. Biochem.* **1998**, *253* (3), 591–597. https://doi.org/10.1046/j.1432-1327.1998.2530591.x.
(27) Munemitsu, S.; Souza, B.; Müller, O.; Albert, I.; Rubinfeld, B.; Polakis, P. The APC Gene Product Associates with Microtubules in Vivo and Promotes Their Assembly in Vitro. *Cancer Res.* **1994**, *54* (14), 3676–3681.
(28) Askham, J. M.; Moncur, P.; Markham, A. F.; Morrison, E. E. Regulation and Function of the Interaction between the APC Tumour Suppressor Protein and EB1. *Oncogene* **2000**, *19* (15), 1950–1958. https://doi.org/10.1038/sj.onc.1203498.
(29) Okada, K.; Bartolini, F.; Deaconescu, A. M.; Moseley, J. B.; Dogic, Z.; Grigorieff, N.; Gundersen, G. G.; Goode, B. L. Adenomatous Polyposis Coli Protein Nucleates Actin Assembly and Synergizes with the Formin MDia1. *J. Cell Biol.* **2010**, *189* (7), 1087–1096. https://doi.org/10.1083/jcb.201001016.
(30) Moseley, J. B.; Bartolini, F.; Okada, K.; Wen, Y.; Gundersen, G. G.; Goode, B. L. Regulated Binding of Adenomatous Polyposis Coli Protein to Actin. *J. Biol. Chem.* **2007**, *282* (17), 12661–12668. https://doi.org/10.1074/jbc.M610615200.
(31) Wang, Y.; Azuma, Y.; Friedman, D. B.; Coffey, R. J.; Neufeld, K. L. Novel Association of APC with Intermediate Filaments Identified Using a New Versatile APC Antibody. *BMC Cell Biol.* **2009**, *10*, 75. https://doi.org/10.1186/1471-2121-10-75.
(32) Matsumine, A.; Ogai, A.; Senda, T.; Okumura, N.; Satoh, K.; Baeg, G. H.; Kawahara, T.; Kobayashi, S.; Okada, M.; Toyoshima, K.; Akiyama, T. Binding of APC to the Human Homolog of the Drosophila Discs Large Tumor Suppressor Protein. *Science* **1996**, *272* (5264), 1020–1023. https://doi.org/10.1126/science.272.5264.1020.
(33) Zhang, Z.; Li, H.; Chen, L.; Lu, X.; Zhang, J.; Xu, P.; Lin, K.; Wu, G. Molecular Basis for the Recognition of Adenomatous Polyposis Coli by the Discs Large 1 Protein. *PloS One* **2011**, *6* (8), e23507. https://doi.org/10.1371/journal.pone.0023507.
(34) Tickenbrock, L.; Cramer, J.; Vetter, I. R.; Müller, O. The Coiled Coil Region (Amino Acids 129–250) of the Tumor Suppressor Protein Adenomatous Polyposis Coli (APC) ITS STRUCTURE AND ITS INTERACTION WITH CHROMOSOME MAINTENANCE REGION 1 (Crm-1). *J. Biol. Chem.* **2002**, *277* (35), 32332–32338. https://doi.org/10.1074/jbc.M203990200.
(35) Day, C. L.; Alber, T. Crystal Structure of the Amino-Terminal Coiled-Coil Domain of the APC Tumor Suppressor11Edited by I. A. Wilson. *J. Mol. Biol.* **2000**, *301* (1), 147–156. https://doi.org/10.1006/jmbi.2000.3895.
(36) Morishita, E. C.; Murayama, K.; Kato-Murayama, M.; Ishizuka-Katsura, Y.; Tomabechi, Y.; Hayashi, T.; Terada, T.; Handa, N.; Shirouzu, M.; Akiyama, T.; Yokoyama, S. Crystal Structures of the Armadillo Repeat Domain of Adenomatous Polyposis Coli and Its Complex with the Tyrosine-Rich Domain of Sam68. *Struct. Lond. Engl. 1993* **2011**, *19* (10), 1496–1508. https://doi.org/10.1016/j.str.2011.07.013.

(37) Zhang, Z.; Lin, K.; Gao, L.; Chen, L.; Shi, X.; Wu, G. Crystal Structure of the Armadillo Repeat Domain of Adenomatous Polyposis Coli Which Reveals Its Inherent Flexibility. *Biochem. Biophys. Res. Commun.* **2011**, *412* (4), 732–736. https://doi.org/10.1016/j.bbrc.2011.08.044.
(38) Spink, K. E.; Fridman, S. G.; Weis, W. I. Molecular Mechanisms of β-Catenin Recognition by Adenomatous Polyposis Coli Revealed by the Structure of an APC–β-Catenin Complex. *EMBO J.* **2001**, *20* (22), 6203–6212. https://doi.org/10.1093/emboj/20.22.6203.
(39) Minde, D. P.; Anvarian, Z.; Rüdiger, S. G.; Maurice, M. M. Messing up Disorder: How Do Missense Mutations in the Tumor Suppressor Protein APC Lead to Cancer? *Mol. Cancer* **2011**, *10* (1), 101. https://doi.org/10.1186/1476-4598-10-101.
(40) Xue, B.; Dunker, A. K.; Uversky, V. N. The Roles of Intrinsic Disorder in Orchestrating the Wnt-Pathway. *J. Biomol. Struct. Dyn.* **2012**, *29* (5), 843–861. https://doi.org/10.1080/073911012010525024.
(41) Minde, D. P.; Radli, M.; Forneris, F.; Maurice, M. M.; Rüdiger, S. G. D. Large Extent of Disorder in Adenomatous Polyposis Coli Offers a Strategy to Guard Wnt Signalling against Point Mutations. *PLoS ONE* **2013**, *8* (10). https://doi.org/10.1371/journal.pone.0077257.
(42) Kaplan, K. B.; Burds, A. A.; Swedlow, J. R.; Bekir, S. S.; Sorger, P. K.; Näthke, I. S. A Role for the Adenomatous Polyposis Coli Protein in Chromosome Segregation. *Nat. Cell Biol.* **2001**, *3* (4), 429–432. https://doi.org/10.1038/35070123.
(43) Lui, C.; Ashton, C.; Sharma, M.; Brocardo, M. G.; Henderson, B. R. APC Functions at the Centrosome to Stimulate Microtubule Growth. *Int. J. Biochem. Cell Biol.* **2016**, *70*, 39–47. https://doi.org/10.1016/j.biocel.2015.10.028.
(44) Bahmanyar, S.; Nelson, W. J.; Barth, A. I. M. Role of APC and Its Binding Partners in Regulating Microtubules in Mitosis. *Adv. Exp. Med. Biol.* **2009**, *656*, 65–74.
(45) Bienz, M.; Hamada, F. Adenomatous Polyposis Coli Proteins and Cell Adhesion. *Curr. Opin. Cell Biol.* **2004**, *16* (5), 528–535. https://doi.org/10.1016/j.ceb.2004.08.001.
(46) Aoki, K.; Taketo, M. M. Adenomatous Polyposis Coli (APC): A Multi-Functional Tumor Suppressor Gene. *J. Cell Sci.* **2007**, *120* (19), 3327–3335. https://doi.org/10.1242/jcs.03485.
(47) Komiya, Y.; Habas, R. Wnt Signal Transduction Pathways. *Organogenesis* **2008**, *4* (2), 68–75.
(48) Stamos, J. L.; Weis, W. I. The β-Catenin Destruction Complex. *Cold Spring Harb. Perspect. Biol.* **2013**, *5* (1). https://doi.org/10.1101/cshperspect.a007898.
(49) Kries, J. P. von; Winbeck, G.; Asbrand, C.; Schwarz-Romond, T.; Sochnikova, N.; Dell'Oro, A.; Behrens, J.; Birchmeier, W. Hot Spots in β-Catenin for Interactions with LEF-1, Conductin and APC. *Nat. Struct. Biol.* **2000**, *7* (9), 800. https://doi.org/10.1038/79039.
(50) Behrens, J.; von Kries, J. P.; Kühl, M.; Bruhn, L.; Wedlich, D.; Grosschedl, R.; Birchmeier, W. Functional Interaction of Beta-Catenin with the Transcription Factor LEF-1. *Nature* **1996**, *382* (6592), 638–642. https://doi.org/10.1038/382638a0.
(51) MacDonald, B. T.; Tamai, K.; He, X. Wnt/β-Catenin Signaling: Components, Mechanisms, and Diseases. *Dev. Cell* **2009**, *17* (1), 9–26. https://doi.org/10.1016/j.devcel.2009.06.016.
(52) Jeong, W.-J.; Ro, E. J.; Choi, K.-Y. Interaction between Wnt/β-Catenin and RAS-ERK Pathways and an Anti-Cancer Strategy via Degradations of β-Catenin and RAS by Targeting the Wnt/β-Catenin Pathway. *Npj Precis. Oncol.* **2018**, *2* (1), 1–10. https://doi.org/10.1038/s41698-018-0049-y.

(53) Sharma, M.; Castro-Piedras, I.; Simmons, G. E.; Pruitt, K. Dishevelled: A Masterful Conductor of Complex Wnt Signals. *Cell. Signal.* **2018**, *47*, 52–64. https://doi.org/10.1016/j.cellsig.2018.03.004.
(54) Parker, T. W.; Neufeld, K. L. APC Controls Wnt-Induced β-Catenin Destruction Complex Recruitment in Human Colonocytes. *Sci. Rep.* **2020**, *10*. https://doi.org/10.1038/s41598-020-59899-z.
(55) Bilic, J.; Huang, Y.-L.; Davidson, G.; Zimmermann, T.; Cruciat, C.-M.; Bienz, M.; Niehrs, C. Wnt Induces LRP6 Signalosomes and Promotes Dishevelled-Dependent LRP6 Phosphorylation. *Science* **2007**, *316* (5831), 1619–1622. https://doi.org/10.1126/science.1137065.
(56) Lykke-Andersen, S.; Jensen, T. H. Nonsense-Mediated MRNA Decay: An Intricate Machinery That Shapes Transcriptomes. *Nat. Rev. Mol. Cell Biol.* **2015**, *16* (11), 665–677. https://doi.org/10.1038/nrm4063.
(57) Miyoshi, Y.; Nagase, H.; Ando, H.; Horii, A.; Ichii, S.; Nakatsuru, S.; Aoki, T.; Miki, Y.; Mori, T.; Nakamura, Y. Somatic Mutations of the APC Gene in Colorectal Tumors: Mutation Cluster Region in the APC Gene. *Hum. Mol. Genet.* **1992**, *1* (4), 229–233. https://doi.org/10.1093/hmg/1.4.229.
(58) Knudson, A. G. Mutation and Cancer: Statistical Study of Retinoblastoma. *Proc. Natl. Acad. Sci. U. S. A.* **1971**, *68* (4), 820–823.
(59) Nagase, H.; Nakamura, Y. Mutations of the APC (Adenomatous Polyposis Coli) Gene. *Hum. Mutat.* **1993**, *2* (6), 425–434. https://doi.org/10.1002/humu.1380020602.
(60) Lamlum, H.; Ilyas, M.; Rowan, A.; Clark, S.; Johnson, V.; Bell, J.; Frayling, I.; Efstathiou, J.; Pack, K.; Payne, S.; Roylance, R.; Gorman, P.; Sheer, D.; Neale, K.; Phillips, R.; Talbot, I.; Bodmer, W.; Tomlinson, I. The Type of Somatic Mutation at APC in Familial Adenomatous Polyposis Is Determined by the Site of the Germline Mutation: A New Facet to Knudson's "two-Hit" Hypothesis. *Nat. Med.* **1999**, *5* (9), 1071–1075. https://doi.org/10.1038/12511.
(61) Noutsou, M.; Duarte, A. M. S.; Anvarian, Z.; Didenko, T.; Minde, D. P.; Kuper, I.; de Ridder, I.; Oikonomou, C.; Friedler, A.; Boelens, R.; Rüdiger, S. G. D.; Maurice, M. M. Critical Scaffolding Regions of the Tumor Suppressor Axin1 Are Natively Unfolded. *J. Mol. Biol.* **2011**, *405* (3), 773–786. https://doi.org/10.1016/j.jmb.2010.11.013.
(62) Dajani, R.; Fraser, E.; Roe, S. M.; Yeo, M.; Good, V. M.; Thompson, V.; Dale, T. C.; Pearl, L. H. Structural Basis for Recruitment of Glycogen Synthase Kinase 3β to the Axin–APC Scaffold Complex. *EMBO J.* **2003**, *22* (3), 494–501. https://doi.org/10.1093/emboj/cdg068.
(63) Sobrado, P.; Jedlicki, A.; Bustos, V. H.; Allende, C. C.; Allende, J. E. Basic Region of Residues 228–231 of Protein Kinase CK1α Is Involved in Its Interaction with Axin: Binding to Axin Does Not Affect the Kinase Activity. *J. Cell. Biochem.* **2005**, *94* (2), 217–224. https://doi.org/10.1002/jcb.20350.
(64) Liu, C.; Li, Y.; Semenov, M.; Han, C.; Baeg, G.-H.; Tan, Y.; Zhang, Z.; Lin, X.; He, X. Control of β-Catenin Phosphorylation/Degradation by a Dual-Kinase Mechanism. *Cell* **2002**, *108* (6), 837–847. https://doi.org/10.1016/S0092-8674(02)00685-2.
(65) Kimelman, D.; Xu, W. Beta-Catenin Destruction Complex: Insights and Questions from a Structural Perspective. *Oncogene* **2006**, *25* (57), 7482–7491. https://doi.org/10.1038/sj.onc.1210055.
(66) Albuquerque, C.; Breukel, C.; van der Luijt, R.; Fidalgo, P.; Lage, P.; Slors, F. J. M.; Leitão, C. N.; Fodde, R.; Smits, R. The "just-Right" Signaling Model: APC Somatic Mutations

Are Selected Based on a Specific Level of Activation of the Beta-Catenin Signaling Cascade. *Hum. Mol. Genet.* **2002**, *11* (13), 1549–1560. https://doi.org/10.1093/hmg/11.13.1549.
(67) Schneikert, J.; Grohmann, A.; Behrens, J. Truncated APC Regulates the Transcriptional Activity of Beta-Catenin in a Cell Cycle Dependent Manner. *Hum. Mol. Genet.* **2007**, *16* (2), 199–209. https://doi.org/10.1093/hmg/ddl464.
(68) Roberts, D. M.; Pronobis, M. I.; Poulton, J. S.; Waldmann, J. D.; Stephenson, E. M.; Hanna, S.; Peifer, M. Deconstructing the SScatenin Destruction Complex: Mechanistic Roles for the Tumor Suppressor APC in Regulating Wnt Signaling. *Mol. Biol. Cell* **2011**, *22* (11), 1845–1863. https://doi.org/10.1091/mbc.E10-11-0871.
(69) Jarrett, C. R.; Blancato, J.; Cao, T.; Bressette, D. S.; Cepeda, M.; Young, P. E.; King, C. R.; Byers, S. W. Human APC2 Localization and Allelic Imbalance. *Cancer Res.* **2001**, *61* (21), 7978–7984.
(70) Schneikert, J.; Chandra, S. H. V.; Ruppert, J. G.; Ray, S.; Wenzel, E. M.; Behrens, J. Functional Comparison of Human Adenomatous Polyposis Coli (APC) and APC-Like in Targeting Beta-Catenin for Degradation. *PLOS ONE* **2013**, *8* (7), e68072. https://doi.org/10.1371/journal.pone.0068072.
(71) Leung, J. Y.; Kolligs, F. T.; Wu, R.; Zhai, Y.; Kuick, R.; Hanash, S.; Cho, K. R.; Fearon, E. R. Activation of AXIN2 Expression by β-Catenin-T Cell Factor A FEEDBACK REPRESSOR PATHWAY REGULATING Wnt SIGNALING. *J. Biol. Chem.* **2002**, *277* (24), 21657–21665. https://doi.org/10.1074/jbc.M200139200.
(72) Huang, P.; Senga, T.; Hamaguchi, M. A Novel Role of Phospho- β -Catenin in Microtubule Regrowth at Centrosome. *Oncogene* **2007**, *26* (30), 4357–4371. https://doi.org/10.1038/sj.onc.1210217.
(73) Huber, A. H.; Weis, W. I. The Structure of the β-Catenin/E-Cadherin Complex and the Molecular Basis of Diverse Ligand Recognition by β-Catenin. *Cell* **2001**, *105* (3), 391–402. https://doi.org/10.1016/S0092-8674(01)00330-0.
(74) Cormier, K. W.; Woodgett, J. R. Recent Advances in Understanding the Cellular Roles of GSK-3. *F1000Research* **2017**, *6*. https://doi.org/10.12688/f1000research.10557.1.
(75) Luo, W.; Lin, S.-C. Axin: A Master Scaffold for Multiple Signaling Pathways. *Neurosignals* **2004**, *13* (3), 99–113. https://doi.org/10.1159/000076563.
(76) Kendrew, J. C.; Bodo, G.; Dintzis, H. M.; Parrish, R. G.; Wyckoff, H.; Phillips, D. C. A Three-Dimensional Model of the Myoglobin Molecule Obtained by x-Ray Analysis. *Nature* **1958**, *181* (4610), 662–666. https://doi.org/10.1038/181662a0.
(77) Tripathi, A.; Bankaitis, V. A. Molecular Docking: From Lock and Key to Combination Lock. *J. Mol. Med. Clin. Appl.* **2017**, *2* (1).
(78) Montelione, G. T. The Protein Structure Initiative: Achievements and Visions for the Future. *F1000 Biol. Rep.* **2012**, *4*. https://doi.org/10.3410/B4-7.
(79) Meng, F.; Uversky, V. N.; Kurgan, L. Comprehensive Review of Methods for Prediction of Intrinsic Disorder and Its Molecular Functions. *Cell. Mol. Life Sci. CMLS* **2017**, *74* (17), 3069–3090. https://doi.org/10.1007/s00018-017-2555-4.
(80) van der Lee, R.; Buljan, M.; Lang, B.; Weatheritt, R. J.; Daughdrill, G. W.; Dunker, A. K.; Fuxreiter, M.; Gough, J.; Gsponer, J.; Jones, D. T.; Kim, P. M.; Kriwacki, R. W.; Oldfield, C. J.; Pappu, R. V.; Tompa, P.; Uversky, V. N.; Wright, P. E.; Babu, M. M. Classification of Intrinsically Disordered Regions and Proteins. *Chem. Rev.* **2014**, *114* (13), 6589–6631. https://doi.org/10.1021/cr400525m.

(81) Oates, M. E.; Romero, P.; Ishida, T.; Ghalwash, M.; Mizianty, M. J.; Xue, B.; Dosztányi, Z.; Uversky, V. N.; Obradovic, Z.; Kurgan, L.; Dunker, A. K.; Gough, J. D2P2: Database of Disordered Protein Predictions. *Nucleic Acids Res.* **2013**, *41* (Database issue), D508–D516. https://doi.org/10.1093/nar/gks1226.
(82) Uversky, V. N. Intrinsically Disordered Proteins and Their "Mysterious" (Meta)Physics. *Front. Phys.* **2019**, *7*. https://doi.org/10.3389/fphy.2019.00010.
(83) Dunker, A. K.; Obradovic, Z.; Romero, P.; Garner, E. C.; Brown, C. J. Intrinsic Protein Disorder in Complete Genomes. *Genome Inform. Workshop Genome Inform.* **2000**, *11*, 161–171.
(84) PubMed https://pubmed.ncbi.nlm.nih.gov/ (accessed Jun 6, 2020).
(85) Miskei, M.; Gregus, A.; Sharma, R.; Duro, N.; Zsolyomi, F.; Fuxreiter, M. Fuzziness Enables Context Dependence of Protein Interactions. *FEBS Lett.* **2017**, *591* (17), 2682–2695. https://doi.org/10.1002/1873-3468.12762.
(86) Mittag, T.; Kay, L. E.; Forman-Kay, J. D. Protein Dynamics and Conformational Disorder in Molecular Recognition. *J. Mol. Recognit. JMR* **2010**, *23* (2), 105–116. https://doi.org/10.1002/jmr.961.
(87) Fu, B.; Vendruscolo, M. Structure and Dynamics of Intrinsically Disordered Proteins. *Adv. Exp. Med. Biol.* **2015**, *870*, 35–48. https://doi.org/10.1007/978-3-319-20164-1_2.
(88) Uversky, V. N.; Gillespie, J. R.; Fink, A. L. Why Are "Natively Unfolded" Proteins Unstructured under Physiologic Conditions? *Proteins* **2000**, *41* (3), 415–427. https://doi.org/10.1002/1097-0134(20001115)41:3<415::aid-prot130>3.0.co;2-7.
(89) Wright, P. E.; Dyson, H. J. Linking Folding and Binding. *Curr. Opin. Struct. Biol.* **2009**, *19* (1), 31–38. https://doi.org/10.1016/j.sbi.2008.12.003.
(90) Mollica, L.; Bessa, L. M.; Hanoulle, X.; Jensen, M. R.; Blackledge, M.; Schneider, R. Binding Mechanisms of Intrinsically Disordered Proteins: Theory, Simulation, and Experiment. *Front. Mol. Biosci.* **2016**, *3*. https://doi.org/10.3389/fmolb.2016.00052.
(91) Shammas, S. L.; Crabtree, M. D.; Dahal, L.; Wicky, B. I. M.; Clarke, J. Insights into Coupled Folding and Binding Mechanisms from Kinetic Studies. *J. Biol. Chem.* **2016**, *291* (13), 6689–6695. https://doi.org/10.1074/jbc.R115.692715.
(92) Wang, W.; Wang, D. Extreme Fuzziness: Direct Interactions between Two IDPs. *Biomolecules* **2019**, *9* (3). https://doi.org/10.3390/biom9030081.
(93) Tompa, P.; Fuxreiter, M. Fuzzy Complexes: Polymorphism and Structural Disorder in Protein-Protein Interactions. *Trends Biochem. Sci.* **2008**, *33* (1), 2–8. https://doi.org/10.1016/j.tibs.2007.10.003.
(94) Miskei, M.; Antal, C.; Fuxreiter, M. FuzDB: Database of Fuzzy Complexes, a Tool to Develop Stochastic Structure-Function Relationships for Protein Complexes and Higher-Order Assemblies. *Nucleic Acids Res.* **2017**, *45* (Database issue), D228–D235. https://doi.org/10.1093/nar/gkw1019.
(95) Dunker, A. K.; Brown, C. J.; Lawson, J. D.; Iakoucheva, L. M.; Obradović, Z. Intrinsic Disorder and Protein Function. *Biochemistry* **2002**, *41* (21), 6573–6582. https://doi.org/10.1021/bi012159+.
(96) Tskhovrebova, L.; Trinick, J. Titin: Properties and Family Relationships. *Nat. Rev. Mol. Cell Biol.* **2003**, *4* (9), 679–689. https://doi.org/10.1038/nrm1198.
(97) Laptenko, O.; Tong, D. R.; Manfredi, J.; Prives, C. The Tail That Wags the Dog: How the Disordered C-Terminal Domain Controls the Transcriptional Activities of the P53 Tumor-Suppressor Protein. *Trends Biochem. Sci.* **2016**, *41* (12), 1022–1034. https://doi.org/10.1016/j.tibs.2016.08.011.

(98) Lassalle, M. W.; Kondou, S. Uncovering the Role of the Flexible C-Terminal Tail: A Model Study with Strep-Tagged GFP. *Biochim. Open* **2016**, *2*, 1–8. https://doi.org/10.1016/j.biopen.2015.11.004.
(99) Cohan, M. C.; Eddelbuettel, A. M. P.; Levin, P. A.; Pappu, R. V. Dissecting the Functional Contributions of the Intrinsically Disordered C-Terminal Tail of Bacillus Subtilis FtsZ. *J. Mol. Biol.* **2020**, *432* (10), 3205–3221. https://doi.org/10.1016/j.jmb.2020.03.008.
(100) Tompa, P.; Kovacs, D. Intrinsically Disordered Chaperones in Plants and Animals. *Biochem. Cell Biol. Biochim. Biol. Cell.* **2010**, *88* (2), 167–174. https://doi.org/10.1139/o09-163.
(101) Daniels, A. J.; Williams, R. J.; Wright, P. E. The Character of the Stored Molecules in Chromaffin Granules of the Adrenal Medulla: A Nuclear Magnetic Resonance Study. *Neuroscience* **1978**, *3* (6), 573–585. https://doi.org/10.1016/0306-4522(78)90022-2.
(102) Pang, X.; Zhou, H.-X. Mechanism and Rate Constants of the Cdc42 GTPase Binding with Intrinsically Disordered Effectors. *Proteins* **2016**, *84* (5), 674–685. https://doi.org/10.1002/prot.25018.
(103) Trzepacz, C.; Lowy, A. M.; Kordich, J. J.; Groden, J. Phosphorylation of the Tumor Suppressor Adenomatous Polyposis Coli (APC) by the Cyclin-Dependent Kinase P34. *J. Biol. Chem.* **1997**, *272* (35), 21681–21684. https://doi.org/10.1074/jbc.272.35.21681.
(104) *Fuzziness: Structural Disorder in Protein Complexes*; Fuxreiter, M., Tompa, P., Eds.; Advances in Experimental Medicine and Biology; Springer-Verlag: New York, 2012. https://doi.org/10.1007/978-1-4614-0659-4.
(105) Borgia, A.; Borgia, M. B.; Bugge, K.; Kissling, V. M.; Heidarsson, P. O.; Fernandes, C. B.; Sottini, A.; Soranno, A.; Buholzer, K. J.; Nettels, D.; Kragelund, B. B.; Best, R. B.; Schuler, B. Extreme Disorder in an Ultrahigh-Affinity Protein Complex. *Nature* **2018**, *555* (7694), 61–66. https://doi.org/10.1038/nature25762.
(106) Dunker, A. K.; Cortese, M. S.; Romero, P.; Iakoucheva, L. M.; Uversky, V. N. Flexible Nets. The Roles of Intrinsic Disorder in Protein Interaction Networks. *FEBS J.* **2005**, *272* (20), 5129–5148. https://doi.org/10.1111/j.1742-4658.2005.04948.x.
(107) Kim, P. M.; Sboner, A.; Xia, Y.; Gerstein, M. The Role of Disorder in Interaction Networks: A Structural Analysis. *Mol. Syst. Biol.* **2008**, *4*, 179. https://doi.org/10.1038/msb.2008.16.
(108) Wright, P. E.; Dyson, H. J. Intrinsically Disordered Proteins in Cellular Signaling and Regulation. *Nat. Rev. Mol. Cell Biol.* **2015**, *16* (1), 18–29. https://doi.org/10.1038/nrm3920.
(109) Haynes, C.; Oldfield, C. J.; Ji, F.; Klitgord, N.; Cusick, M. E.; Radivojac, P.; Uversky, V. N.; Vidal, M.; Iakoucheva, L. M. Intrinsic Disorder Is a Common Feature of Hub Proteins from Four Eukaryotic Interactomes. *PLoS Comput. Biol.* **2006**, *2* (8). https://doi.org/10.1371/journal.pcbi.0020100.
(110) Flock, T.; Weatheritt, R. J.; Latysheva, N. S.; Babu, M. M. Controlling Entropy to Tune the Functions of Intrinsically Disordered Regions. *Curr. Opin. Struct. Biol.* **2014**, *26*, 62–72. https://doi.org/10.1016/j.sbi.2014.05.007.
(111) Mukherjee, S. P.; Behar, M.; Birnbaum, H. A.; Hoffmann, A.; Wright, P. E.; Ghosh, G. Analysis of the RelA:CBP/P300 Interaction Reveals Its Involvement in NF-KB-Driven Transcription. *PLOS Biol.* **2013**, *11* (9), e1001647. https://doi.org/10.1371/journal.pbio.1001647.
(112) Shi, J.; Shen, Q.; Cho, J.-H.; Hwang, W. Entropy Hotspots for the Binding of Intrinsically Disordered Ligands to a Receptor Domain. *Biophys. J.* **2020**, *118* (10), 2502–2512. https://doi.org/10.1016/j.bpj.2020.03.026.

(113) Shoemaker, B. A.; Portman, J. J.; Wolynes, P. G. Speeding Molecular Recognition by Using the Folding Funnel: The Fly-Casting Mechanism. *Proc. Natl. Acad. Sci. U. S. A.* **2000**, *97* (16), 8868–8873.
(114) Zhou, H.-X. Intrinsic Disorder: Signaling via Highly Specific but Short-Lived Association. *Trends Biochem. Sci.* **2012**, *37* (2), 43–48. https://doi.org/10.1016/j.tibs.2011.11.002.
(115) Iakoucheva, L. M.; Radivojac, P.; Brown, C. J.; O'Connor, T. R.; Sikes, J. G.; Obradovic, Z.; Dunker, A. K. The Importance of Intrinsic Disorder for Protein Phosphorylation. *Nucleic Acids Res.* **2004**, *32* (3), 1037–1049. https://doi.org/10.1093/nar/gkh253.
(116) Tompa, P.; Davey, N. E.; Gibson, T. J.; Babu, M. M. A Million Peptide Motifs for the Molecular Biologist. *Mol. Cell* **2014**, *55* (2), 161–169. https://doi.org/10.1016/j.molcel.2014.05.032.
(117) Wang, Y.; Azuma, Y.; Moore, D.; Osheroff, N.; Neufeld, K. L. Interaction between Tumor Suppressor Adenomatous Polyposis Coli and Topoisomerase IIα: Implication for the G2/M Transition. *Mol. Biol. Cell* **2008**, *19* (10), 4076–4085. https://doi.org/10.1091/mbc.E07-12-1296.
(118) Wang, Y.; Coffey, R. J.; Osheroff, N.; Neufeld, K. L. Topoisomerase IIα Binding Domains of Adenomatous Polyposis Coli Influence Cell Cycle Progression and Aneuploidy. *PLoS ONE* **2010**, *5* (4). https://doi.org/10.1371/journal.pone.0009994.
(119) Deweese, J. E.; Osheroff, M. A.; Osheroff, N. DNA Topology and Topoisomerases: Teaching a "Knotty" Subject. *Biochem. Mol. Biol. Educ. Bimon. Publ. Int. Union Biochem. Mol. Biol.* **2008**, *37* (1), 2–10. https://doi.org/10.1002/bmb.20244.
(120) Watson, J. D.; Crick, F. H. Genetical Implications of the Structure of Deoxyribonucleic Acid. *Nature* **1953**, *171* (4361), 964–967. https://doi.org/10.1038/171964b0.
(121) Kouzine, F.; Levens, D.; Baranello, L. DNA Topology and Transcription. *Nucleus* **2014**, *5* (3), 195–202. https://doi.org/10.4161/nucl.28909.
(122) Alberts, B.; Johnson, A.; Lewis, J.; Raff, M.; Roberts, K.; Walter, P. Chromosomal DNA and Its Packaging in the Chromatin Fiber. *Mol. Biol. Cell 4th Ed.* **2002**.
(123) Pommier, Y.; Sun, Y.; Huang, S. N.; Nitiss, J. L. Roles of Eukaryotic Topoisomerases in Transcription, Replication and Genomic Stability. *Nat. Rev. Mol. Cell Biol.* **2016**, *17* (11), 703–721. https://doi.org/10.1038/nrm.2016.111.
(124) Berger, J. M.; Fass, D.; Wang, J. C.; Harrison, S. C. Structural Similarities between Topoisomerases That Cleave One or Both DNA Strands. *Proc. Natl. Acad. Sci. U. S. A.* **1998**, *95* (14), 7876–7881.
(125) Chen, S.-F.; Huang, N.-L.; Lin, J.-H.; Wu, C.-C.; Wang, Y.-R.; Yu, Y.-J.; Gilson, M. K.; Chan, N.-L. Structural Insights into the Gating of DNA Passage by the Topoisomerase II DNA-Gate. *Nat. Commun.* **2018**, *9* (1), 3085. https://doi.org/10.1038/s41467-018-05406-y.
(126) Sengupta, T.; Mukherjee, M.; Mandal, C.; Das, A.; Majumder, H. K. Functional Dissection of the C-Terminal Domain of Type II DNA Topoisomerase from the Kinetoplastid Hemoflagellate Leishmania Donovani. *Nucleic Acids Res.* **2003**, *31* (18), 5305–5316. https://doi.org/10.1093/nar/gkg727.
(127) Meczes, E. L.; Gilroy, K. L.; West, K. L.; Austin, C. A. The Impact of the Human DNA Topoisomerase II C-Terminal Domain on Activity. *PloS One* **2008**, *3* (3), e1754. https://doi.org/10.1371/journal.pone.0001754.

(128) Dickey, J. S.; Osheroff, N. Impact of the C-Terminal Domain of Topoisomerase IIalpha on the DNA Cleavage Activity of the Human Enzyme. *Biochemistry* **2005**, *44* (34), 11546–11554. https://doi.org/10.1021/bi0508111.
(129) Kozuki, T.; Chikamori, K.; Surleac, M. D.; Micluta, M. A.; Petrescu, A. J.; Norris, E. J.; Elson, P.; Hoeltge, G. A.; Grabowski, D. R.; Porter, A. C. G.; Ganapathi, R. N.; Ganapathi, M. K. Roles of the C-Terminal Domains of Topoisomerase IIα and Topoisomerase IIβ in Regulation of the Decatenation Checkpoint. *Nucleic Acids Res.* **2017**, *45* (10), 5995–6010. https://doi.org/10.1093/nar/gkx325.
(130) Chen, S. H.; Chan, N.-L.; Hsieh, T. New Mechanistic and Functional Insights into DNA Topoisomerases. *Annu. Rev. Biochem.* **2013**, *82*, 139–170. https://doi.org/10.1146/annurev-biochem-061809-100002.
(131) Champoux, J. J. DNA Topoisomerases: Structure, Function, and Mechanism. *Annu. Rev. Biochem.* **2001**, *70*, 369–413. https://doi.org/10.1146/annurev.biochem.70.1.369.
(132) Nitiss, J. L. DNA Topoisomerase II and Its Growing Repertoire of Biological Functions. *Nat. Rev. Cancer* **2009**, *9* (5), 327–337. https://doi.org/10.1038/nrc2608.
(133) Chan, S. K.; Griffith, O. L.; Tai, I. T.; Jones, S. J. M. Meta-Analysis of Colorectal Cancer Gene Expression Profiling Studies Identifies Consistently Reported Candidate Biomarkers. *Cancer Epidemiol. Biomark. Prev. Publ. Am. Assoc. Cancer Res. Cosponsored Am. Soc. Prev. Oncol.* **2008**, *17* (3), 543–552. https://doi.org/10.1158/1055-9965.EPI-07-2615.
(134) Murphy, K. J.; Nielson, K. R.; Albertine, K. H. Defining a Molecularly Normal Colon. *J. Histochem. Cytochem. Off. J. Histochem. Soc.* **2001**, *49* (5), 667–668. https://doi.org/10.1177/002215540104900516.
(135) Shigematsu, H.; Ozaki, S.; Yasui, D.; Yamamoto, H.; Zaitsu, J.; Taniyama, D.; Saitou, A.; Kuraoka, K.; Hirata, T.; Taniyama, K. Overexpression of Topoisomerase II Alpha Protein Is a Factor for Poor Prognosis in Patients with Luminal B Breast Cancer. *Oncotarget* **2018**, *9* (42), 26701–26710. https://doi.org/10.18632/oncotarget.25468.
(136) St Pierre, J.; Wright, D. J.; Rowe, T. C.; Wright, S. J. DNA Topoisomerase II Is Essential for Preimplantation Mouse Development. *Mol. Reprod. Dev.* **2002**, *61* (3), 347–357. https://doi.org/10.1002/mrd.10015.
(137) Negri, C.; Bernardi, R.; Donzelli, M.; Scovassi, A. I. Induction of Apoptotic Cell Death by DNA Topoisomerase II Inhibitors. *Biochimie* **1995**, *77* (11), 893–899. https://doi.org/10.1016/0300-9084(95)90009-8.
(138) Akimitsu, N.; Adachi, N.; Hirai, H.; Hossain, M. S.; Hamamoto, H.; Kobayashi, M.; Aratani, Y.; Koyama, H.; Sekimizu, K. Enforced Cytokinesis without Complete Nuclear Division in Embryonic Cells Depleting the Activity of DNA Topoisomerase IIalpha. *Genes Cells Devoted Mol. Cell. Mech.* **2003**, *8* (4), 393–402. https://doi.org/10.1046/j.1365-2443.2003.00643.x.
(139) Nitiss, J. L. Targeting DNA Topoisomerase II in Cancer Chemotherapy. *Nat. Rev. Cancer* **2009**, *9* (5), 338–350. https://doi.org/10.1038/nrc2607.
(140) Liu, L. F. DNA Topoisomerase Poisons as Antitumor Drugs. *Annu. Rev. Biochem.* **1989**, *58*, 351–375. https://doi.org/10.1146/annurev.bi.58.070189.002031.
(141) Pommier, Y. Drugging Topoisomerases: Lessons and Challenges. *ACS Chem. Biol.* **2013**, *8* (1), 82–95. https://doi.org/10.1021/cb300648v.
(142) Ezoe, S. Secondary Leukemia Associated with the Anti-Cancer Agent, Etoposide, a Topoisomerase II Inhibitor. *Int. J. Environ. Res. Public. Health* **2012**, *9* (7), 2444–2453. https://doi.org/10.3390/ijerph9072444.

(143) Long, B. H.; Wang, L.; Lorico, A.; Wang, R. C.; Brattain, M. G.; Casazza, A. M. Mechanisms of Resistance to Etoposide and Teniposide in Acquired Resistant Human Colon and Lung Carcinoma Cell Lines. *Cancer Res.* **1991**, *51* (19), 5275–5283.
(144) Jeremic, B.; Acimovic, L.; Mijatovic, L. Carboplatin and Etoposide in Advanced Colorectal Carcinoma. A Phase II Study. *Cancer* **1993**, *71* (9), 2706–2708. https://doi.org/10.1002/1097-0142(19930501)71:9<2706::aid-cncr2820710903>3.0.co;2-4.
(145) Green, R. A.; Kaplan, K. B. Chromosome Instability in Colorectal Tumor Cells Is Associated with Defects in Microtubule Plus-End Attachments Caused by a Dominant Mutation in APC. *J. Cell Biol.* **2003**, *163* (5), 949–961. https://doi.org/10.1083/jcb.200307070.
(146) Tighe, A.; Johnson, V. L.; Taylor, S. S. Truncating APC Mutations Have Dominant Effects on Proliferation, Spindle Checkpoint Control, Survival and Chromosome Stability. *J. Cell Sci.* **2004**, *117* (26), 6339–6353. https://doi.org/10.1242/jcs.01556.
(147) Huang, L.; Shitashige, M.; Satow, R.; Honda, K.; Ono, M.; Yun, J.; Tomida, A.; Tsuruo, T.; Hirohashi, S.; Yamada, T. Functional Interaction of DNA Topoisomerase IIα With the β-Catenin and T-Cell Factor-4 Complex. *Gastroenterology* **2007**, *133* (5), 1569–1578. https://doi.org/10.1053/j.gastro.2007.08.011.

CHAPTER 2

STRUCTURAL ANALYSIS OF THE 15-AA REPEAT REGION OF APC

Abstract

Most cancers of the colon and rectum present with truncated APC that retains the 15-aa repeat region. Understanding the structure and function of this region will be critical for untangling the mechanism of the β-catenin destruction complex. The data presented in this chapter firmly establish the 15-aa repeat region of APC as intrinsically disordered, containing only transient and heterogeneous secondary structural features. Our findings will help to shape the understanding of the architecture of the β-catenin destruction complex, and how that architecture may be altered upon APC truncation.

Introduction

Acquisition of mutations that truncate the tumor-suppressor Adenomatous polyposis coli (APC) has long been established as an early, if not initiating event in the development of sporadic and familial colorectal cancer [1,2]. Central to the tumor-suppressive function of APC is its key role in the so-called β-catenin destruction complex[3]. This complex, consisting of APC, Axin, and the kinases GSK3β and CK1, is responsible for regulating levels of the transcription co-factor β-catenin, and is inhibited by extracellular Wnt ligands. Binding of ligand to Wnt co-receptors inhibits the destruction complex, resulting in an accumulation of cytosolic β-catenin, which translocates to the nucleus and activates genes responsible for cellular proliferation, among others[3].

C-terminally truncated APC protein fragments are presumed to alter the β-catenin destruction complex architecture and function. The landscape of the mutations is depicted in Figure 2.1A, with a majority of mutations occurring C-terminal to the 15-aa repeat region. The clustered location of these mutations raises the possibility that the 15-aa repeats impart some selective growth advantage to cells that eventually become tumors. The precise consequences of

these truncations have proven difficult to resolve, in part due to the high degree of intrinsic structural disorder proposed for APC. Algorithms developed to estimate degrees of secondary structure and disorder have predicted >70% of APC to be in an extended, disordered conformation[4]. Intrinsically disordered proteins (IDPs) or intrinsically disordered regions (IDRs) of proteins are gaining increasing attention for their importance in signaling cascades, scaffolding, and other molecular functions[5,6].

Proteins that contain few elements of secondary structure are more extended, which has led to development of the proposed 'fly-casting' mechanism. This mechanism suggests that disorder increases the capture radius for specific interactions and speeds molecular recognition[7]. In the context of the β-catenin destruction complex, this 'fly-casting' ability of APC would function to rapidly sequester cytosolic β-catenin and increase its local concentration within the destruction complex. Disorder of bound proteins could also increase access to post-translational modification enzymes, and speed dissociation.[8] Very few structural biology tools have been used to evaluate the C-terminal ~2000 amino acids of APC, due primarily to the large extent of predicted intrinsic disorder. To our knowledge, the only structural information available for the 15-aa repeat region is a crystal structure solved by Weis *et al.*[9] of β-catenin bound with a 15-mer peptide representing the first of four 15-aa repeats, repeat "A". Of the APC 15-aa repeats, repeats B, C, and D are separated by 4 and 2 residues, respectively, whereas repeat A is separated from repeat B by 101 residues. Figure 2.1C shows the alignment of the 15-aa repeats, indicating completely conserved residues as well as charge conserved residues. Figure 2.1D shows the full linear layout of the APC15R-BCD construct, indicating where the 15-aa repeats lie in proximity to one another, and showing where the linker region and His tag are separated from the APC coding sequence.

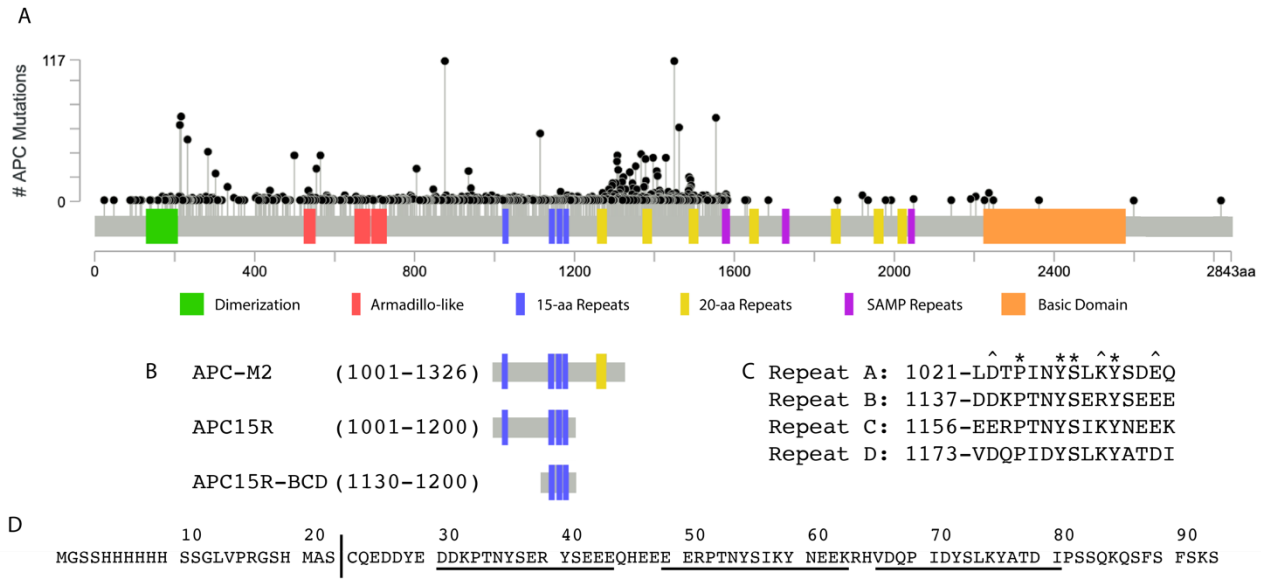

FIGURE 2.1. Linear representation of full-length APC protein and regions used in this study. A) Schematic of the APC protein. Black lollipops indicate location and number of truncating *APC* mutations in colorectal tumors of 8 compiled studies of 3,504 colorectal tumors[10,11]. B) Proteins used in this study, with amino acids of APC indicated. C) Primary sequence alignment of the 15-aa repeats. Asterisks denote conserved residues, carrots denote charge-conserved residues. D) Primary sequence of APC15R-BCD. 15-aa repeats B-D are underlined. Vertical line indicates beginning of *APC* sequence. Residues to the left of vertical line contain 6X-His tag and linker sequence.

I made many attempts to crystallize fragments of APC encompassing the 15-aa repeat region, but all were unsuccessful. Therefore, we turned to solution NMR to study the structural features and characteristics of the 15-aa repeat region of APC. Numerous NMR techniques have been developed in recent years to study proteins that sample multiple conformations across different timescales[12]. Residue-level information about local structure and backbone chain dynamics can also be obtained by observing protein in the solution state.

For this study, we generated APC peptides to model the 15-aa repeat region (APC15R), and the tightly clustered repeats B-D (APC15R-BCD) absent repeat A and the linker region (Figure 2.1B). Here, we show that the 15-aa repeat region of APC largely lacks classical secondary structural features such as α-helices and β-strands, though it can be induced to form a helix as measured by circular dichroism. We have completed the NMR backbone assignment of APC15R-BCD, performed an NMR solution characterization of APC15R-BCD, and predicted residues and/or regions that may have contributions to transient secondary structural features.

Results

Expression and purification of human APC fragments

For this study, three constructs of APC were generated. The first construct spanned residues 1000 – 1326, encompassing all of the 15-aa repeats as well as the first of the 20-aa repeats, and is herein referred to as APC-M2. The second construct spanned residues 1000 – 1200 and encompassed all of the 15-aa repeats but none of the 20-aa repeats, and is herein referred to as APC15R. The third construct spanned residues 1106 – 1200 and encompassed only the second (B), third (C), and fourth (D) repeats of the 15-aa repeat region, herein referred to as APC15R-BCD (see figure 2.1) Each protein construct was screened for optimal expression conditions

from BL21 (DE3) *E. coli* cells, and for optimal buffer stability. Each protein was subject to nickel chelating chromatography, followed by size exclusion chromatography, achieving >95% purity as estimated by polyacrylamide gel electrophoresis.

NMR analysis of APC15R

For our initial structural analysis, we used NMR, an attractive method to study proteins that do not fold in a classic globular shape of sheets and helices. The heteronuclear single quantum coherence (HSQC) spectrum of APC15R recorded at 25°C revealed a narrow dispersion of peak signals from 7.5 – 8.5 ppm (Figure 2.2A). This narrow dispersion is typical of proteins that are classified as IDPs, and reveals that APC15R is extended and not well folded. Acquisition parameters were optimized for the spectral width and number of scans to limit acquisition time to approximately 1 hour, and the experiment was repeated approximately 24 and 48 hours after the first sample was analyzed. Between the 2nd and 3rd experiments, the sample temperature was lowered to 5° C for approximately 2 hours, then raised to 45° C for approximately 8 hours before resetting to room temperature. Figure 2.2B shows an overlay of the ^{1}H-^{15}N transverse relaxation-optimized spectroscopy (TROSY) NMR spectra recorded at t = 24 and 48 hrs (in blue and red, respectively), with Figure 2.2C and 2.2D showing representative spectrum recorded during the temperature alterations. Taking into account differences in the signal-to-noise resulting from different numbers of scans, the TROSY spectrum is identical at all three 25° C time points. This observation implies that the protein is stable over the time frame of several days and any temperature-induced changes are reversible. Table 2.1 indicates a summary of the observable

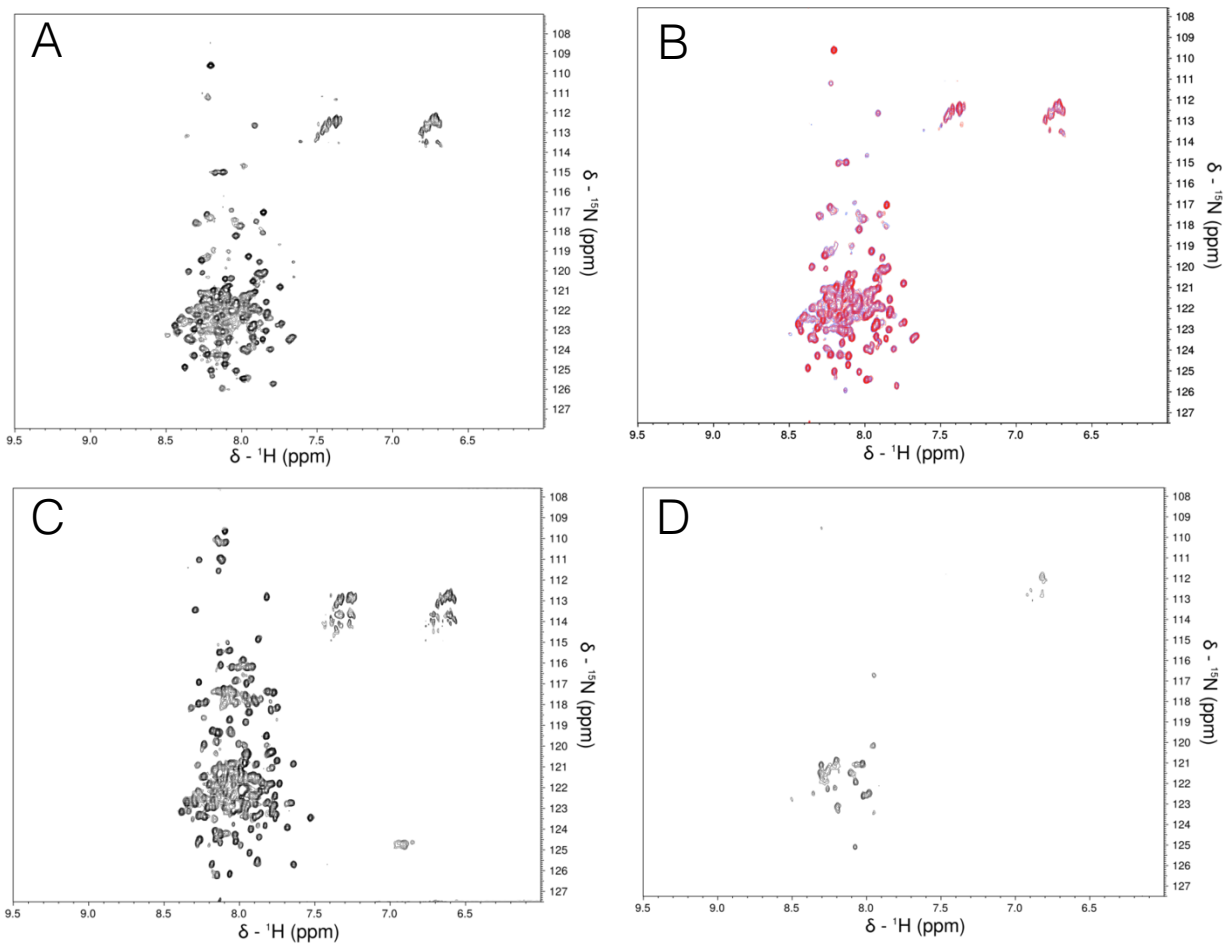

Figure 2.2 ^{1}H-^{15}N TROSY NMR spectrum of ^{15}N-APC15R A) Spectrum of ^{15}N-APC15R acquired immediately after sample buffer exchange. B) Overlay of the spectrum of ^{15}N-APC15R 24 hours (blue) and 48 hours (red) after delivery, and after temperature cycling. C) TROSY NMR spectrum of ^{15}N-APC15R recorded at 5°C. D) TROSY NMR spectrum of ^{15}N-APC15R recorded at 45°C.

Number of peaks[1] in 2D ^{1}H-^{15}N TROSY of ^{15}N-APC15R		
Temperature	Number of Peaks	Fraction of expected peaks[2]
25°C (~24 hrs after delivery)	119	0.56
5°C	170	0.80
45°C	27	0.13
25°C (~48 hrs after delivery)	120	0.57
1 measured using the nmrDraw peak detection algorith with manual subtraction of suspected side chain peaks 2 number of residues minus one (to account for the N-terminus) and minus the number of proline residues		

Table 2.1 Fraction of Detectable Peaks at Various Temperatures Summary of the number of backbone cross peaks in the ^{1}H-^{15}N TROSY NMR spectra of APC15R at each temperature measured. This number was measured using the nmrDraw peak detection algorithm with manual subtraction of suspected side chain (N and Q) peaks. The number of cross peaks expected in the ^{1}H-^{15}N TROSY NMR spectrum of a globular, folded protein equals the number of residues minus one (to account for the N-terminus) and minus the number of proline residues.

peaks at each time point and temperature recorded. The sample at 5° C revealed 80% of expected peaks, while only 13% of expected peaks were visible when the sample was heated to 45° C.

NMR analysis and backbone assignment of APC15R-BCD

One of our goals for this project was to identify key residues important for the interaction of APC with binding partner β-catenin. While basic HSQC data is useful, assigning the backbone resonances of each specific residue is critical to performing more sophisticated and detailed NMR experiments. After analyzing APC15R, it was determined that the peak overlap was too significant to perform triple resonance assignment. We therefore expressed and purified ^{15}N-labeled APC15R-BCD. Not only was this fragment smaller in size and thus more suitable for resonance assignment, but it also allowed us to compare observations of a polypeptide containing all four 15-aa repeats (APC15R), with a construct that contains only three clustered repeats (Figure 2.1B). Figure 2.4 shows overlay of the ^{1}H-^{15}N HSQC spectra of APC15R (red) and APC15R-BCD (blue). 71 of the backbone amide peaks (93.4%) from the APC15R-BCD spectrum matched peaks from the APC15R spectrum and 5 of the backbone amide peaks showed small chemical shift changes, which are deemed insignificant. Nearly all of the peaks in the fingerprint spectrum of BCD fragment overlap with peaks in the larger APC15R construct, indicating that truncating the A repeat and linker region does not impact the ^{1}H and ^{15}N chemical shifts of the smaller BCD construct. We envision that the APC15R protein adopts an extended conformation that does not resemble a globular protein with standard α-helix or β-sheet secondary structure elements. Segments of this protein that are expressed and purified still maintain a conformation identical to that of the complete region *in vitro*.

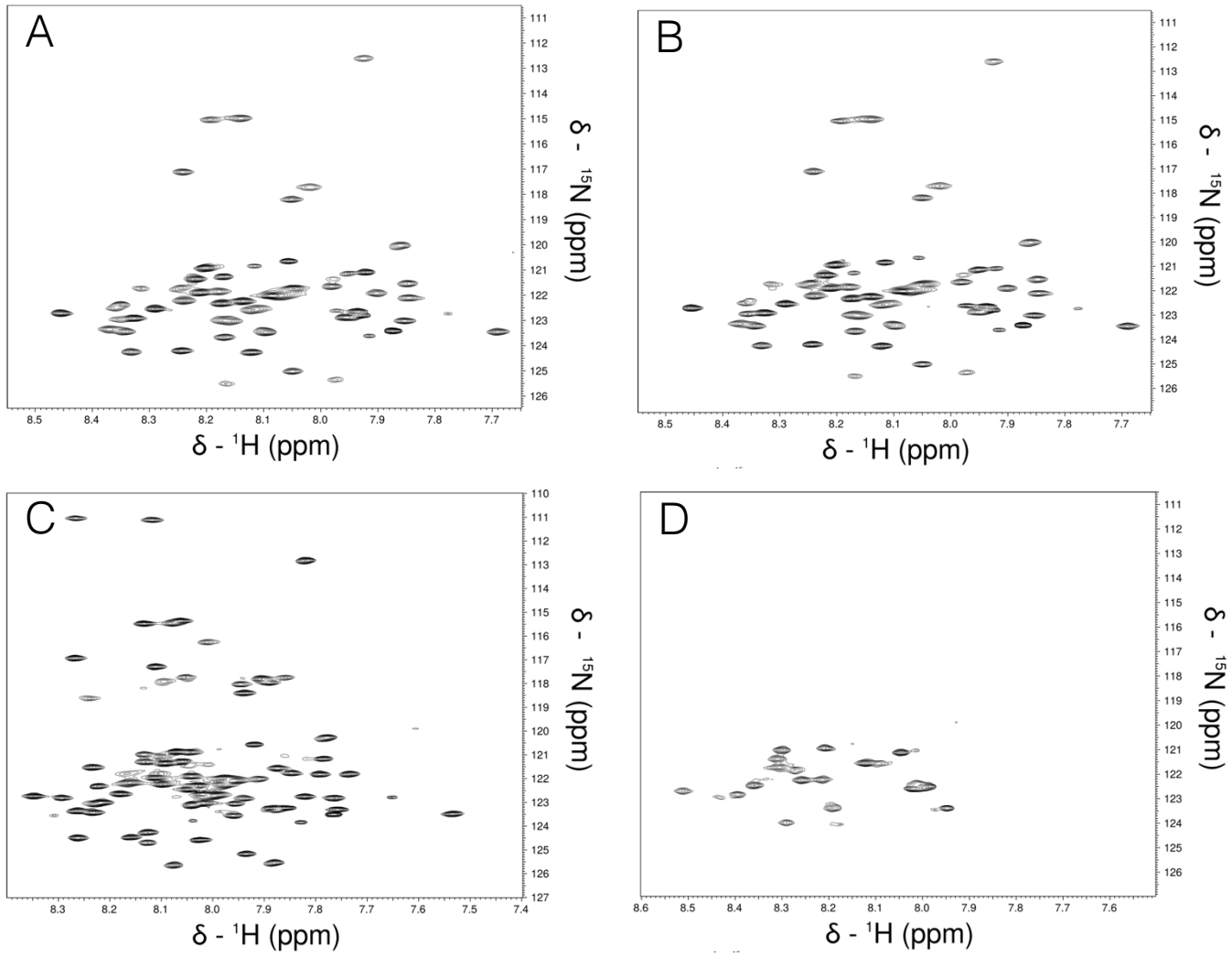

Figure 2.3 ^{1}H-^{15}N TROSY NMR spectrum of ^{15}N-APC15R-BCD A) 2D ^{1}H-^{15}N TROSY spectrum of ^{15}N-APC15R-BCD acquired after sample buffer exchange. B) 2D ^{1}H-^{15}N TROSY NMR spectrum of ^{15}N-APC15R-BCD acquired 20 hours after first sample. C) 2D ^{1}H-^{15}N TROSY NMR spectrum of ^{15}N-APC15R-BCD recorded at 5°C. D) 2D ^{1}H-^{15}N TROSY NMR spectrum of ^{15}N-APC15R-BCD recorded at 45°C. Note: Sidechain residues omitted from these plots

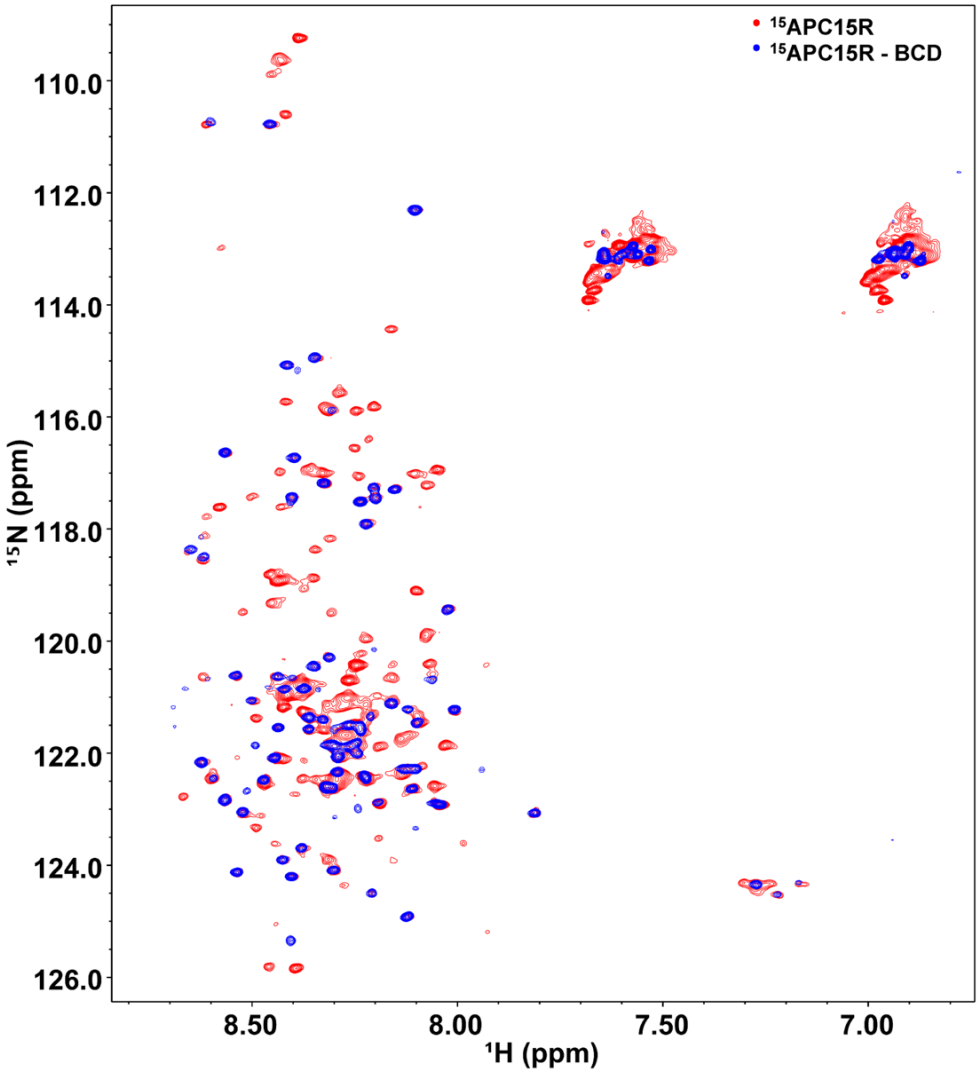

Figure 2.4 Comparison of APC15R and APC15R-BCD Overlay of ^{1}H-^{15}N HSQC spectra of ^{15}N-APC15R (red) and ^{15}N-APC15R-BCD (blue)

Temperature cycling and time course spectra were repeated as performed with APC15R. Figure 2.3A-D shows that no significant differences between the spectra before and after temperature cycling, nor after a full day in solution were observed, indicating that the protein is stable over several days and that any temperature-induced changes are reversible.

After it was determined that the APC15R-BCD construct was stable in solution over the timescale required for data acquisition, and that the spectra was of sufficient quality, the backbone resonances ^{1}HN, ^{15}N, ^{13}Cα, ^{13}Cβ, and ^{13}CO were assigned for APC15R-BCD. Figure 2.5 shows the 2D ^{1}H-^{15}N HSQC spectrum of APC15R-BCD annotated with the ^{1}HN, ^{15}N assignment of residues S12-S94. Overall, 88.7% of the non-proline backbone resonances were assigned. Residues of APC15R-BCD not assigned were M1, S3, and H6 through S11 of the hexa-histidine tag. Backbone ^{1}H, ^{15}N, and ^{13}C assignments have been deposited in the biological magnetic resonance data bank (BMRB) under accession number 27766.

Predictions of structure based on NMR backbone resonance assignments

With the backbone resonances of APC15R-BCD assigned, we sought to investigate whether the intrinsically disordered 15-aa repeats of APC possessed any pre-formed structural elements. Proteins mostly devoid of standard secondary structure elements such as helices and sheets can still possess preformed structural elements that play important roles in molecular recognition[13]. Using the Neighbor Corrected Structural Propensity Calculator (ncSPC)[14] and the backbone chemical shift data from NMR, we predicted the possible transient secondary structures in APC. Figure 4A shows the secondary structure propensity of APC15R-BCD calculated using ncSPC, with the Tamiola, Acar and Mulder (2010) random coil chemical shift library used for analysis. Positive values indicate α-helix structure, negative values indicate β-sheet structure, and the

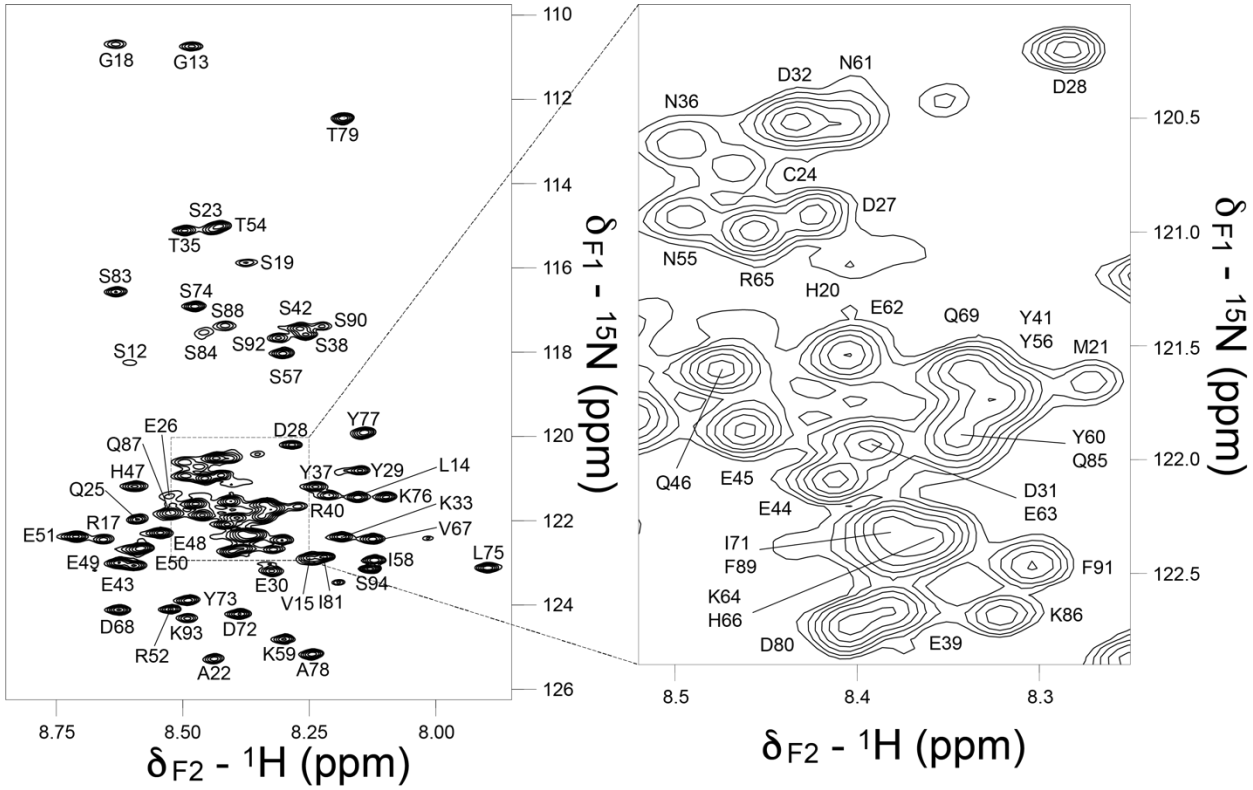

Figure 2.5 Backbone chemical shift assignment of APC15R-BCD. ^{1}H-15N HSQC spectrum of ^{15}N labeled APC15R-BCD in PBS buffer. The assignments of S12-S94 backbone (^{1}HN, ^{15}N) are annotated. Box to right details central region with crowded peaks in left panel.

dashed lines indicate the thresholds for random coil conformation. Our ncSPC analysis revealed that APC15R-BCD is an intrinsically disordered protein with some possible transient α-helicity at residues 16-18, 31-40, 50-59, 63-76, 81-86 and 90-93, and possible transient β-sheet structures at residues 26-30 (Figure 2.6A). We also utilized the web server CSI 3.0 to identify and predict regions of secondary structure. CSI 3.0 takes input from assigned backbone NMR chemical shifts (Cα, CO, Cβ, N, Hα, NH) and uses a multi-step algorithm combining four separate programs to predict 11 different types of secondary structure[15]. Figure 2.6B shows the secondary structure assignment for APC15R-BCD. CSI 3.0 calculated a short segment from residues 26-33 to be β-turn type I, with no predictions of α-helix or β-sheet. Therefore, it is likely any secondary structural features observable in the previous analyses are highly transient and heterogeneous in nature.

To further examine the global structural state of APC15R-BCD, backbone chemical shifts were entered into CS-ROSETTA. CS-ROSETTA has been effective in *de novo* structure prediction for small proteins (≤16 kDa)[16,17]. A total of 3,000 structures were generated for APC15R-BCD. The five best scoring structures were selected, and their averaged Cα root-mean-square-deviation (RMSD) against the lowest energy structure was 17.0 ± 1.1 Å. The RMSD value is used to estimate calculation precision, and hence convergence. A final RMSD of less than 1 Å indicates an acceptable convergence while anything less than 0.5 Å indicates a very well converged structure model. The very high RMSD value with poor convergence measured for the five best scoring structures of APC15R-BCD indicates that CS-ROSETTA is unable to make a prediction based on any known structures.

Finally, in an attempt to identify specific residues that may be involved in preformed structural elements, we predicted the ^{15}N chemical shifts of APC15R-BCD using the sequence-

corrected "random coil" ^{15}N chemical shift library developed by Braun et al.[18] This library was created to test the hypothesis that the greatest predictor of the ^{15}N chemical shift of a given residue is the identity of the preceding amino acid. Braun et al. demonstrated that for denatured proteins the predicted chemical shift agrees with experimental data within ± 2 ppm. Additional studies have shown that this strategy is effective at predicting unfolded peptides from those which are partially and fully folded.[19] Figure 2.6C plots the measured ^{15}N chemical shifts for APC15R-BCD in PBS versus the predicted ^{15}N chemical shifts based the random coil library (black dots). Points along the diagonal agree well ($R^2 = 0.87$) between the measured and predicted values, suggesting that these residues are not part of well-structured regions. On the other hand, residues whose predicted and measured values differ by more than one z-score suggest that these portions of the APC15R-BCD are contributing to intramolecular structural elements, i.e. hydrogen bonds or salt bridges. The predicted ordered residues include V15, R65, H66, I71, Y73, Y77, I81, and S94. We hypothesize that these residues are important in regulating the local order present in APC15R-BCD. As a control, this method was tested on ubiquitin (a model for a well-folded protein). The measured ^{15}N chemical shift values were taken from BMRB entry 5387. The plot of measured versus predicted ^{15}N chemical shifts for ubiquitin (Fig. 4D, pink dots) are highly scattered, indicating a stable, compact secondary structure. The absence of correlation ($R^2 = 0.54$) for ubiquitin demonstrates the ability of this prediction method to distinguish highly-structured proteins from those with less compact structural elements.

A

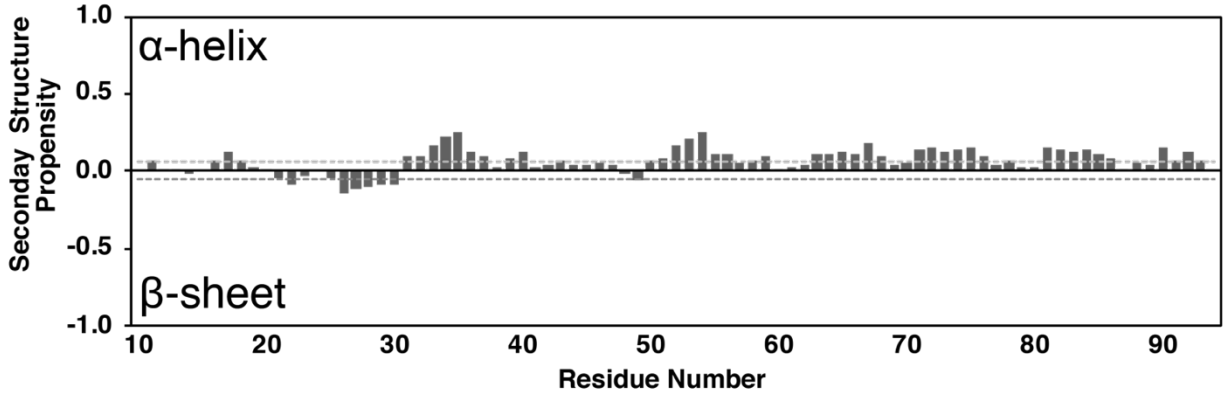

B

```
1              10         20         30         40           50
1   MGSSHHHHHHSSGLVPRGSHMASCQEDDYEDDKPTNYSERYSEEEQHEEE 50
1   CCCCCCCCCCCCCCCCCCCCCCCCCCTTTTTTTCCCCCCCCCCCCCCCCC 50


51             60         70         80         90     94
51  ERPTNYSIKYNEEKRHVDQPIDYSLKYATDIPSSQKQSFSFSKS 94
51  CCCCCCCCCCCCCCCCCCCCCCCCCCCCCCCCCCCCCCCCCCCCC 94
```

C

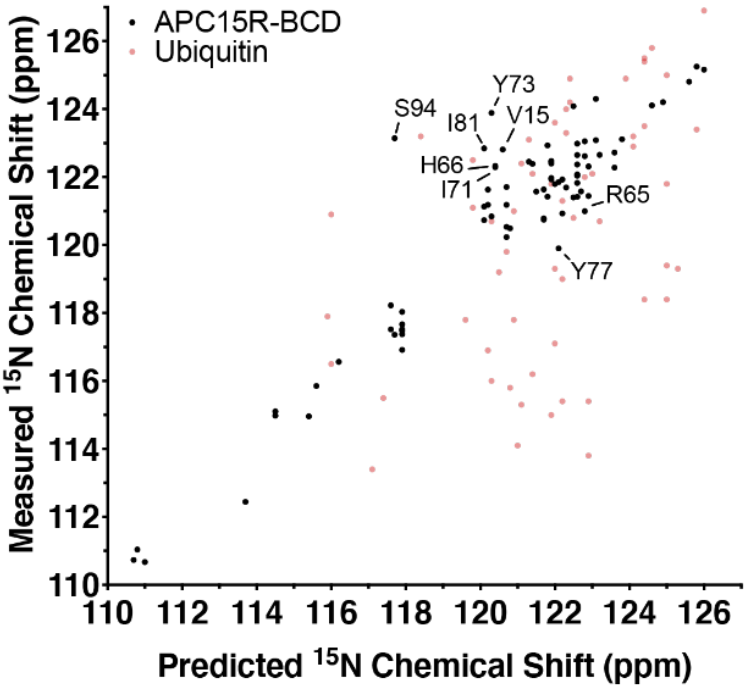

Figure 2.6 Structural Predictions for APC15R-BCD A) Secondary structure propensity of APC15R-BCD calculated using the Neighbor Corrected Structural Propensity Calculator (ncSPC). Positive values indicate α-helix structure and negative values indicate β-sheet structure. Dashed lines indicate the thresholds for random coil conformation. B) Secondary structural elements predicted for APC15R-BCD by the web server CSI 3.0 using backbone NMR chemical shifts (Cα, Cβ, CO, N, Hα, NH)[15]. Black C indicates coil, pink T indicates type I β-turn. C) Plot of measured ^{15}N chemical shifts of APC15R-BCD vs ^{15}N shifts predicted by a primary sequence-based algorithm developed by Braun et. al.[18]. Residues falling outside 1 z-score from mean regression are indicated.

Structural analysis of APC15R-BCD by circular dichroism

Servers that predict protein structure based on an analysis of primary structure alone indicate that the 15-aa repeat region of APC is primarily disordered, with some small regions of potential secondary features[4,20,21]. Proteins mostly devoid of classical secondary structure elements such as helices and sheets can still possess preformed structural elements that play important roles in molecular recognition[13]. To test whether any pre-formed structural elements could be discerned by conventional secondary structural analysis, we examined APC15R-BCD using circular dichroism (CD) spectroscopy. Initial CD spectra acquired at 25°C and pH 7.0 showed a large minimum at 200 nm, as well as a slight shoulder minimum at 222 nm for both constructs analyzed (Figure 2.7A). Using the program CDSSTR[22], we estimate a 4% α-helical and 18% β-sheet propensity of APC15R-BCD. These results suggest APC15R-BCD may possesses a small fraction of transient α-helix and/or β-sheet.

To determine if APC15R-BCD could be induced to form a helix, we performed a titration with 2,2,2-trifluoroethanol (TFE). Experimental evidence has suggested that titration with TFE is an effective method to identify regions of proteins that undergo helical transitions upon binding to a protein partner.[23] Titration with TFE resulted in a coil-helix transition, as is apparent by the gradual loss of the 200 nm minimum with concomitant appearance of minimums at 208 nm and 222 nm by 20% TFE addition (Figure 2.7B). We used CDSSTR to quantify the spectra and estimate the fraction of α-helix formed upon addition of TFE. Figure 2.7C, which plots the fraction of α-helix as calculated by the CDSSTR program versus percent TFE, shows an inflection point at around ~30% TFE addition. This result demonstrates that APC15R-BCD is inclined to form α-helical or helix-like structure under conditions favorable to helix formation.

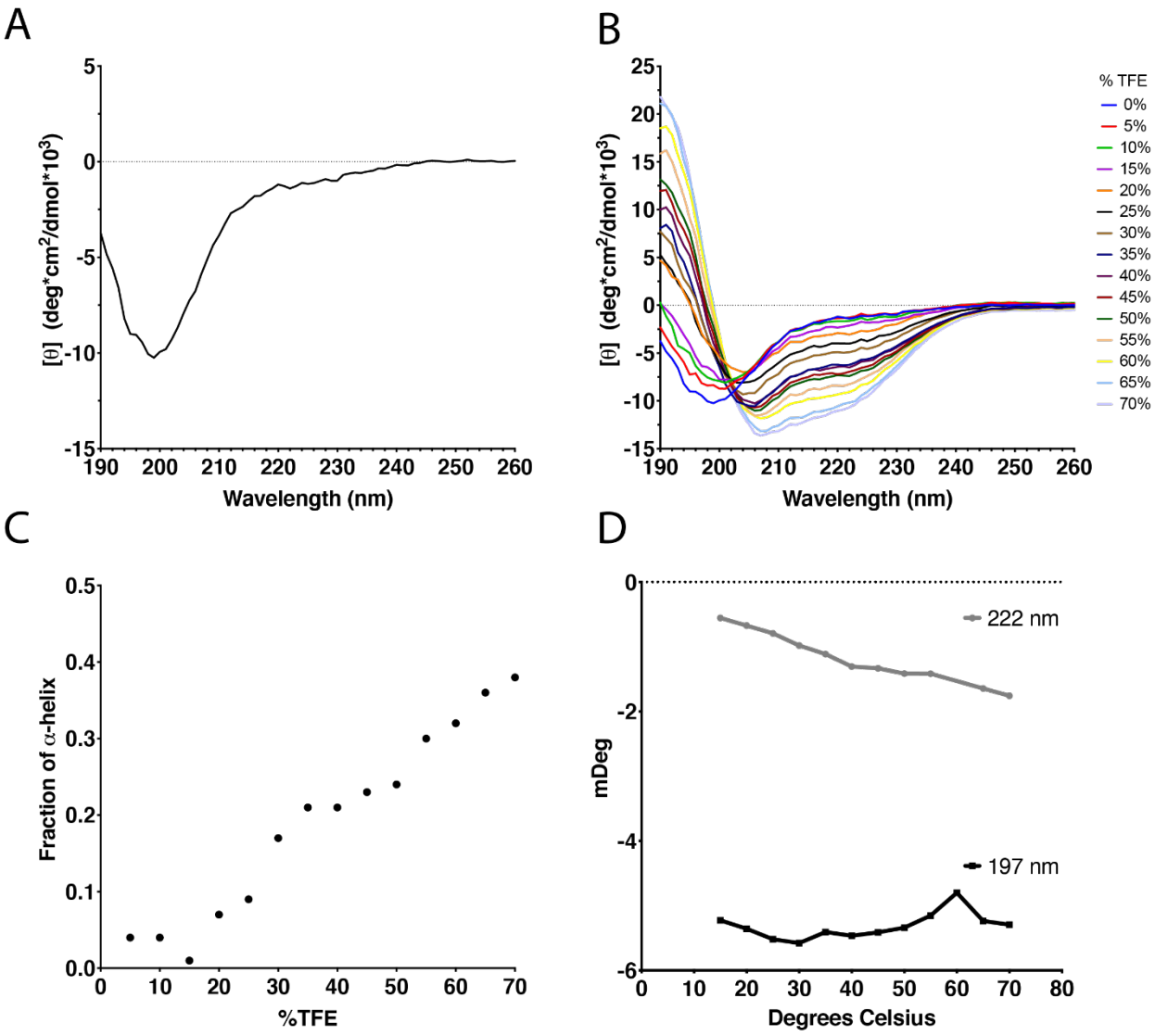

Figure 2.7. Structural analysis of APC15R-BCD by Circular Dichroism A) CD Spectra of APC15R-BCD. B) TFE titration of APC15R-BCD. C) Plot of estimated α-helical content vs %TFE for APC15R-BCD. D) mDeg of APC15R-BCD at 222 nm (grey) and 197 nm (black) over an increasing range of temperatures. Plots indicate no folding transitions occurred upon temperature increase.

Lastly, a melting curve of APC15R-BCD was acquired to determine if any unfolding transitions could be detected. Figure 2.7D shows that there were no observable transitions or inflection points at wavelengths 222 nm and 197 nm.

The central binding region of APC is susceptible to rapid proteolysis

In an effort to identify regions of APC that possess greater stability, or regions that are protected from exposure to proteases, we incubated our APC fragments with a mixture of proteases including chymotrypsin, trypsin, elastase, papain, subtilisin and endoproteinase Glu-C. This method has been successfully used to identify the most stable domains of a protein that can be the target of further structural studies[24]. Figure 2.8 shows that, upon incubation with proteases, all fragments of APC were fully degraded, even at very low concentrations. As a control, the well folded serum albumin protein BSA showed no degradation, even at the highest concentration of protease used. Minde and colleagues previously showed that a more C-terminal region of APC that encompasses the 20-aa repeats was completely susceptible to proteolysis[20]. Therefore, as a positive control, a region of APC spanning residues 1211 – 2075 (herein referred to as APC-M3) was expressed and purified, and analyzed along with the other constructs. Our data is consistent with the results from Minde et al., showing complete proteolytic degradation of APC-M3. These data indicate that the central region of APC is extended, and susceptible to rapid protease digestion. These findings raise interesting questions about how APC is protected from this rapid digestion in the cell.

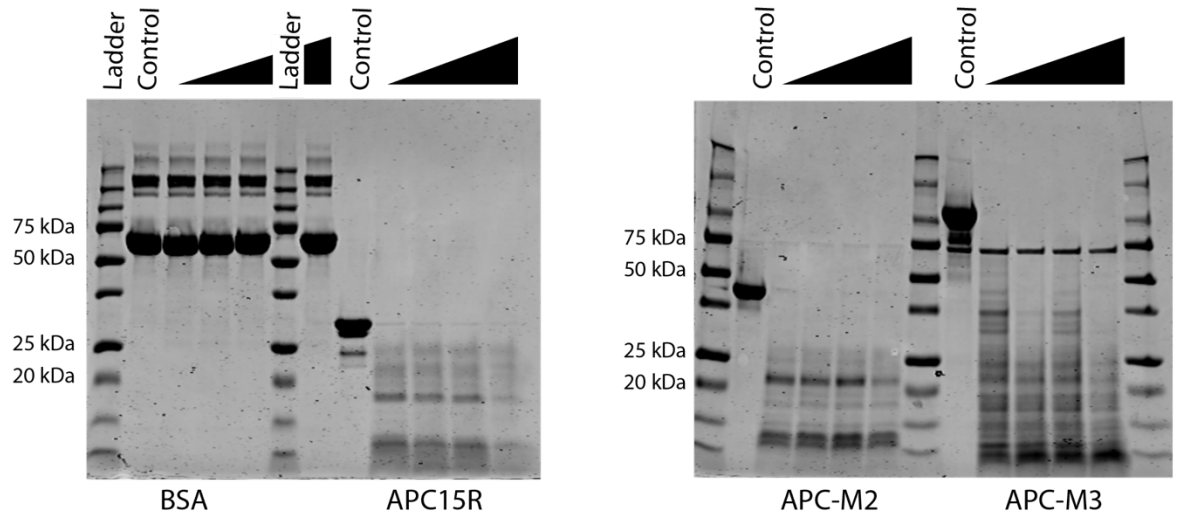

Figure 2.8. Limited Proteolytic Digestion of APC Protein samples were diluted to 10 mg/mL and incubated with increasing concentrations of a solution of proteases. No degradation observed for the well folded serum albumin BSA. For all APC constructs, complete degradation was observed across all concentrations screened, resulting in lower molecular weight banding patterns.

Discussion

Missense *APC* mutations are common in colorectal tumors, however the impact missense mutations have independent of truncating mutations has not been investigated thoroughly[4]. It has been proposed that the extensive intrinsic disorder present throughout the central binding repeat region of APC and high degree of binding redundancy may be a mechanism that guards against missense mutations[25]. It has also been proposed that the β-catenin destruction complex functions as a stochastic machine, driven by the random chemical interactions of kinases, substrates, and other proteins[26]. This model is centered on the high degree of intrinsic disorder within individual components of the β-catenin destruction complex and contends that the binding redundancy and flexibility function to colocalize and greatly increase the rate of associations. Our findings that APC is extended fit into this stochastic machine model, as fewer elements of secondary structure would result in a greater likelihood of collisions.

Previous computational predictions suggested that the 15-aa repeat region is intrinsically disordered.[4] Our CD and NMR analyses are in line with those predictions, and provide evidence of only limited or transient traditional secondary structure such as helices and sheets. The chemical shift overlap of APC15R and APC15R-BCD indicates that Repeat A (and the linker region) of APC15R does not influence the local structure of APC15R-BCD. Instead, we observe a striking similarity between the 15-aa repeat region and the central mutation cluster region of APC, both in ability to be induced to form helix in the presence of TFE, and in its extended nature[25]. Together, our data lead us to conclude that this region of APC contains significant flexibility, is able to form a helix under conditions favorable to helix formation, and is susceptible to rapid proteolytic degradation.

Materials and Methods

Protein Expression and Purification

Gene sequences for the APC constructs used in this study were cloned from a previously generated plasmid containing full-length human APC[27]. Cloned fragments were ligated into the pET28b (Novagen) expression vector, which contains an N-terminal 6X-His tag. Sequence-verified plasmids were transformed into BL21-CodonPlus-(DE3)-RIPL *E. coli* cells (NEB) for expression. Cells were grown in standard LB broth containing 50 μg/mL kanamycin at 37°C with shaking (225 rpm), and induced with 0.2 mM isopropyl-β-D-thiogalactopyranoside (IPTG) for protein expression when an OD of 0.4-0.6 was reached. Cells were allowed to express induced protein product for 3-4 hours at 37°C with shaking before harvested by centrifugation at 4,000 rpm, 15 min, 4°C. Cellular pellets were resuspended in a buffer containing 50 mM Tris pH 8.0, 50 mM NaCl, 50 mM imidazole, 10% glycerol, and HALT protease cocktail (Thermo). Cells were lysed by a French pressure cell (35,000 psi), and the insoluble cellular debris was removed by centrifugation at 16,000 x g for 45 min, 4°C. Supernatant was applied to a chelating sepharose fast-flow column (Amersham Biosciences) charged with nickel chloride and pre-equilibrated in resuspension buffer. Protein retained on the column was washed with a 3 column volumes (C.V.) salt gradient (50 mM potassium phosphate pH 8.0, 500 mM NaCl, 50 mM imidazole, 10% glycerol). Protein was eluted with an imidazole buffer gradient (50 mM Tris pH 8.0, 500 mM NaCl, 500 mM imidazole, 10% glycerol). Fractions containing recombinant protein were pooled and applied to a Superdex 200 size-exclusion column (Amersham Biosciences) pre-equilibrated with 25 mM Tris, pH 8.0, 100 mM NaCl, and 10% glycerol. Fractions containing recombinant protein were pooled and concentrated with Amicon Ultra centrifugal filters (Millipore).

^{15}N- and ^{13}C-labeled Protein Expression and Purification

For protein labeling, 4 liters of cells were grown in standard LB broth containing 50 μg/mL kanamycin at 37°C with shaking (225 rpm) to an OD of 0.7-0.8. Cells were harvested at room temperature (RT), washed once in M9 salt solution and spun down again. All cells were resuspended in 1 liter of minimal media containing the following: 100 mL 10X M9 salt solution (30 g/L KH_2PO_4, 66.5 g/L Na_2HPO_4, 5 g/L mM NaCl), 2 mL trace element solution (0.6 mg/mL $CaCl_2$, 0.07 mg/mL $ZnSO_4$, 0.5 mg/mL EDTA, 0.115 mg/mL $MnCl_2 \bullet 4H_2O$, 0.025 mg/mL $(NH_4)6Mo_7O_{24} \bullet 4H_2O$, 0.002 mg/mL H_3BO_3, 0.08 mg/mL $CoCl_2$, 0.6 mg/mL $FeCl_3$, 0.03 mg/mL $CuSO_4$), 4 mM $MgSO_4$, 0.2 mM $CaCl_2$, 6 mg/mL Thiamine, 10 mL 100X BME Vitamins (Sigma), 50 μg/mL kanamycin, 4 g D-glucose, and 1.5 g ^{15}N-NH_4Cl (Cambridge Isotope Laboratories). For ^{13}C-labeled protein, 4 g uniformly labeled ^{13}C-D-glucose (Cambridge Isotope Laboratories) was substituted for D-glucose. Cells were allowed to recover from spinning and washing for 1 hour, before induction with 1 mM IPTG. Cells were incubated at 37°C with shaking (225 rpm) for 7 hours. After 7 hours, cells were harvested and protein was purified as described above.

Circular Dichroism

CD spectra were acquired at 25°C using a JASCO J-815, under continual purge of N_2. Data were collected in triplicate at a scan speed of 20 nm/min, with a 1.37 nm slit width, a response of 4 seconds, and a pathlength of 0.1 cm. Samples were exchanged into 100 μM potassium phosphate, pH 7.0 using a PD-10 desalting column (GE Healthcare Life Sciences). Sample concentration was determined by Bradford assay. Final protein concentration was 15 μM. Measurements in millidegrees (mDeg) were converted to molar ellipticity (θ) by the formula

mDeg*M/(10*L*C), where M is the average molecular weight of the amino acids (mean residual weight), L is the path length of the cell in cm, and C is the concentration of the protein in g/L. Final protein concentration was 15 μM. To induce alpha-helix, 2,2,2-trifluoroethanol (TFE) (Sigma) was added to pre-mixed solutions of potassium phosphate buffer and protein to indicated final percentages. Solutions were incubated at RT for 10 minutes before spectra were acquired.

Limited Proteolysis

Manufacturer's protocol for the Proti-Ace Kit (Hamton Research, HR2-429) used for limited proteolysis experiments. BSA (Sigma) was measured by weight. All proteins exchanged into PBS buffer by overnight dialysis, with a 10,000 Da cutoff membrane. Protein samples were then diluted to 10 mg/mL by Bradford Assay in provided Proti-Ace dilution buffer. Protease mixture was diluted to final concentrations of 2.0, 3.0, 4.0, and 5.0 μg/mL. Reactions were incubated for 15 minutes at room temperature, before being halted by addition of SDS loading buffer. Samples were resolved by SDS-PAGE and stained by Coomassie Blue for visualization of bands.

Protein NMR Spectroscopy

All NMR data were collected on a Bruker AV 800 MHz NMR spectrometer equipped with a triple resonance cryoprobe. Data were processed using the NMRPipe[28] program and visualized and analyzed using NMRDraw and NMRViewJ[29] and CCPN analysis[30] on the NMRBox platform[31]. Triple resonance NMR data were collected using 0.5 mM ^{13}C and ^{15}N labeled APC15R-BCD in 50 mM PBS, pH7.4 and 0.5% (v/v) trimethylsilyl propanoic acid (TSP) for chemical shift referencing in a standard 5 mm NMR tube. Backbone resonance assignments were made by analyzing HNCACB, CBCACONH, and HNCO spectra. ^{1}H chemical shifts were

referenced to the internal TSP signal, whereas ^{15}N and ^{13}C chemical shifts were referenced indirectly using nuclei-specific gyromagnetic ratios.

References

(1) Kinzler, K. W.; Vogelstein, B. Lessons from Hereditary Colorectal Cancer. *Cell* **1996**, *87* (2), 159–170. https://doi.org/10.1016/S0092-8674(00)81333-1.
(2) Rowan, A. J.; Lamlum, H.; Ilyas, M.; Wheeler, J.; Straub, J.; Papadopoulou, A.; Bicknell, D.; Bodmer, W. F.; Tomlinson, I. P. M. APC Mutations in Sporadic Colorectal Tumors: A Mutational "Hotspot" and Interdependence of the "Two Hits." *Proc. Natl. Acad. Sci.* **2000**, *97* (7), 3352–3357. https://doi.org/10.1073/pnas.97.7.3352.
(3) Stamos, J. L.; Weis, W. I. The β-Catenin Destruction Complex. *Cold Spring Harb. Perspect. Biol.* **2013**, *5* (1). https://doi.org/10.1101/cshperspect.a007898.
(4) Minde, D. P.; Anvarian, Z.; Rüdiger, S. G.; Maurice, M. M. Messing up Disorder: How Do Missense Mutations in the Tumor Suppressor Protein APC Lead to Cancer? *Mol. Cancer* **2011**, *10* (1), 101. https://doi.org/10.1186/1476-4598-10-101.
(5) Uversky, V. N. A Decade and a Half of Protein Intrinsic Disorder: Biology Still Waits for Physics. *Protein Sci. Publ. Protein Soc.* **2013**, *22* (6), 693–724. https://doi.org/10.1002/pro.2261.
(6) Wright, P. E.; Dyson, H. J. Intrinsically Disordered Proteins in Cellular Signaling and Regulation. *Nat. Rev. Mol. Cell Biol.* **2015**, *16* (1), 18–29. https://doi.org/10.1038/nrm3920.
(7) Shoemaker, B. A.; Portman, J. J.; Wolynes, P. G. Speeding Molecular Recognition by Using the Folding Funnel: The Fly-Casting Mechanism. *Proc. Natl. Acad. Sci. U. S. A.* **2000**, *97* (16), 8868–8873.
(8) Borgia, A.; Borgia, M. B.; Bugge, K.; Kissling, V. M.; Heidarsson, P. O.; Fernandes, C. B.; Sottini, A.; Soranno, A.; Buholzer, K. J.; Nettels, D.; Kragelund, B. B.; Best, R. B.; Schuler, B. Extreme Disorder in an Ultrahigh-Affinity Protein Complex. *Nature* **2018**, *555* (7694), 61–66. https://doi.org/10.1038/nature25762.
(9) Spink, K. E.; Fridman, S. G.; Weis, W. I. Molecular Mechanisms of β-Catenin Recognition by Adenomatous Polyposis Coli Revealed by the Structure of an APC–β-Catenin Complex. *EMBO J.* **2001**, *20* (22), 6203–6212. https://doi.org/10.1093/emboj/20.22.6203.
(10) Gao, J.; Aksoy, B. A.; Dogrusoz, U.; Dresdner, G.; Gross, B.; Sumer, S. O.; Sun, Y.; Jacobsen, A.; Sinha, R.; Larsson, E.; Cerami, E.; Sander, C.; Schultz, N. Integrative Analysis of Complex Cancer Genomics and Clinical Profiles Using the CBioPortal. *Sci. Signal.* **2013**, *6* (269), pl1. https://doi.org/10.1126/scisignal.2004088.
(11) Cerami, E.; Gao, J.; Dogrusoz, U.; Gross, B. E.; Sumer, S. O.; Aksoy, B. A.; Jacobsen, A.; Byrne, C. J.; Heuer, M. L.; Larsson, E.; Antipin, Y.; Reva, B.; Goldberg, A. P.; Sander, C.; Schultz, N. The CBio Cancer Genomics Portal: An Open Platform for Exploring Multidimensional Cancer Genomics Data. *Cancer Discov.* **2012**, *2* (5), 401–404. https://doi.org/10.1158/2159-8290.CD-12-0095.
(12) Brutscher, B.; Felli, I. C.; Gil-Caballero, S.; Hošek, T.; Kümmerle, R.; Piai, A.; Pierattelli, R.; Sólyom, Z. NMR Methods for the Study of Instrinsically Disordered Proteins Structure, Dynamics, and Interactions: General Overview and Practical Guidelines. *Adv. Exp. Med. Biol.* **2015**, *870*, 49–122. https://doi.org/10.1007/978-3-319-20164-1_3.

(13) Fuxreiter, M.; Simon, I.; Friedrich, P.; Tompa, P. Preformed Structural Elements Feature in Partner Recognition by Intrinsically Unstructured Proteins. *J. Mol. Biol.* **2004**, *338* (5), 1015–1026. https://doi.org/10.1016/j.jmb.2004.03.017.
(14) Tamiola, K.; Mulder, F. A. A. Using NMR Chemical Shifts to Calculate the Propensity for Structural Order and Disorder in Proteins. *Biochem. Soc. Trans.* **2012**, *40* (5), 1014–1020. https://doi.org/10.1042/BST20120171.
(15) Hafsa, N. E.; Arndt, D.; Wishart, D. S. CSI 3.0: A Web Server for Identifying Secondary and Super-Secondary Structure in Proteins Using NMR Chemical Shifts. *Nucleic Acids Res.* **2015**, *43* (Web Server issue), W370–W377. https://doi.org/10.1093/nar/gkv494.
(16) Lange, O. F.; Rossi, P.; Sgourakis, N. G.; Song, Y.; Lee, H.-W.; Aramini, J. M.; Ertekin, A.; Xiao, R.; Acton, T. B.; Montelione, G. T.; Baker, D. Determination of Solution Structures of Proteins up to 40 KDa Using CS-Rosetta with Sparse NMR Data from Deuterated Samples. *Proc. Natl. Acad. Sci.* **2012**, *109* (27), 10873–10878. https://doi.org/10.1073/pnas.1203013109.
(17) Shen, Y.; Lange, O.; Delaglio, F.; Rossi, P.; Aramini, J. M.; Liu, G.; Eletsky, A.; Wu, Y.; Singarapu, K. K.; Lemak, A.; Ignatchenko, A.; Arrowsmith, C. H.; Szyperski, T.; Montelione, G. T.; Baker, D.; Bax, A. Consistent Blind Protein Structure Generation from NMR Chemical Shift Data. *Proc. Natl. Acad. Sci.* **2008**, *105* (12), 4685–4690. https://doi.org/10.1073/pnas.0800256105.
(18) Braun, D.; Wider, G.; Wuethrich, K. Sequence-Corrected 15N "Random Coil" Chemical Shifts. *J. Am. Chem. Soc.* **1994**, *116* (19), 8466–8469. https://doi.org/10.1021/ja00098a005.
(19) Tamiola, K.; Acar, B.; Mulder, F. A. A. Sequence-Specific Random Coil Chemical Shifts of Intrinsically Disordered Proteins. *J. Am. Chem. Soc.* **2010**, *132* (51), 18000–18003. https://doi.org/10.1021/ja105656t.
(20) Minde, D. P.; Radli, M.; Forneris, F.; Maurice, M. M.; Rüdiger, S. G. D. Large Extent of Disorder in Adenomatous Polyposis Coli Offers a Strategy to Guard Wnt Signalling against Point Mutations. *PLoS ONE* **2013**, *8* (10). https://doi.org/10.1371/journal.pone.0077257.
(21) Liu, J.; Xing, Y.; Hinds, T. R.; Zheng, J.; Xu, W. The Third 20 Amino Acid Repeat Is the Tightest Binding Site of APC for Beta-Catenin. *J. Mol. Biol.* **2006**, *360* (1), 133–144. https://doi.org/10.1016/j.jmb.2006.04.064.
(22) Johnson, W. C. Analyzing Protein Circular Dichroism Spectra for Accurate Secondary Structures. *Proteins Struct. Funct. Bioinforma.* **1999**, *35* (3), 307–312. https://doi.org/10.1002/(SICI)1097-0134(19990515)35:3<307::AID-PROT4>3.0.CO;2-3.
(23) Glover, K.; Mei, Y.; Sinha, S. C. Identifying Intrinsically Disordered Protein Regions Likely to Undergo Binding-Induced Helical Transitions. *Biochim. Biophys. Acta* **2016**, *1864* (10), 1455–1463. https://doi.org/10.1016/j.bbapap.2016.05.005.
(24) Wernimont, A.; Edwards, A. In Situ Proteolysis to Generate Crystals for Structure Determination: An Update. *PLOS ONE* **2009**, *4* (4), e5094. https://doi.org/10.1371/journal.pone.0005094.
(25) Minde, D. P.; Radli, M.; Forneris, F.; Maurice, M. M.; Rüdiger, S. G. D. Large Extent of Disorder in Adenomatous Polyposis Coli Offers a Strategy to Guard Wnt Signalling against Point Mutations. *PLOS ONE* **2013**, *8* (10), e77257. https://doi.org/10.1371/journal.pone.0077257.
(26) Xue, B.; Romero, P. R.; Noutsou, M.; Maurice, M. M.; Rüdiger, S. G. D.; William, A. M.; Mizianty, M. J.; Kurgan, L.; Uversky, V. N.; Dunker, A. K. Stochastic Machines as a Colocalization Mechanism for Scaffold Protein Function. *FEBS Lett.* **2013**, *587* (11), 1587–1591. https://doi.org/10.1016/j.febslet.2013.04.006.

(27) Neufeld, K. L.; Nix, D. A.; Bogerd, H.; Kang, Y.; Beckerle, M. C.; Cullen, B. R.; White, R. L. Adenomatous Polyposis Coli Protein Contains Two Nuclear Export Signals and Shuttles between the Nucleus and Cytoplasm. *Proc. Natl. Acad. Sci.* **2000**, *97* (22), 12085–12090. https://doi.org/10.1073/pnas.220401797.
(28) Delaglio, F.; Grzesiek, S.; Vuister, G. W.; Zhu, G.; Pfeifer, J.; Bax, A. NMRPipe: A Multidimensional Spectral Processing System Based on UNIX Pipes. *J. Biomol. NMR* **1995**, *6* (3), 277–293.
(29) Johnson, B. A.; Blevins, R. A. NMR View: A Computer Program for the Visualization and Analysis of NMR Data. *J. Biomol. NMR* **1994**, *4* (5), 603–614. https://doi.org/10.1007/BF00404272.
(30) Vranken, W. F.; Boucher, W.; Stevens, T. J.; Fogh, R. H.; Pajon, A.; Llinas, M.; Ulrich, E. L.; Markley, J. L.; Ionides, J.; Laue, E. D. The CCPN Data Model for NMR Spectroscopy: Development of a Software Pipeline. *Proteins* **2005**, *59* (4), 687–696. https://doi.org/10.1002/prot.20449.
(31) Maciejewski, M. W.; Schuyler, A. D.; Gryk, M. R.; Moraru, I. I.; Romero, P. R.; Ulrich, E. L.; Eghbalnia, H. R.; Livny, M.; Delaglio, F.; Hoch, J. C. NMRbox: A Resource for Biomolecular NMR Computation. *Biophys. J.* **2017**, *112* (8), 1529–1534. https://doi.org/10.1016/j.bpj.2017.03.011.

CHAPTER 3

THE ASSOCIATION OF β-CATENIN AND THE 15-AA REPEAT REGION OF APC

Abstract

Oncogenic *APC* mutations typically result in a truncated protein product that is expressed in cells. This truncated APC often retains the 15-amino acid repeats, implicating this region in the initiation of cancer. The roles of this region within the β-catenin destruction complex are poorly understood, and mechanisms of binding are ill-defined. In this chapter, we investigate the backbone dynamics of the 15-aa repeat region of APC, as well as how those dynamics change once bound to β-catenin. We find that the 15-aa region of APC retains flexibility upon binding β-catenin and that APC does not have a single, observable "highest affinity" binding site for β-catenin. This flexibility potentially allows β-catenin to be more readily captured by APC and then remain accessible to other elements of the destruction complex for subsequent processing.

Introduction

Mutations that truncate APC most often occur in a central region aptly named the mutation cluster region[1]. The middle portion of APC includes a series of 15-amino acid (aa) repeats and 20-aa repeats. The 15- and 20-aa repeat regions can each bind β-catenin directly[2,3]. Phosphorylation of the 20-aa repeats, but not the 15-aa repeats, greatly increases binding affinity *in vitro*[2–4]. It is intriguing that, while the 20-aa repeats bind the same groove of β-catenin as the 15-aa repeats, modification by phosphorylation only regulates the 20-aa repeats. Retention of the APC 15-aa repeats in a majority of colon tumors has led to the proposed "just-right" signaling model[5]. In this model, APC mutations that retain some capacity to bind and regulate β-catenin provide a selective advantage over complete abolition of all binding sites[5]. Because the 15-aa repeat region of APC is retained in the majority of colon cancer-associated truncated APC proteins, this region is predicted to possess functions necessary for oncogenesis and thus, is an

important area to focus our attention. Sequence similarity of the 15-aa repeats (Figure 2.1C) raises the potential that each of the four repeats maintains the capacity to bind β-catenin. While the contribution of the 15-aa repeats in regulating cellular β-catenin levels[4] and the binding affinities of some individual repeats[2] have been investigated, the stoichiometry of β-catenin binding to the 15-aa repeat region as a whole, and how β-catenin specifically associates with APC have not been determined.

In chapter 2, we established that the 15-aa repeat region of APC is intrinsically disordered and extended. The presence of multiple binding motifs is a common observation with intrinsically disordered proteins (IDPs)[6], and is true also of APC. Some IDPs contain multiple binding repeats that, as a whole, only weakly interact with binding partners, with certain hotspots that contribute strongly to the binding affinity[7,8]. For this study, we used APC constructs described in the previous chapter along with recombinant human β-catenin to investigate biophysical characteristics of their interaction. We were unable to detect a specific binding site for β-catenin on APC, leading us to conclude that binding of β-catenin to APC is heterogenous in nature. We also reveal that APC retains a high proportion of disorder both before and after binding to β-catenin, an interaction which has been characterized as "fuzzy"[9]. These findings will help to shape our understanding of how the β-catenin complex is assembled, and how β-catenin is precisely regulated in the cell.

Results

Expression and purification of human β-catenin

Initially for this study, full-length (FL) human β-catenin was cloned, and screened for optimal expression conditions in BL21 (DE3) *E. coli* cells, and for optimal buffer stability. FL-β-catenin

was subject to nickel chelating chromatography, followed by size exclusion chromatography, achieving >95% purity as estimated by polyacrylamide gel electrophoresis.

FL-β-catenin was moderately stable in the Tris buffer, however upon exchange into PBS for NMR analysis and protein-protein interaction studies, FL-β-catenin rapidly precipitated out of solution. The armadillo repeats, which take their name from sequence homology to the *Drosophila* protein *armadillo,* are well folded and comprise most of the β-catenin protein. The N- and C-termini of β-catenin, however, contain high degrees of flexibility. Nearly all of the structures of β-catenin solved by X-ray crystallography remove the N- and C-terminal domains in order to obtain crystals[10–13]. The terminal domains of β-catenin are implicated in regulation, signal processing and transduction, and are targets of post-translational modification, however they have not been identified as binding sites for APC[11,14,15]. Therefore, primers were designed to remove the N-terminal 149 amino acids, as well as the C-terminal 116 amino acids. This left only the 12 core well-folded armadillo repeats of β-catenin. The construct of β-catenin encompassing residues 150-665 was used throughout this study, and is herein referred to as β-catenin (Figure 3.1). β-catenin protein was subjected to nickel chelating chromatography, followed by size exclusion chromatography, achieving >95% purity as estimated by polyacrylamide gel electrophoresis and Coomassie stain. While removal of the flexible N- and C-terminal domains improved stability, we still observed aggregation over time, especially when combined with our APC fragments. Screening for optimal buffer conditions revealed that a buffer composed of potassium phosphate, sodium citrate, and glycerol was suitable for both β-catenin and our APC constructs. For all association studies presented in this chapter, APC was exchanged into the phosphate/citrate buffer (see methods).

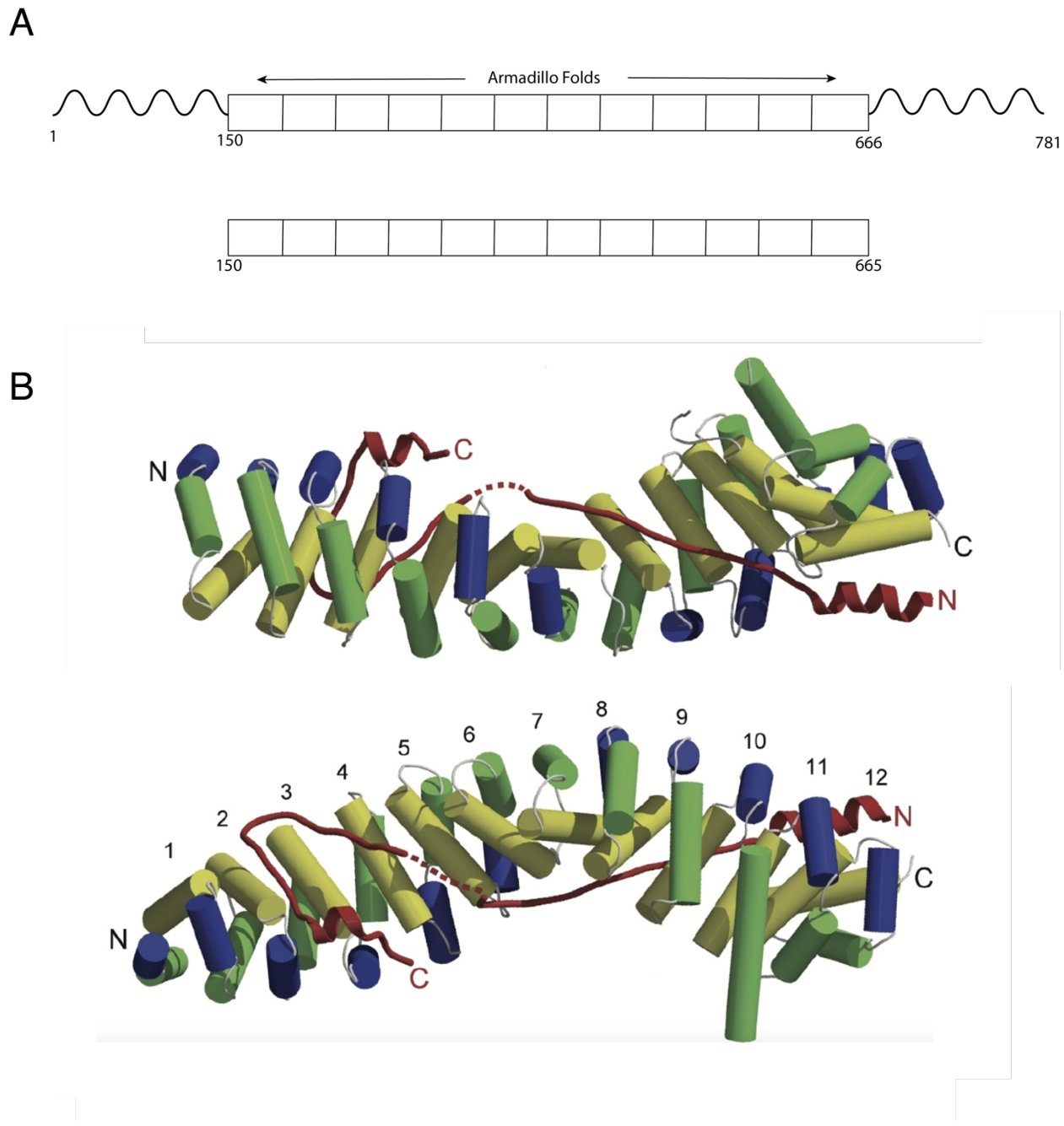

Figure 3.1 β-catenin Constructs and Structure A) Linear schematic of human β-catenin (top) and schematic of construct used in this study, with disordered termini not a part of the armadillo region removed (bottom). Relevant residues marking boundaries indicated. B) Crystal structure of β-catenin with a short fragment of the 20-aa repeats of APC (red) bound, reproduced with permission from Xing et al.[11].

The 15-aa repeat region of APC forms a complex with β-catenin in solution

Human APC contains four 15-aa repeats labeled A-D, as shown in Figure 2.1. Previous studies have suggested that individual repeats are each capable of binding to one β-catenin, and that repeat "A" has the highest affinity for β-catenin[2–4]. However, *in vitro* binding analyses have not been performed on the complete 15-aa repeat region. To further examine the stoichiometry, we incubated β-catenin with APC protein fragments that contained the 15-aa repeats in different contexts. Addition of dimethyl pimelimidate (DMP), which has a (9.2 Å) spacer arm, allowed chemical cross-linking of proteins in close proximity. Figure 3.2A shows efficient crosslinking of heavy and light chains of IgG which serves as a positive control. SDS-PAGE analysis comparing the migration of test proteins to that of molecular weight standards led to estimated molecular weights of APC15R-BCD, APC15R, and β-catenin of 15, 30 and 48 kDa, respectively (Figure 3.2B). These values match the expected molecular weight for these proteins. The migration does not change in the presence of DMP crosslinker. The failure of DMP to covalently trap homo-oligomers indicates that these proteins do not self-associate or aggregate at the concentrations tested. As negative controls, Figure 3.2C shows that no APC protein fragment nor β-catenin cross-link with lysozyme, nor was DMP able to cross-link lysozyme to itself. Lysozyme (pI 11.35) was chosen because it is positively charged at our experimental pH of 8.0, as is β-catenin (pI 8.71). Based on previous isothermal titration calorimetry data[2], we expected two β-catenin molecules to bind one APC15R-BCD. When incubated together at equal molar ratios, the primary APC15R-BCD / β-catenin protein band we observed migrated at a molecular weight that corresponded to a 1:1 interaction (Figure 3.2D). With β-catenin in 2-fold molar excess (1:2 ratio APC:β-catenin), a band appeared at a molecular weight that approximated binding of two β-catenins for each

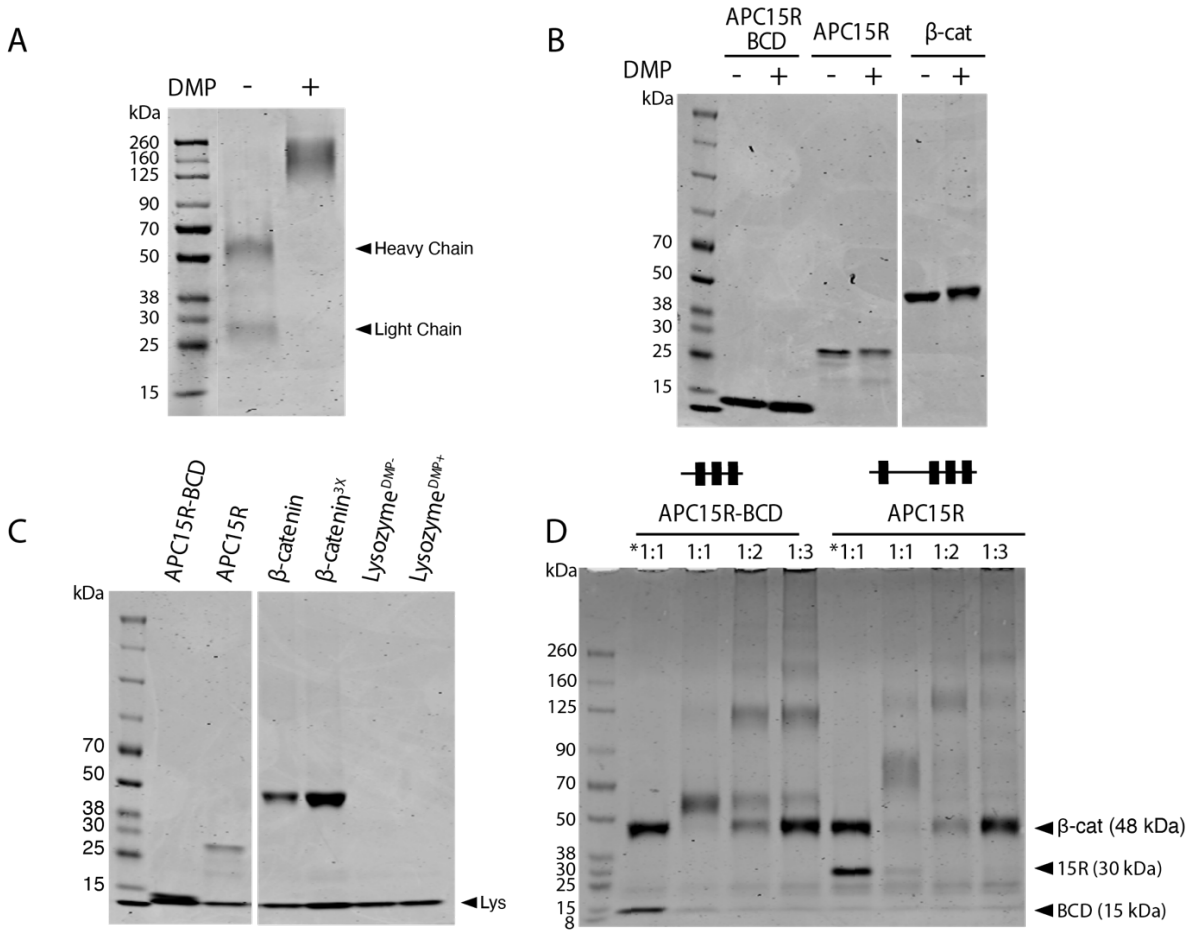

Figure 3.2 Chemical Crosslinking of the 15-aa repeat region of APC with β-catenin.

A-D) Products of *in vitro* reactions resolved by SDS-PAGE and visualized by Coomassie stain. A) IgG incubated with and without DMP. B) Constructs tested for self-association with DMP. C) Lysozyme negative control. All samples with DMP added, except where denoted. All concentrations 10 μM. 3X β-catenin = 30μM β-catenin with 10 μM Lysozyme to control for 1:3 molar ratio. D) All reactions included 10 μM APC protein fragment and 10 μM (1:1), 20 μM (1:2), or 30 μM (1:3) β-catenin (150-665). Reactions without DMP indicated with *. Apparent molecular weight of unbound proteins denoted in parenthesis.

APC15R-BCD. The band corresponding to a 1:1 interaction diminished, but remained visible. The difference in molecular weight between a 1:2 or 2:2 stoichiometry is small (~15 kDa). Therefore, the bands approximating a 1:1 and a 1:2 interaction were each excised, digested with trypsin, and analyzed by LC-coupled high-resolution mass spectrometry to determine the stoichiometry. By measuring the ratio of peptide intensities between these two bands, we determined that there was a greater ratio of β-catenin vs. APC in the upper band, consistent with a 1:2 stoichiometry of APC15R-BCD to β-catenin (Figure 3.3). With 3-fold molar excess of β-catenin, band migration was similar to that at a 2-fold molar excess, also indicating a 1:2 ratio of APC15R-BCD to β-catenin. We did observe faint higher molecular-weight bands, however we were unable to estimate the molecular weight of these bands as accurately due to limitations in gel resolution.

The cross-linking experiments were repeated with APC15R, which contains the entire 15-aa repeat region. At a 1:1 molar ratio of APC15R:β-catenin, the major visible protein band was consistent with a 1:1 complex. We also observed a faint band which would be consistent with a complex of 1:2 or 2:2 ratio of APC15R:β-catenin. At a 2-fold molar excess of β-catenin, the dominant observed band was at a molecular weight that was consistent with a 1:2 or 2:2 ratio. Finally, at 3-fold molar excess of β-catenin, the band consistent with a molecular weight of a 1:2 or 2:2 ratio was diminished, and a band at a higher molecular weight appeared. This band may be a 1:3 molar ratio of APC15R-BCD:β-catenin, however we cannot rule out the possibility that it is comprised of some other stable stoichiometric ratio, such as 2:4. In any case, it is apparent that as the local concentration of β-catenin rises, APC facilitates formation of higher-order species.

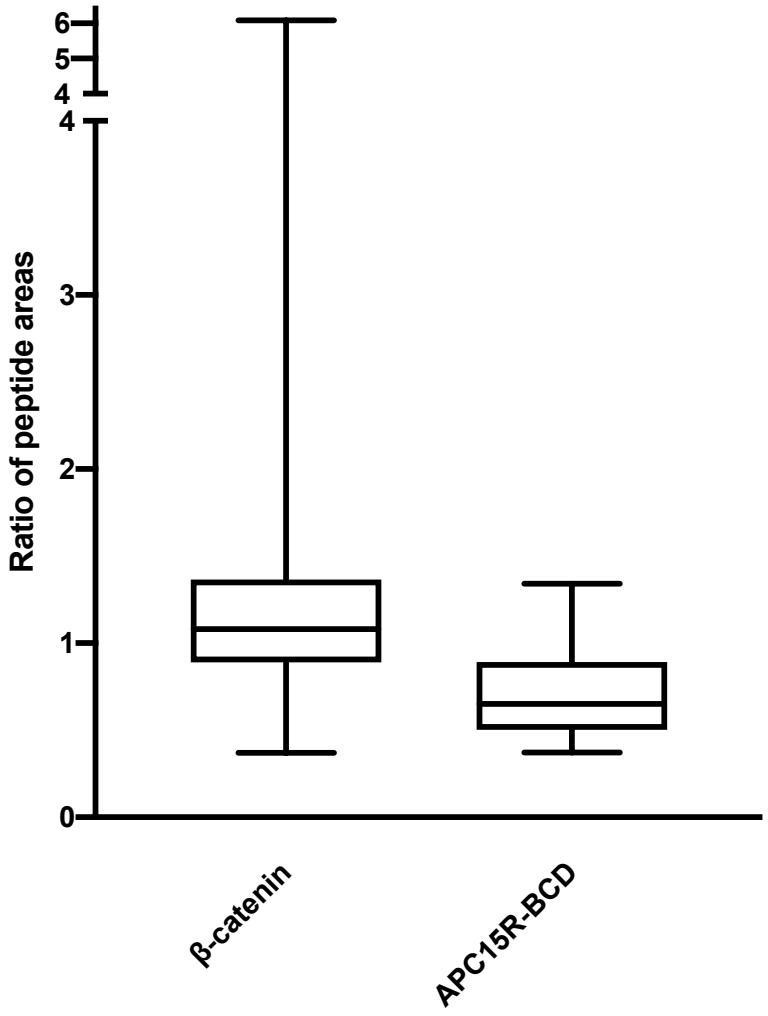

Figure 3.3 Mass Spectrometry Analysis Crosslinked Products Ratio of peptide areas from excised 1:1 band vs 1:2 (APC15R-BCD:β-catenin). Mean ratio for β-catenin was 1.34, mean ratio for APC15R-BCD was 0.699. Data are consistent with twice as much β-catenin as APC15R-BCD in higher band (1:2) compared to lower band (1:1).

Native association of APC and β-catenin

To confirm that the observed APC/β-catenin interactions were not an artifact of crosslinking, APC15R-BCD was incubated with β-catenin without addition of DMP, and the solution was subjected to size exclusion chromatography. Figure 3.4A shows the peaks representing the individual proteins, as well as the chromatogram of protein mixed in a 1:1 ratio. Apparent molecular weights were estimated based on column calibration with a standard mix of globular proteins. Because this APC15R-BCD is not likely globular, but rather in a more extended conformation, it is not surprising that the apparent molecular weights of APC and bound complexes of APC/β-catenin eluted as if they were larger in molecular weight. Three peaks appeared in the elution of 1:1 molar ratio of APC15R-BCD:β-catenin. The right-most peak elutes at a volume consistent with the elution time of the unbound APC15R–BCD. The middle peak likely contains the complex in a 1:1 molar ratio. The left-most peak contains a higher order complex. Because there is a substantial peak of monomer APC15R-BCD in this sample, it seems most likely that the highest molecular weight elution represents two β-catenin molecules binding a single APC15R-BCD and thus leaving surplus unbound APC15R-BCD. We did not observe peaks at higher estimated molecular weights, indicating that the proteins were not aggregating or forming detectable higher order oligomers. We examined whether APC15R-BCD would dimerize or form higher order oligomers at the higher concentrations necessary for NMR analysis. APC15R-BCD was concentrated to above 1 mM, allowed to incubate for 10 minutes, and injected onto the sizing column. Figure 3.4B shows no higher order peaks, again indicating that APC15R-BCD does not dimerize or form higher order species alone. Lastly, to determine an approximate time-scale of association, APC15R-BCD was incubated at a 1:1 molar ratio with β-

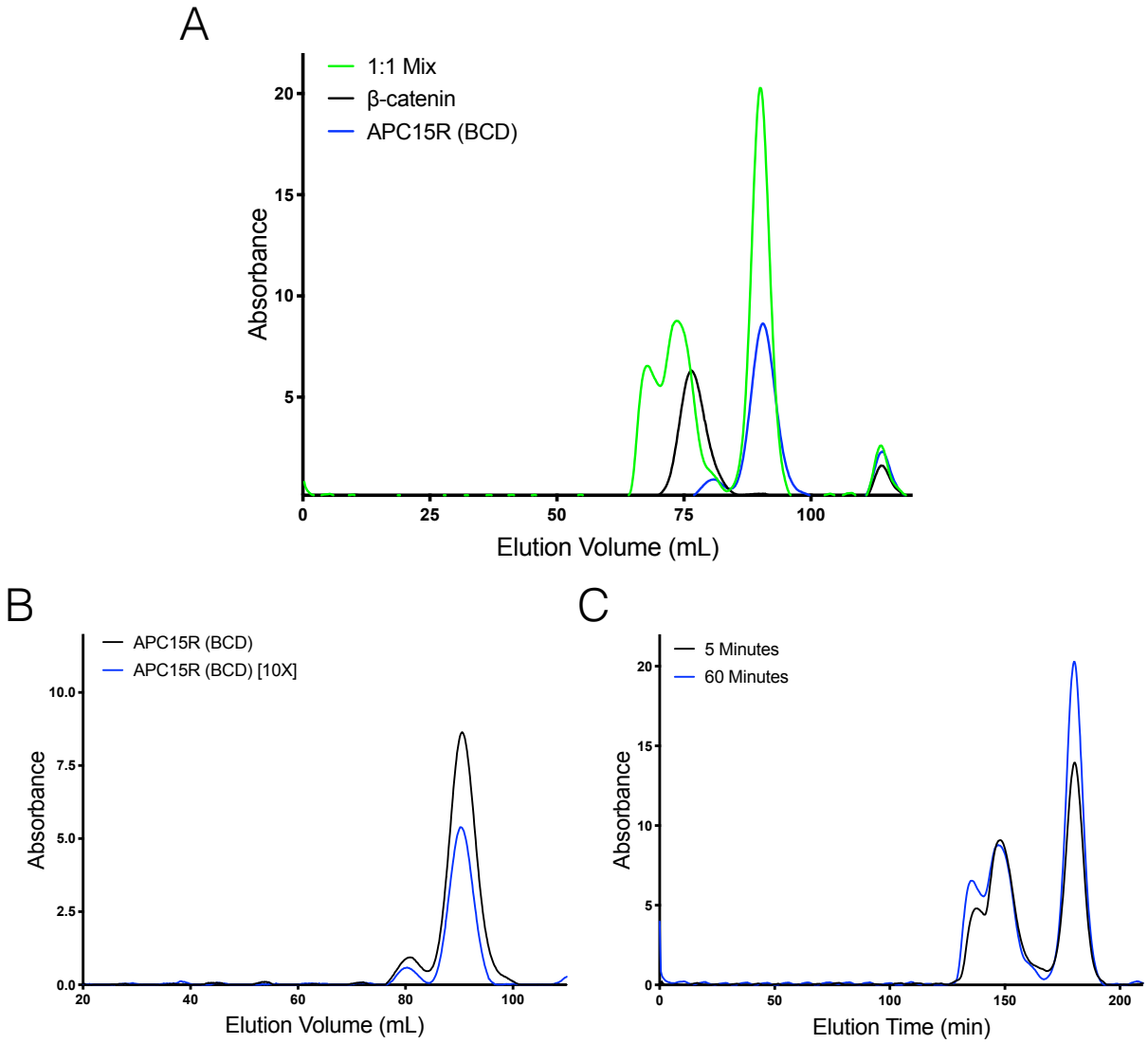

Figure 3.4 Native Association of APC15R-BCD and β-catenin monitored by Size Exclusion Chromatography A) Size exclusion chromatography (SEC) spectra of APC15R – BCD and β-catenin run independently, and at a 1:1 molar ratio with no added crosslinker. B) SEC spectra of APC15R-BCD ran at 136 μM (black) and at 1.2 mM (blue). We did not observe any peaks forming in a concentration-dependent fashion. C) SEC Spectra of APC15R-BCD after incubation for 5 min before injection to column (black) and incubation for 60 min before injection (blue). In general, peaks were largely unchanged with longer incubation times, with slightly more unbound APC15R-BCD moving into the left-most elution peak.

catenin for 5 minutes, and for 60 minutes. Figure 3.4C shows that spectra at both points were similar, with slightly more unbound APC15R-BCD moving into the complex peak after one hour. This indicates that the association of β-catenin and APC is rapid, and verifies that the timescales used throughout these studies are acceptable for characterizing their interaction.

Next, we used analytical ultracentrifugation as a second method of estimating binding stoichiometry in a native state, absent chemical cross-linking. Figure 3.5 shows representative spectra from APC15R-BCD and β-catenin alone, overlaid with spectra from mixtures at the indicated molar ratios. The 1:1 molar ratio mixture showed a shift of sedimentation coefficient consistent with the predicted molecular weight of a 1:1 interaction. Unexpectedly, for the 2:1 and 3:1 molar ratio samples, we observed only one prominent peak that lined up with the 1:1 peak but with a broad tail. Overall, the chromatograms were consistent with the cross-linking data for APC15R–BCD.

In total, our results demonstrate that the 15-aa repeat region of APC is capable of inducing formation of a complex containing multiple β-catenin molecules. However, only a 1:1 association was clearly observable under native experimental conditions, indicating that additional binding events after the initial 1:1 association are of weaker affinity.

Titration of APC15R-BCD with β-catenin

With 88.7% of the backbone NMR peaks for APC15R-BCD assigned to specific residues, we sought to identify key features of the β-catenin/APC interaction. The β-catenin protein was not soluble in the PBS buffer in which the backbone peaks of APC15R-BCD were assigned. Buffer screening revealed that citrate buffer was suitable for both APC and β-catenin

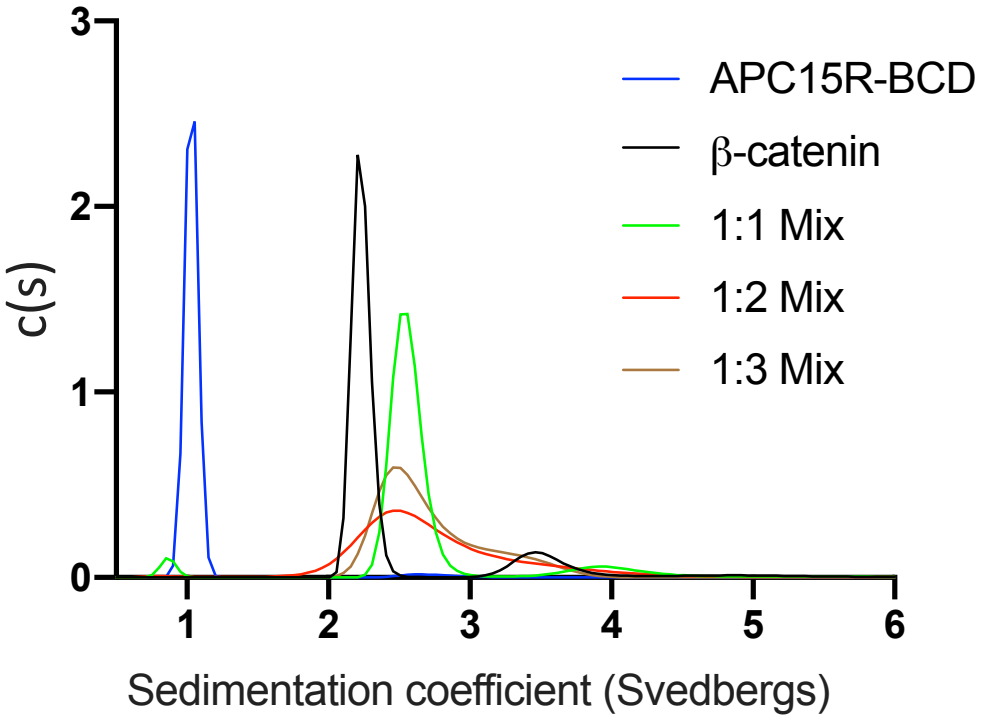

Figure 3.5 Native Association of APC15R-BCD and β-catenin monitored by Analytical Ultracentrifugation Analytical ultracentrifugation spectra of APC15R-BCD alone, β-catenin alone, and indicated ratios of APC:β-catenin mixed together with no crosslinker included.

(see methods). Because the 1H-15N-HSQC spectra of APC15R-BCD in PBS and citrate buffer did not overlap perfectly, we analyzed a new 3D ^{1}H-^{15}N TOCSY-HSQC spectrum of the ^{15}N-labeled APC15R-BCD in the citrate buffer. This confirmed to us that the resonance assignments were transferred correctly to APC15R-BCD in the new citrate buffer (Figure 3.6, Table 3.1).

Titration of APC15R-BCD (Figure 3.7A) with equivalent moles of β-catenin, half as much β-catenin, or a 2.0-fold molar excess resulted in a general decrease in peak intensities. This result confirms that APC15R-BCD binds to β-catenin *in vitro*, and that all APC residues appear impacted in response to β-catenin binding. Unexpectedly, no significant chemical shift changes were observed. ^{1}H-^{15}N TROSY spectra acquired for each of the titration points also showed a decrease in peak intensities and no discernable chemical shift changes (data not shown). Figure 3.7C shows the ratio of peak heights upon titration of a 1:1 to 1:0 APC/β-catenin molar ratio. APC15R has a linker region that is not predicted to associate with β-catenin. We hypothesized that in a titration of APC15R with β-catenin, peaks from this linker region would not change in response to β-catenin binding. However, as was seen with APC15R-BCD, titration of APC15R with 0.5 – 2.0 molar equivalent of β-catenin also resulted in a general decrease in all peak intensities, including those from the linker region (Figure 3.7B).

In order to test the specificity of the 15-aa repeat region of APC for β-catenin binding, we incubated APC15R with lysozyme at a 1:1 molar ratio. Lysozyme was again chosen because, like β-catenin, it is positively charged at our experimental pH (pI 11.35). As expected, we observed no changes to the APC15R spectra (Figure 3.8) confirming that APC15R (pI 5.61) does not interact with lysozyme. We conclude that APC15R does not merely interact with protein partners simply by electrostatic attraction.

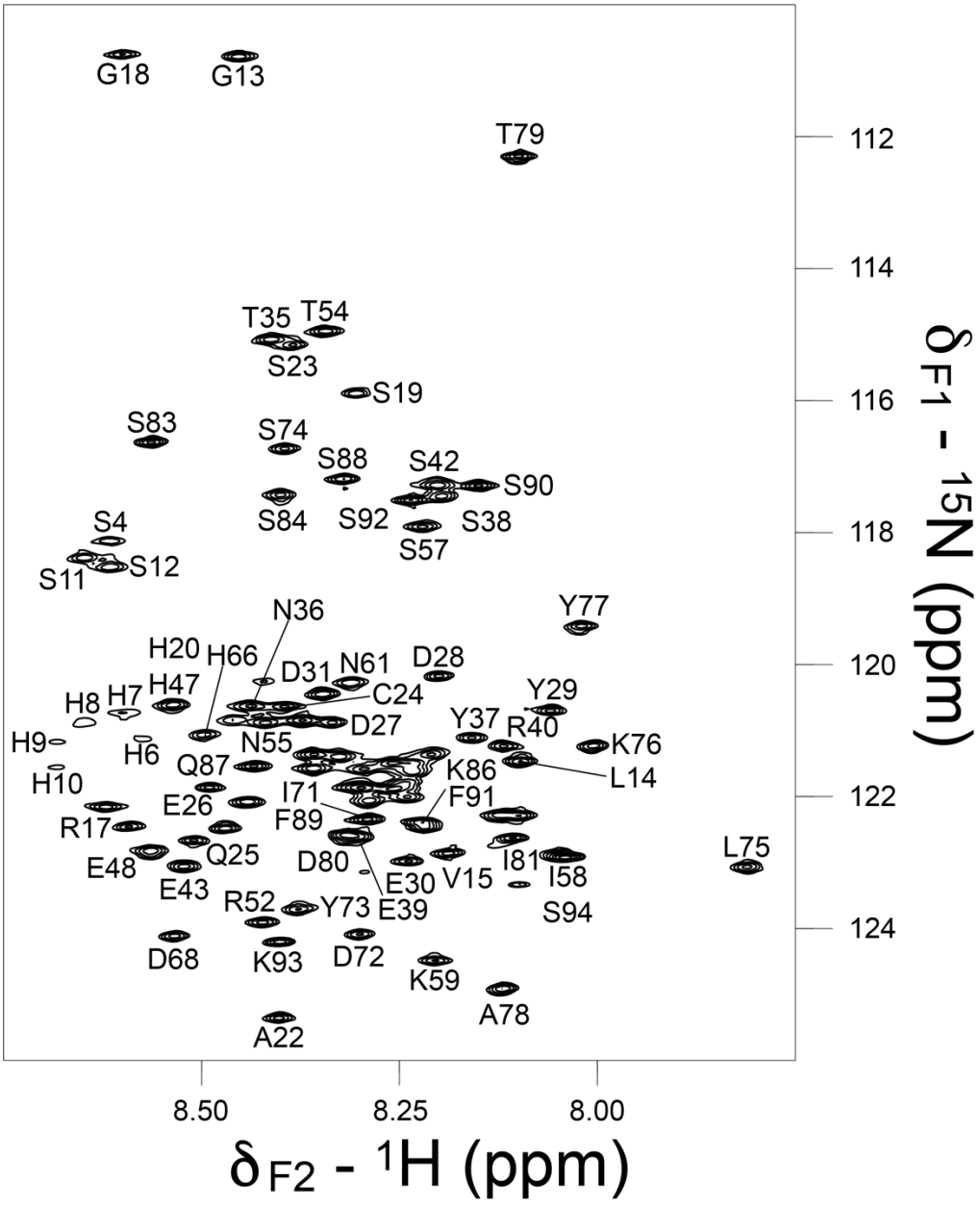

Figure 3.6 Citrate Backbone Resonance Assignments of APC15R-BCD. ^{1}H-^{15}N HSQC spectrum of ^{15}N labeled APC15R-BCD in 100 mM sodium citrate, 50 mM potassium phosphate, 10% glycerol, pH 7.0. The backbone assignments (^{1}HN, ^{15}N) are annotated. Assignments were transferred from those of APC15R-BCD in PBS buffer based on the ^{15}N TOCSY-HSQC spectrum.

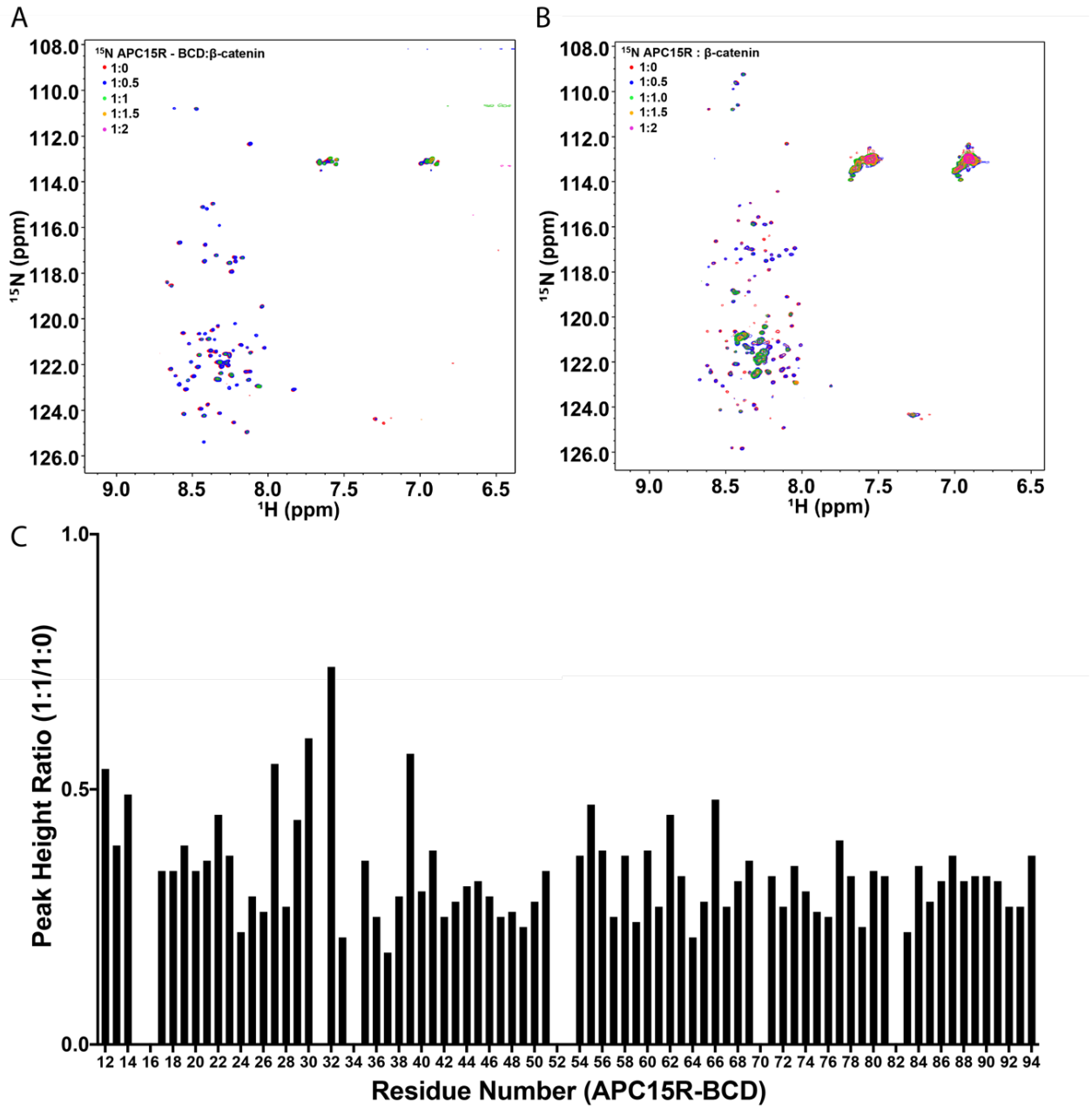

Figure 3.7 Titration of APC15R-BCD and APC15R with β-catenin. A) Overlay of ^{1}H-^{15}N HSQC spectra of ^{15}N APC15R-BCD titrated with increasing molar ratios of β-catenin. B) Overlay of ^{1}H-^{15}N HSQC spectra of ^{15}N APC15R titrated with increasing molar ratios of β-catenin. C) Peak height ratio of APC15R-BCD with 1.0 molar equivalence of β-catenin (1:1) to the peak height of free APC15R-BCD in solution (1:0). Global reduction of peak heights with no discernable chemical shift changes indicates a highly heterogenous association.

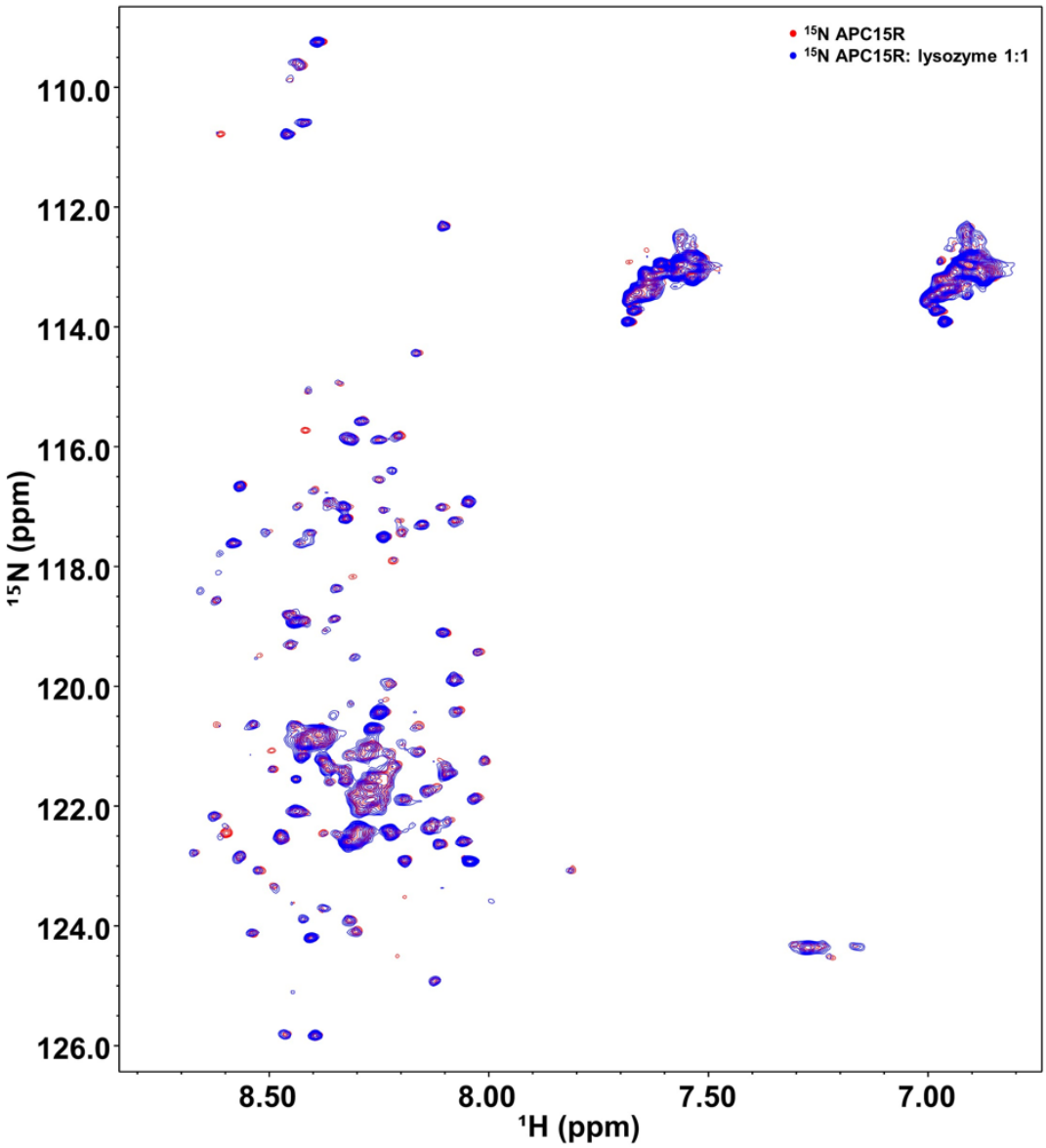

Figure 3.8 Negative Control for APC15R-BCD Association Overlay of ^{1}H-^{15}N HSQC spectra of ^{15}N-APC15R and ^{15}N-APC15R: lysozyme (1:1 molar ratio). The lack of peak shifts or peak broadening indicates that lysozyme and APC15R-BCD do not physically interact.

Backbone dynamics of APC15R-BCD

To gain insight into the backbone dynamics of the 15-aa repeat region of APC that interacts with β-catenin, we collected heteronuclear $\{^1H\}$-^{15}N NOE relaxation rates for APC15R-BCD in both the unbound, free state as well as upon addition of 0.2 molar-ratio β-catenin to the solution. The $\{^1H\}$-^{15}N NOE values (Figure 3.9) of free APC15R-BCD reinforced our conclusions that this region is highly flexible, as we do not observe continuous stretches of residues with NOE values close to 0.8, which would indicate higher degrees of rigidity. NOE values very low or negative are indicative of highly flexible, "random coil" like regions. Interestingly, a majority of the residues fall into a middle range between a ratio of 0.3 and 0.6. We did not observe significant changes in NOE values when a 0.2 molar ratio of β-catenin was added. 0.2 ratio was chosen to avoid signal loss due to peak broadening. Of note, residues spanning "repeat D" show a general increase in flexibility (decrease in NOE value) upon binding with β-catenin. These results indicate that the backbone dynamics of APC15R-BCD remain largely unchanged upon association with β-catenin, and that no major fold-upon-binding events are discernable.

Discussion

β-catenin binds to Repeat A of APC using the same binding groove as other binding partners E-cadherin, XTcf3, and TCF[3]. Indeed, the crystal structure of β-catenin with a peptide representing Repeat A showed that APC residues D1022, P1024, I1025, Y1027, and E1034 directly contact β-catenin[3]. A different study reported that mutation of Y1027, S1028, and Y1031 of Repeat A (as well as the corresponding residues for repeats B-D, see Fig. 1C) was sufficient to abolish β-catenin binding to an APC fragment expressed transiently in HEK293T cells[1]. Interestingly, crystal structures solved with TCF fragments bound to β-catenin revealed at least two distinct

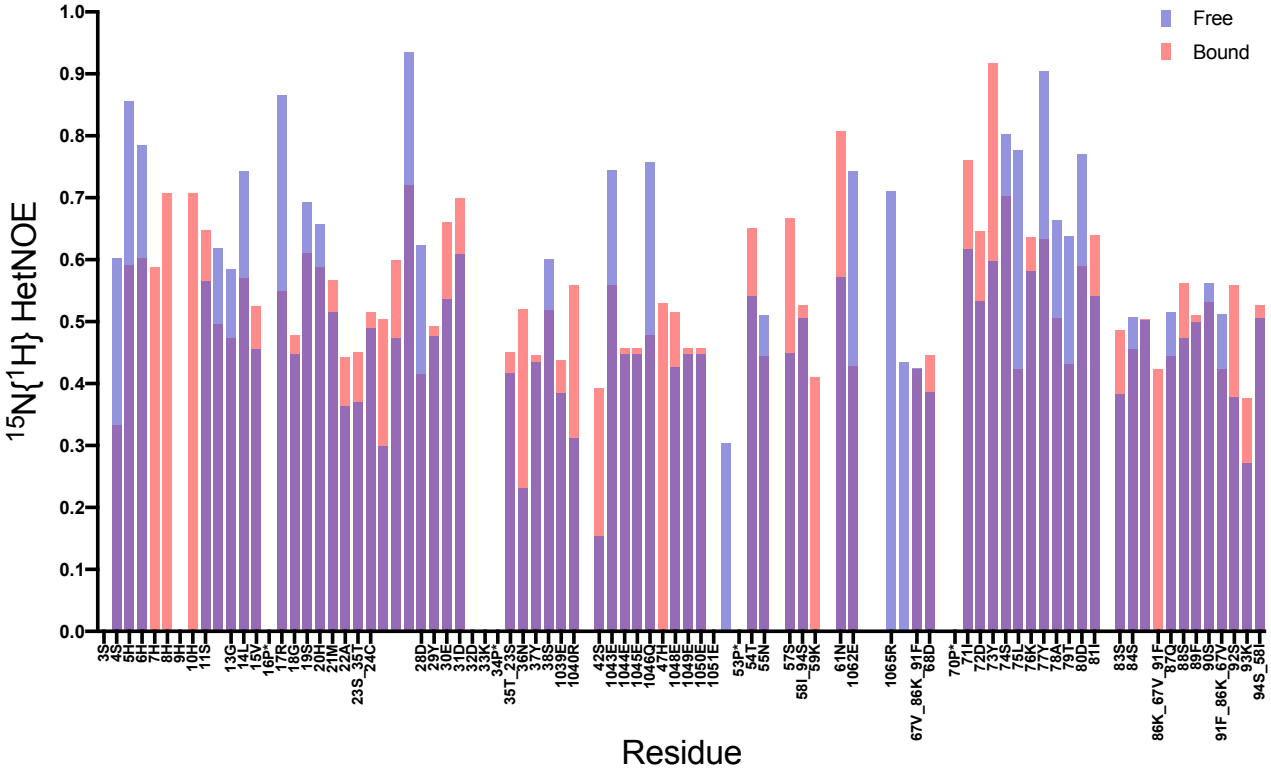

Figure 3.9 ^{1}H- ^{15}N Heteronuclear NOE of APC15R-BCD bound with β-catenin. Overlay of $^{15}N\{^{1}H\}$ HetNOE spectra of APC15R-BCD (blue) with the $^{15}N\{^{1}H\}$ HetNOE spectra after 0.2 molar equivalent of β-catenin was added to the sample tube. HetNOE values indicate general flexibility throughout the APC15R-BCD construct. A region of HetNOE values higher than mean (0.51 for free APC15R-BCD) from S74-S84 decreases upon interactions with β-catenin, suggesting a partial unfolding upon binding in this region.

modes of binding, with TCF utilizing variable residues to form salt bridges with specific β-catenin residues[16]. We hypothesize that APC can also recognize and bind β-catenin specifically, yet in alternative conformations similar to the TCF studies. Our NMR studies revealed no chemical shift changes for APC15R-BCD in solution with β-catenin titration, but rather, the simultaneous disappearance of peaks, even at sub-1:1 stoichiometric ratios. A longer peptide fragment, APC15R, produced overlapping NMR peaks with APC15R-BCD and these peaks also disappeared rather than shifted with β-catenin titration. These observations that the bound state is NMR invisible, that we observe no shifts upon binding, and that we do not observe large complexes of oligomers at the ratios used support the conclusion that APC15R–BCD binds in a heterogenous fashion with β-catenin that is in intermediate chemical exchange on the NMR time scale.

The high sequence similarity of the four 15-aa repeats raises the potential that each could bind β-catenin. Our crosslinking data indicates that APC15R-BCD can facilitate formation of complexes involving more than one β-catenin when β-catenin is at a molar excess. These data support the conclusion of previous isothermal titration calorimetry data that a peptide containing repeats B, C, and D could bind two β-catenin molecules[2].

For both APC constructs tested at a 1:1 molar ratio, a majority of the observed cross-linked protein products were at molecular weights that corresponded to a 1:1 ratio, with minor products at higher molecular weight complexes. We initially wondered if certain binding sites had a higher affinity for β-catenin, and if we could identify those sites. However, our NMR results did not reveal any peak shifts that would be consistent with one specific bound conformation. Therefore, we suggest that there is no specific site in the span of repeats B – D that is of significantly higher affinity than any other site. These results are consistent with the

"binding cloud" model which proposes that certain disordered regions of proteins dynamically present multiple identical, rapidly interchangeable binding sites to partners at once, existing in a "cloud" of bound conformations.[17–19] In the context of the β-catenin destruction complex, this flexibility in binding would provide APC the ability to sequester β-catenin when appropriate, and to release it to the higher affinity, 20-aa repeat region for phosphorylation and eventual degradation.

We also observe that APC retains conformational flexibility upon binding with β-catenin. This flexibility has been described as "fuzzy", or a disorder-to-disorder association in order to differentiate this type of binding from traditional lock-and-key or induced fit ordered binding models.[20,18] The β-catenin destruction complex is often modeled as a large globular complex with 1:1 molar ratios of all components. However, some proteins of this complex exist in extended conformations, which complicates this model and our understanding of how β-catenin is regulated. Our data as a whole support a model whereby, as β-catenin concentrations increase in the cell, APC is able to act as a molecular sponge, binding excess β-catenin in a sequential manner. The extended nature of the 15-aa repeats likely speeds molecular recognition, and allows APC to rapidly regulate free β-catenin.

Materials and Methods

Protein Expression and Purification

Gene sequences for the β-catenin used in this study were cloned from a previously generated plasmid containing full-length human β-catenin[21]. Cloned fragments were ligated into the pET28b (Novagen) expression vector, which contains an N-terminal 6X-His tag. Sequence-verified plasmids were transformed into BL21-CodonPlus-(DE3)-RIPL *E. coli* cells (NEB) for

expression. Cells were grown in standard LB broth containing 50 μg/mL kanamycin at 37°C with shaking (225 rpm), and induced with 0.2 mM isopropyl-β-D-thiogalactopyranoside (IPTG) for protein expression when an OD of 0.4-0.6 was reached. Cells were allowed to express induced protein product for 3-4 hours at 37°C with shaking before harvested by centrifugation at 4,000 rpm, 15 min, 4°C. Cellular pellets were resuspended in a buffer containing 50 mM Tris pH 8.0, 50 mM NaCl, 50 mM imidazole, 10% glycerol, and HALT protease cocktail (Thermo). Cells were lysed by a French pressure cell (35,000 psi), and the insoluble cellular debris was removed by centrifugation at 16,000 x g for 45 min, 4°C. Supernatant was applied to a chelating sepharose fast-flow column (Amersham Biosciences) charged with nickel chloride and pre-equilibrated in resuspension buffer. Protein retained on the column was washed with a 3 column volumes (C.V.) salt gradient (50 mM potassium phosphate pH 8.0, 500 mM NaCl, 50 mM imidazole, 10% glycerol). Protein was eluted with an imidazole buffer gradient (50 mM Tris pH 8.0, 500 mM NaCl, 500 mM imidazole, 10% glycerol). As soon as β-catenin was eluted from the nickel column, pooled protein fractions were placed in 10,000 Da SnakeSkin dialysis tubing (Thermo), and dialyzed against a citrate buffer containing 50 mM KPi pH 8.0, 100 mM Sodium Citrate, and 10% glycerol. Dialyzed protein samples were applied to a Superdex 200 size-exclusion column (Amersham Biosciences) pre-equilibrated with 50 mM KPi, pH 8.0, 100 mM Sodium Citrate, and 10% glycerol. Fractions containing recombinant protein were pooled and concentrated with Amicon Ultra centrifugal filters (Millipore) and stored at -80°C.

In vitro Protein Crosslinking

Frozen protein aliquots were thawed, and concentration determined by Bradford assay. Proteins were diluted in triethanolamine, pH 8.0 to 10 μM final volume, and mixed according to indicated molar ratios. Protein solutions were cross-linked using 5 mM dimethyl pimelimidate (DMP)

(Thermo) overnight at 4°C. Final reactions contained 0.1M triethanolamine, pH 8.0. Crosslinking reactions were quenched with Tris, pH 8.0 for one hour, RT before boiling in SDS-PAGE buffer and resolution by gel electrophoresis. Protein bands were visualized by Coomassie stain and imaged on an Odyssey CLx imaging system (LiCor).

Size Exclusion Chromatography

Frozen protein aliquots were thawed on ice, and concentration was determined by Bradford assay. Individual proteins were injected onto a Superdex 200 gel filtration column pre-equilibrated with a citrate buffer containing 50 mM KPi pH 8.0, 100 mM Sodium Citrate, and 10% glycerol. 1:1 protein mixture was incubated for 1 hour at 4°C before injection.

Analytical Ultracentrifugation

SV-AUC experiments were performed on a Proteome Lab XL-I (Beckman Coulter) analytical ultracentrifuge equipped with a scanning ultraviolet-visible optical system. Prior to SV-AUC analysis, all samples were dialyzed into 50 mM potassium phosphate, 100 mM sodium citrate, 5% glycerol, pH 7.0 buffer. Concentrations of the samples were adjusted to 0.5 OD (approximately 3.0 mg/mL for β-catenin, 1.5 mg/mL for APC15R, and 2.5 mg/mL for APC15R-BCD) at 280nm to optimize the absorbance for the SV-AUC measurements. All experiments were conducted at 20°C after ≥1 h of equilibration and after the rotor had reached the set temperature, at a rotor speed of 40,000 RPM and with detection at 280 nm. Samples and corresponding buffer alone were loaded into Beckman charcoal-epon two sector centerpiece (12 mm) with sapphire windows. The data were analyzed using Sedfit (Dr. Peter Schuck, NIH). Partial specific volumes of the samples were calculated using Sednterp (Professor Thomas Laue, University of New Hampshire and BITC) based on amino acid sequence and used in the analysis

(0.6985 mL/g for APC-15R B-D, 0.7449 mL/g for β-catenin, and 0.7372 mL/g for the complex of the two). The buffer density and viscosity used in the analysis were also calculated using Sednterp based on buffer composition. For the 50 mM potassium phosphate, 100 mM sodium citrate, 5% glycerol, pH 7.0 buffer, a density of 1.0373 g/mL and viscosity of 0.012858 Poise were used. A continuous c(s) distribution model and a range of 0 to 15 svedbergs were used to integrate the data, with a resolution of 300 points per distribution and a confidence level of 0.95. Baseline, radial independent noise, and time independent noise were fit, while the meniscus and bottom positions were set manually. Distributions were imported into Origin (OriginLab) for analyzing peak area distribution before reporting.

Protein NMR Spectroscopy

All NMR data were collected at 5 °C on a Bruker AV 800 MHz NMR spectrometer equipped with a triple resonance cryoprobe. Data were processed using the NMRPipe[22] program and visualized and analyzed using NMRDraw and NMRViewJ[23] and CCPN analysis[24] on the NMRBox platform[25]. ^{1}H-^{15}N TOCSY-HSQC spectrum was acquired using 1 mM ^{15}N labeled APC15R-BCD in 100 mM sodium citrate, 50 mM potassium phosphate, 10% glycerol, pH 7.0. ^{1}H-^{15}N HSQC titration experiments were performed using 80 μM ^{15}N-labeled APC15R-BCD and 80 μM ^{15}N-labeled APC15R. Unlabeled β-catenin stock solution was titrated into the APC15R-BCD and APC15R samples, and ^{1}H-^{15}N HSQC spectra were recorded for each titration point.

The ^{15}N{^{1}H} heteronuclear nuclear Overhauser effect (HetNOE) experiments were acquired using 200 μM ^{15}N APC15R-BCD in the absence or presence of 40 μM β-catenin in 50 mM KPi pH 7.0, 100 mM Sodium Citrate, and 10% glycerol buffer with 1 mM TCEP. The reference and NOE spectra were collected in an interleaved manner with each 2D was consisting

of 1024 × 128 complex data points with 64 scans. The interscan delay is set to 11.75 and 6.75s for the reference and NOE experiments, respectively. The NOE experiment used a train of 120° hard pulses with 18 ms delays for a total saturation time set to 5 s. The total experiment time equaled 5 days, 16 hours. The acquisition parameters match the recommendation of Renner et al.[26] for accurate/precise characterization of fast dynamics on highly flexible proteins.

Collaborations and Workload Allocations

Experiments in this chapter were designed, conducted, and analyzed by Aaron Rudeen except the following: Figure 3.3 – Samples were prepared by A. Rudeen and sent to the Mass Spectrometry Research Center at Vanderbilt University for analysis. Dr. Hayes McDonald, Co-Associate Director, Department of Biochemistry assisted with data analysis. Figure 3.5 – Samples were prepared by A. Rudeen and sent to the Vaccine Analytics and Formulation Center at the University of Kansas for analysis. Dr. Jian Xiong performed the measurements and assisted with data analysis. Figures 3.6, 3.7, 3.8, 3.9 – Samples were prepared by A. Rudeen and sent to the Nuclear Magnetic Resonance Laboratory at the University of Kansas. Dr. Minli Xing and Dr. Justin Douglas performed the measurements and assisted with data analysis. Dr. Minli Xing and Dr. Justin Douglas assigned the backbone resonance chemical shifts.

Supporting Materials

Table 3.1 Chemical shift table of APC15R-BCD in citrate buffer

#	Residue	HN(ppm)	N(ppm)	Note
1	Met			
2	Gly			
3	Ser			
4	Ser			
5	His			
6	His			
7	His			
8	His			
9	His			
10	His			
11	Ser			missing
12	Ser	8.617	118.523	
13	Gly	8.455	110.788	
14	Leu	8.098	121.466	
15	Val			Missing in both PBS buffer and citrate buffer spectrum
16	Pro			
17	Arg	8.593	122.459	
18	Gly	8.602	110.754	
19	Ser	8.306	115.893	
20	His	8.317	122.584	
21	Met	8.211	121.359	
22	Ala	8.403	125.356	
23	Ser	8.386	115.158	
24	Cys	8.336	120.883	
25	Gln	8.359	121.361	
26	Glu	8.499	121.066	
27	Asp	8.297	121.584	
28	Asp	8.349	120.449	
29	Tyr	8.061	120.702	
30	Glu	8.239	122.979	
31	Asp			missing
32	Asp	8.201	120.173	
33	Lys	8.006	121.233	
34	Pro			

35	Thr	8.414	115.070	
36	Asn	8.439	120.629	
37	Tyr	8.16	121.111	
38	Ser	8.198	117.444	
39	Glu	8.511	122.663	
40	Arg	8.425	123.909	
41	Tyr	8.235	121.618	
42	Ser	8.203	117.284	
43	Glu	8.524	123.061	
44	Glu	8.443	122.078	
45	Glu	8.36	121.573	
46	Gln	8.359	121.361	
47	His	8.120	121.237	
48	Glu	8.491	121.862	
49	Glu	8.565	122.821	
50	Glu	8.472	122.483	
51	Glu	8.622	122.157	
52	Arg			missing
53	Pro			
54	Thr	8.345	114.945	
55	Asn	8.462	120.844	
56	Tyr	8.235	121.618	
57	Ser	8.222	117.911	
58	Ile	8.042	122.922	
59	Lys	8.206	124.484	
60	Tyr	8.235	121.618	
61	Asn	8.313	120.277	
62	Glu	8.327	121.398	
63	Glu	8.300	121.865	
64	Lys	8.289	122.060	
65	Arg	8.258	121.888	
66	His	8.421	120.883	
67	Val	8.101	122.290	
68	Asp	8.536	124.113	
69	Gln	8.260	121.492	
70	Pro			
71	Ile	8.292	122.346	
72	Asp	8.302	124.087	
73	Tyr	8.379	123.706	
74	Ser	8.397	116.727	
75	Leu	7.811	123.062	

76	Lys	8.190	122.862	
77	Tyr	8.021	119.415	
78	Ala	8.120	124.910	
79	Thr	8.101	112.294	
80	Asp	8.317	122.584	
81	Ile	8.108	122.624	
82	Pro			
83	Ser	8.565	116.633	
84	Ser	8.402	117.430	
85	Gln	8.258	121.888	
86	Lys	8.224	122.395	
87	Gln	8.436	121.542	
88	Ser	8.323	117.186	
89	Phe	8.292	122.346	
90	Ser	8.152	117.287	
91	Phe	8.224	122.395	
92	Ser	8.236	117.511	
93	Lys	8.402	124.202	
94	Ser	8.042	122.922	

References

(1) Kohler, E. M.; Derungs, A.; Daum, G.; Behrens, J.; Schneikert, J. Functional Definition of the Mutation Cluster Region of Adenomatous Polyposis Coli in Colorectal Tumours. *Hum. Mol. Genet.* **2008**, *17* (13), 1978–1987. https://doi.org/10.1093/hmg/ddn095.

(2) Liu, J.; Xing, Y.; Hinds, T. R.; Zheng, J.; Xu, W. The Third 20 Amino Acid Repeat Is the Tightest Binding Site of APC for Beta-Catenin. *J. Mol. Biol.* **2006**, *360* (1), 133–144. https://doi.org/10.1016/j.jmb.2006.04.064.

(3) Spink, K. E.; Fridman, S. G.; Weis, W. I. Molecular Mechanisms of β-Catenin Recognition by Adenomatous Polyposis Coli Revealed by the Structure of an APC–β-Catenin Complex. *EMBO J* **2001**, *20* (22), 6203–6212. https://doi.org/10.1093/emboj/20.22.6203.

(4) Kohler, E. M.; Brauburger, K.; Behrens, J.; Schneikert, J. Contribution of the 15 Amino Acid Repeats of Truncated APC to Beta-Catenin Degradation and Selection of APC Mutations in Colorectal Tumours from FAP Patients. *Oncogene* **2010**, *29* (11), 1663–1671. https://doi.org/10.1038/onc.2009.447.

(5) Albuquerque, C.; Breukel, C.; van der Luijt, R.; Fidalgo, P.; Lage, P.; Slors, F. J. M.; Leitão, C. N.; Fodde, R.; Smits, R. The "just-Right" Signaling Model: APC Somatic Mutations Are Selected Based on a Specific Level of Activation of the Beta-Catenin Signaling Cascade. *Hum. Mol. Genet.* **2002**, *11* (13), 1549–1560. https://doi.org/10.1093/hmg/11.13.1549.

(6) Flock, T.; Weatheritt, R. J.; Latysheva, N. S.; Babu, M. M. Controlling Entropy to Tune the Functions of Intrinsically Disordered Regions. *Curr. Opin. Struct. Biol.* **2014**, *26*, 62–72. https://doi.org/10.1016/j.sbi.2014.05.007.

(7) Mukherjee, S. P.; Behar, M.; Birnbaum, H. A.; Hoffmann, A.; Wright, P. E.; Ghosh, G. Analysis of the RelA:CBP/P300 Interaction Reveals Its Involvement in NF-KB-Driven Transcription. *PLOS Biology* **2013**, *11* (9), e1001647. https://doi.org/10.1371/journal.pbio.1001647.

(8) Shi, J.; Shen, Q.; Cho, J.-H.; Hwang, W. Entropy Hotspots for the Binding of Intrinsically Disordered Ligands to a Receptor Domain. *Biophysical Journal* **2020**, *118* (10), 2502–2512. https://doi.org/10.1016/j.bpj.2020.03.026.

(9) Tompa, P.; Fuxreiter, M. Fuzzy Complexes: Polymorphism and Structural Disorder in Protein-Protein Interactions. *Trends Biochem. Sci.* **2008**, *33* (1), 2–8. https://doi.org/10.1016/j.tibs.2007.10.003.

(10) Xing, Y.; Takemaru, K.-I.; Liu, J.; Berndt, J. D.; Zheng, J. J.; Moon, R. T.; Xu, W. Crystal Structure of a Full-Length β-Catenin. *Structure* **2008**, *16* (3), 478–487. https://doi.org/10.1016/j.str.2007.12.021.

(11) Xing, Y.; Clements, W. K.; Le Trong, I.; Hinds, T. R.; Stenkamp, R.; Kimelman, D.; Xu, W. Crystal Structure of a β-Catenin/APC Complex Reveals a Critical Role for APC Phosphorylation in APC Function. *Molecular Cell* **2004**, *15* (4), 523–533. https://doi.org/10.1016/j.molcel.2004.08.001.

(12) Xing, Y.; Clements, W. K.; Kimelman, D.; Xu, W. Crystal Structure of a β-Catenin/Axin Complex Suggests a Mechanism for the β-Catenin Destruction Complex. *Genes Dev.* **2003**, *17* (22), 2753–2764. https://doi.org/10.1101/gad.1142603.

(13) Huber, A. H.; Weis, W. I. The Structure of the β-Catenin/E-Cadherin Complex and the Molecular Basis of Diverse Ligand Recognition by β-Catenin. *Cell* **2001**, *105* (3), 391–402. https://doi.org/10.1016/S0092-8674(01)00330-0.

(14) Gottardi, C. J.; Peifer, M. Terminal Regions of β-Catenin Come into View. *Structure* **2008**, *16* (3), 336–338. https://doi.org/10.1016/j.str.2008.02.005.
(15) Kries, J. P. von; Winbeck, G.; Asbrand, C.; Schwarz-Romond, T.; Sochnikova, N.; Dell'Oro, A.; Behrens, J.; Birchmeier, W. Hot Spots in β-Catenin for Interactions with LEF-1, Conductin and APC. *Nature Structural Biology* **2000**, *7* (9), 800. https://doi.org/10.1038/79039.
(16) Graham, T. A.; Ferkey, D. M.; Mao, F.; Kimelman, D.; Xu, W. Tcf4 Can Specifically Recognize Beta-Catenin Using Alternative Conformations. *Nat. Struct. Biol.* **2001**, *8* (12), 1048–1052. https://doi.org/10.1038/nsb718.
(17) Uversky, V. N. A Decade and a Half of Protein Intrinsic Disorder: Biology Still Waits for Physics. *Protein Sci* **2013**, *22* (6), 693–724. https://doi.org/10.1002/pro.2261.
(18) Uversky, V. N. Intrinsic Disorder-Based Protein Interactions and Their Modulators. *Curr. Pharm. Des.* **2013**, *19* (23), 4191–4213.
(19) Uversky, V. N. Multitude of Binding Modes Attainable by Intrinsically Disordered Proteins: A Portrait Gallery of Disorder-Based Complexes. *Chem. Soc. Rev.* **2011**, *40* (3), 1623–1634. https://doi.org/10.1039/C0CS00057D.
(20) Miskei, M.; Gregus, A.; Sharma, R.; Duro, N.; Zsolyomi, F.; Fuxreiter, M. Fuzziness Enables Context Dependence of Protein Interactions. *FEBS Lett.* **2017**, *591* (17), 2682–2695. https://doi.org/10.1002/1873-3468.12762.
(21) Liu, J.; Stevens, J.; Rote, C. A.; Yost, H. J.; Hu, Y.; Neufeld, K. L.; White, R. L.; Matsunami, N. Siah-1 Mediates a Novel Beta-Catenin Degradation Pathway Linking P53 to the Adenomatous Polyposis Coli Protein. *Molecular cell* **2001**. https://doi.org/10.1016/S1097-2765(01)00241-6.
(22) Delaglio, F.; Grzesiek, S.; Vuister, G. W.; Zhu, G.; Pfeifer, J.; Bax, A. NMRPipe: A Multidimensional Spectral Processing System Based on UNIX Pipes. *J. Biomol. NMR* **1995**, *6* (3), 277–293.
(23) Johnson, B. A.; Blevins, R. A. NMR View: A Computer Program for the Visualization and Analysis of NMR Data. *J. Biomol. NMR* **1994**, *4* (5), 603–614. https://doi.org/10.1007/BF00404272.
(24) Vranken, W. F.; Boucher, W.; Stevens, T. J.; Fogh, R. H.; Pajon, A.; Llinas, M.; Ulrich, E. L.; Markley, J. L.; Ionides, J.; Laue, E. D. The CCPN Data Model for NMR Spectroscopy: Development of a Software Pipeline. *Proteins* **2005**, *59* (4), 687–696. https://doi.org/10.1002/prot.20449.
(25) Maciejewski, M. W.; Schuyler, A. D.; Gryk, M. R.; Moraru, I. I.; Romero, P. R.; Ulrich, E. L.; Eghbalnia, H. R.; Livny, M.; Delaglio, F.; Hoch, J. C. NMRbox: A Resource for Biomolecular NMR Computation. *Biophysical Journal* **2017**, *112* (8), 1529–1534. https://doi.org/10.1016/j.bpj.2017.03.011.
(26) Renner, C.; Schleicher, M.; Moroder, L.; Holak, T. A. Practical Aspects of the 2D 15N-[1h]-NOE Experiment. *J. Biomol. NMR* **2002**, *23* (1), 23–33. https://doi.org/10.1023/a:1015385910220.

CHAPTER 4

TOPOISOMERASEIIα, APC, AND CANCER

Abstract

Topoisomerase IIα (TopoIIα) is a critical modulator of the cell cycle and is upregulated in colorectal cancers. Due to the essential nature of TopoIIα for cell survival, it has become a target for many chemotherapeutic agents. However, cancers of the colon and rectum are often resistant to TopoIIα-targeting drugs. Our lab discovered a novel association between the tumor-suppressor APC and TopoIIα, which has implications in colon cancer progression and initiation. In this chapter, I look into potential contributions of APC in the molecular mechanisms driving resistance of tumors to TopoIIα-targeting compounds. Here, we show that tumors that harbor *APC* mutation are more resistant to compounds targeting topoisomerases than tumors with wild-type *APC*. We observe that the levels of TopoIIα and APC correlate across cell lines regardless of APC status, but that APC does not directly regulate TopoIIα levels. We show that APC does not associate with the β-cat/TCF transcriptional complex, but that it does associate with both β-catenin and TopoIIα in the nucleus. We also show that TopoIIα contained in the nuclear extract from cells with mutant or no APC has enhanced catalytic activity compared to TopoIIα from cells with wild type APC. Finally, we report the generation of a new polyclonal antibody raised in chicken that recognizes the 15-aa repeat region of APC. This new tool will be a valuable addition to the field of APC research.

Introduction

The tumor-suppressor APC is mutated in greater than 80% of colorectal cancers[1]. Due to APC's major role in the β-catenin destruction complex, much of the research focus on APC's contribution to cancer is centered around Wnt signaling. While it is know that *APC* mutations disrupt Wnt signaling, this is an active ongoing area of research and other functions of APC have

been identified that have implications in cell growth and development. Several studies indicate that APC has a role in cell cycle regulation[2–4]. APC can bind and be phosphorylated by the spindle assembly checkpoint kinases[4], and localizes to kinetochores during metaphase in a microtubule-dependent fashion[2,4,5]. The spindle assembly checkpoint is a feedback-driven system that signals the cell to pause before entering anaphase when improper spindle-kinetochore attachments are present[6]. APC's roles in spindle assembly and microtubule arrangement are likely due to C-terminal microtubule binding and EB1 binding domains, which are lost by truncating mutation[2]. Aside from the spindle assembly checkpoint, our lab has identified a possible role for APC in another cell-cycle checkpoint: the G2/M decatenation checkpoint. The decatenation checkpoint is a safety mechanism the cell uses to ensure that chromosomes are detangled from one another before transitioning to anaphase and chromosome segregation. A defective G2/M checkpoint can lead to chromosome breakage, nondisjunction, aneuploidy and chromosome rearrangements[7]. Critical to the G2/M checkpoint is the type II DNA topoisomerase IIα (TopoIIα)[8]. TopoIIα catalyzes double-strand DNA breaks and re-ligation in order to detangle or "decatenate" chromosomes prior to segregation.

Our lab first identified APC as a possible binding partner of TopoIIα by conducting an immunoprecipitation of APC from the colon cancer cell line HCT116βw and performing matrix-assisted laser desorption/ionization time of flight (MALDI-TOF) mass spectrometry on unique bands (Neufeld and White, unpublished). Reciprocal immunoprecipitations, colocalization, and förster resonance energy transfer analysis confirmed the association[9]. Having established that TopoIIα and APC could associate in the nucleus of the cell, a more detailed analysis of the role of APC in the nucleus was performed. Fragments of APC encompassing the 15-aa repeats (aa's 959-1338, APC-M2) and the 20-aa repeats (aa's 1211-2075, APC-M3) were exogenously

expressed in cells. APC-M2 and M3 were each able to immunoprecipitate with TopoIIα from HCT116βw cell lysates, implicating these regions as important for the interaction[9,10]. Interestingly, expression of APC-M2 altered the nuclear morphology of colon cancer cells from lines HCT116-βw, SW480, and HCA7[9]. In a cell line with wild-type APC, exogenous expression of either APC-M2 or APC-M3 resulted in cell arrest in G2 and an increased percentage of aneuploid cells. However, in cells containing mutant APC, or cells that were selected for very low endogenous TopoIIα activity, cells did not arrest in G2[10]. Importantly, these effects were both p53 and β-catenin independent, as mutation of either did not change the ability of APC fragments to induce G2 accumulation. Finally, addition of recombinant APC-M2 or APC-M3 to *in vitro* TopoIIα catalytic activity assays resulted in enhanced TopoIIα activity, suggesting a possible direct interaction resulting in allosteric activation[9,10].

Taken together, these results demonstrate that APC has a role in TopoIIα-mediated cell cycle progression. We proposed a model by which mutated APC induces cell cycle arrest in G2 via an activated G2 decatenation checkpoint. A small percentage of cells then escape this arrest and become aneuploid. This aneuploidy, combined with aberrant Wnt signaling driving cell proliferation, greatly increases the likelihood of acquiring additional mutation en route to carcinoma formation.

Previous studies were primarily performed in cell lines overexpressing various portions of APC, which could contribute to observed effects. For this study, I examine what effect endogenous truncations of APC have on TopoIIα binding and activity.

Results

TopoIIα-targeted therapeutics are less effective in APC-mutant tumors

An early cancer therapy, etoposide was first synthesized in 1966 and put into clinical use by 1983[11]. Etoposide targets TopoII, and is an effective chemotherapy for small cell lung cancer and testicular cancer[12]. Despite elevated levels of TopoII in cancers of the colon and rectum, etoposide has been deemed ineffective in such cancers, and is not a tenable treatment option[12–14]. Recent studies in the Neufeld lab have revealed that APC associates with TopoIIα, and fragments of APC can alter the catalytic activity of TopoIIα *in vitro*[9,10]. We hypothesized that part of the resistance mechanism of colorectal cancers to TopoII-targeting drugs was due to mutation of APC. As a first step to test this, I queried the Genomics of Drug Sensitivity in Cancer (GDSC) database to analyze the half maximal inhibitory concentration (IC50) of different chemical compounds and cell lines harboring mutation of *APC* or other genetic events[15–17]. The GDSC has collected over 1000 genetically characterized human tumor cell lines, and determined IC50 values for a large panel of compounds under similar growth conditions to minimize the effect of environmental variation. Figure 4.1A shows the fold change IC50 of cells (pan-cancer) harboring mutant *APC* vs wild-type *APC*. The specific target of each compound is listed below the x-axis. Raw data are provided in supplemental materials. Cells with mutated *APC* show an increased resistance to compounds targeting topoisomerase I or II as compared to compounds that target other proteins of the Wnt signaling pathway. As one might expect, cells with mutation of *APC* show a slight sensitivity to compounds currently used as therapeutics for colorectal cancer (80% of which contain *APC* mutations). Figure 4.1B compares cells with genes commonly mutated

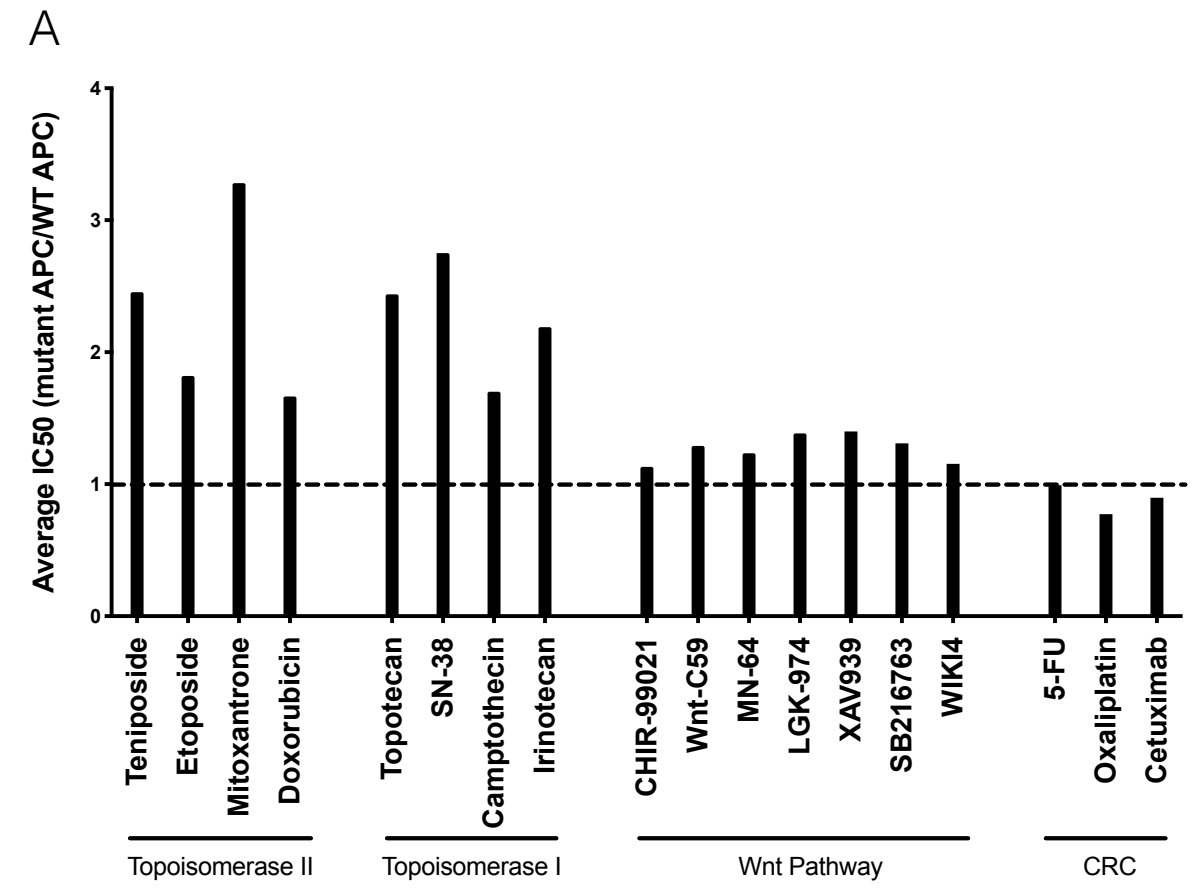
A
Average IC50 (mutant APC/WT APC)
4
3
2
1
0
Teniposide
Etoposide
Mitoxantrone
Doxorubicin
Topotecan
SN-38
Camptothecin
Irinotecan
CHIR-99021
Wnt-C59
MN-64
LGK-974
XAV939
SB216763
WIKI4
5-FU
Oxaliplatin
Cetuximab
Topoisomerase II
Topoisomerase I
Wnt Pathway
CRC

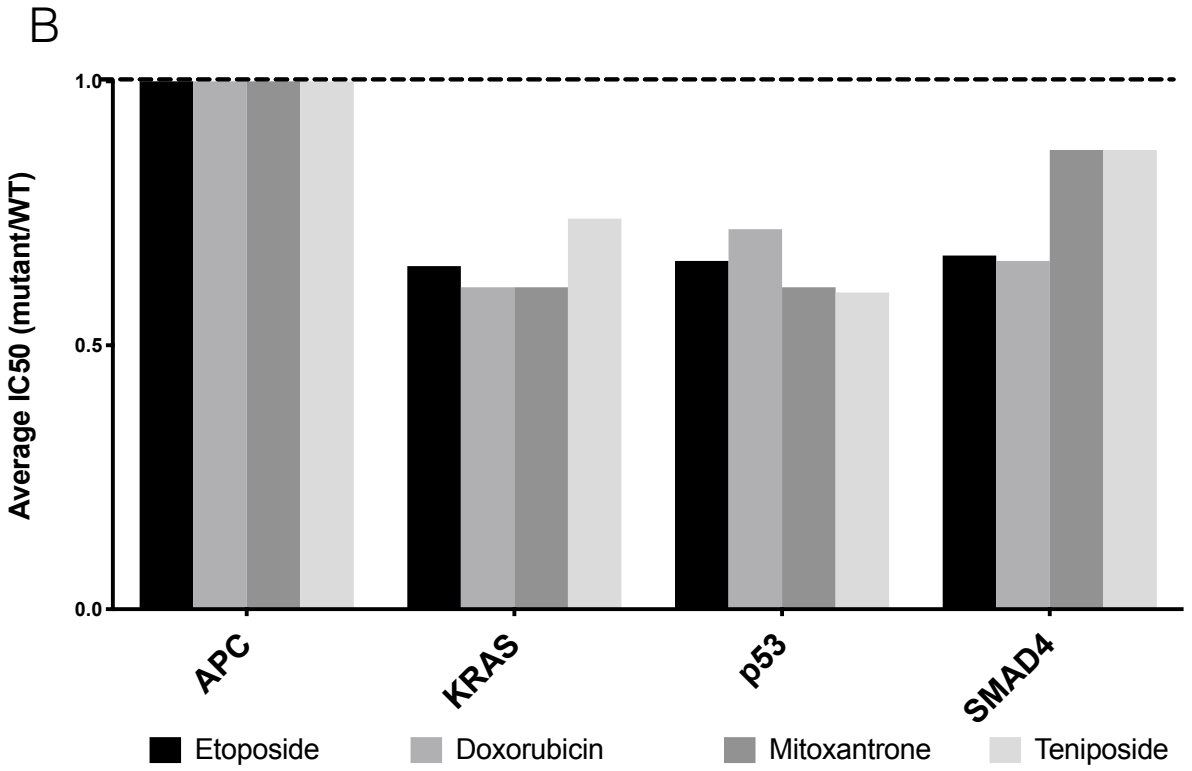
B
Average IC50 (mutant/WT)
1.0
0.5
0.0
APC
KRAS
p53
SMAD4
Etoposide
Doxorubicin
Mitoxantrone
Teniposide

Figure 4.1 APC Mutant Cells Resistance to TopoIIα Targeted Therapeutics A) IC50 values for a panel of compounds expressed as average IC50 in cell lines containing mutant *APC* compared to wild-type APC. Higher values indicate that cells with mutant *APC* are more resistant to compounds targeting topoisomerase than cells with wild-type *APC*. Notably, cells with mutant *APC* are more sensitive than cells with wild-type *APC* to compounds included in standard therapy for colorectal cancer (CRC). B) IC50 of four different TopoIIα-targeting compounds in cells of all cancer types containing four of the most common colorectal cancer mutations. For each mutation, the average IC50 is compared to the average IC50 of *APC* mutant lines which are set at a value of 1. Cells with *APC* mutations are more resistant to TopoIIα targeted compounds than cells with mutations of *KRAS*, *p53*, and *SMAD4*. Data sourced from the Genomics of Drug Sensitivity in Cancer database, a joint project by the Sanger Institute and Massachusetts General Hospital Cancer Center[15–17].

in colorectal cancer. Cells with *APC* mutations are more resistant to drugs targeting topoisomerase than are cells with mutations in *KRAS*, *SMAD4*, or *p53*. Together, our analysis of this dataset indicate that *APC* mutation correlates with an increased resistance to chemotherapeutic agents that target topoisomerase.

Generation of a novel anti-APC IgY antibody

Current commercially available antibodies for the analysis of APC have limited applications and specificity[18,19]. Our most reliable APC antibody was developed and characterized by our lab in a rabbit host[20]. Likewise, the most reliable antibody available to specifically probe TopoIIα and not TopoIIβ (requiring C-terminal domain specificity) was also raised in a rabbit[21]. To overcome this limitation and expand the repertoire of antibody species available, we generated a chicken polyclonal antibody using the same central region of APC (amino acids 1001-1326) which we had successfully used to generate rabbit antisera[20]. The new IgY antibody was purified from yolk extracts and tested by western immunoblot (Figure 4.2A). The major band detected by the purified antibody migrated with an apparent molecular weight of 310 kDa with only faint signals for the smaller sized bands. When compared to a commercially available APC antibody, and our in-house generated rabbit APC antibody, our chicken antibody shows a robust signal. Using siRNA to efficiently knockdown APC, we confirm that the 310 kDa band is reduced upon APC-depletion (Figure 4.2B). This new tool will allow specific detection of APC, simultaneously with other proteins detected using mouse or rabbit antibodies.

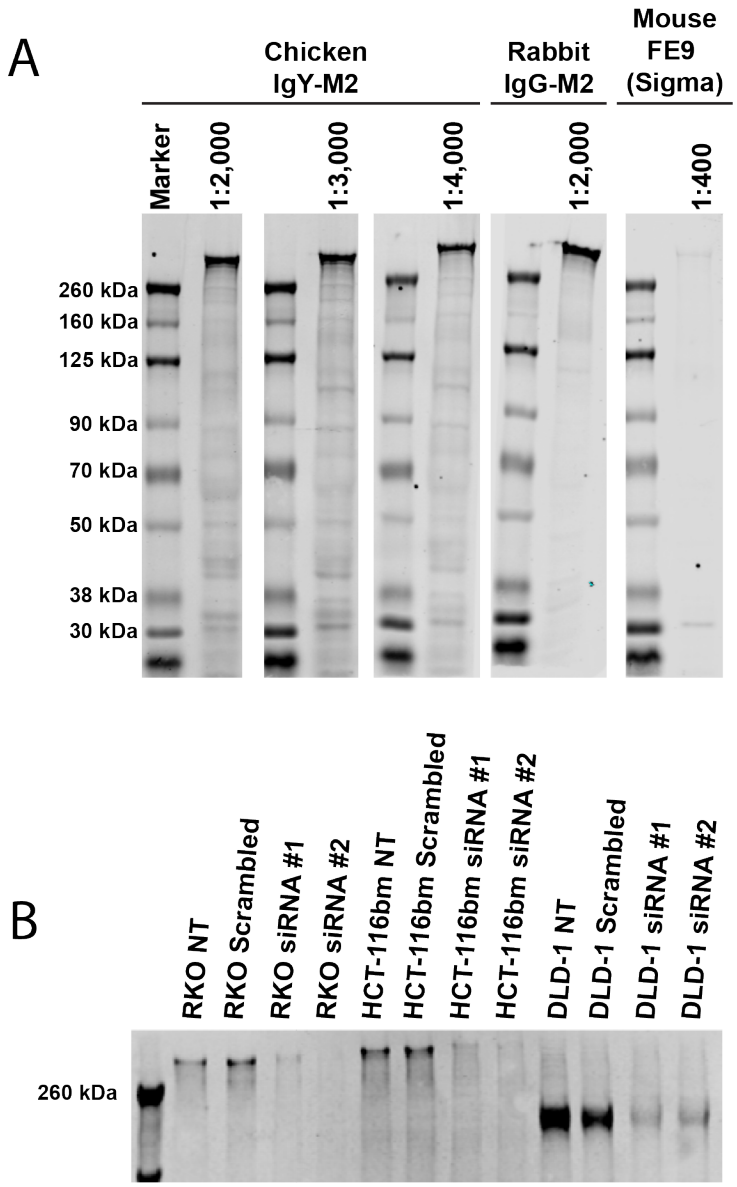

Figure 4.2 Validation of new anti-APC IgY-APC A) Western blot of HCT116βm cell lysates separated by SDS-PAGE and transferred to 0.45μm nitrocellulose membrane. The membrane was cut into strips and probed with varying concentrations of the chicken IgY APC-M2 antibody, our previously developed rabbit APC-M2 antibody, or FE9 antibody (Millipore Sigma). Each lane is flanked by Chameleon DuoLadder (LI-COR). B) siRNA-mediated knock-down of APC. Reduction of band at ~310 kDa for RKO and HCT116bm and ~160 kDa for DLD-1 confirms APC protein detection by our IgY antibody. NT = No Treatment

APC Associates with TopoIIα and β-catenin in the nucleus, but not TCF4

β-catenin forms a complex in the nucleus with LEF/TCF4 to drive transcription[22,23]. TopoIIα can co-immunoprecipitate with both β-catenin and TCF4, indicating TopoIIα may have a role in β-catenin/TCF4-mediated transcriptional activity[24,25]. APC is present in the nucleus, alters TopoIIα catalytic activity, and can bind β-catenin directly. Therefore, we hypothesized APC would also be present in this transcriptional complex. Figure 4.3 shows the immunoprecipitation of APC from the nuclear extracts of RKO (wild-type APC) and DLD-1 (truncated APC) cells using our rabbit IgG APC antibody. While both TopoIIα and β-catenin were able to co-precipitate with APC, we did not detect TCF4 as a part of this complex. Counter to our hypothesis, this observation indicates that APC is not part of the TCF/β-catenin transcriptional complex.

Cellular TopoIIα levels correlate with APC levels

TopoIIα levels are elevated in colorectal cancers, and positively associate with advanced disease[26,27]. Due to the high rate of *APC* mutation in CRC, we hypothesized that *APC* mutation directly leads to TopoIIα upregulation. A panel of CRC cell lines expressing both wild-type and truncated (mutant) APC was analyzed for expression of APC and TopoIIα. Figure 4.4A shows a representative Western blot from total cell lysates from each indicated cell line. Two different loading controls were used in this analysis, β-actin and HSC70. As an additional standard for image quantification, each Western blot contained a 2-fold and a 10-fold dilution of one lysate to ensure linearity of signal. Figure 4.4B and C shows plots of the quantified protein levels normalized against β-actin and HSC70, respectively. While we did not observe TopoIIα levels

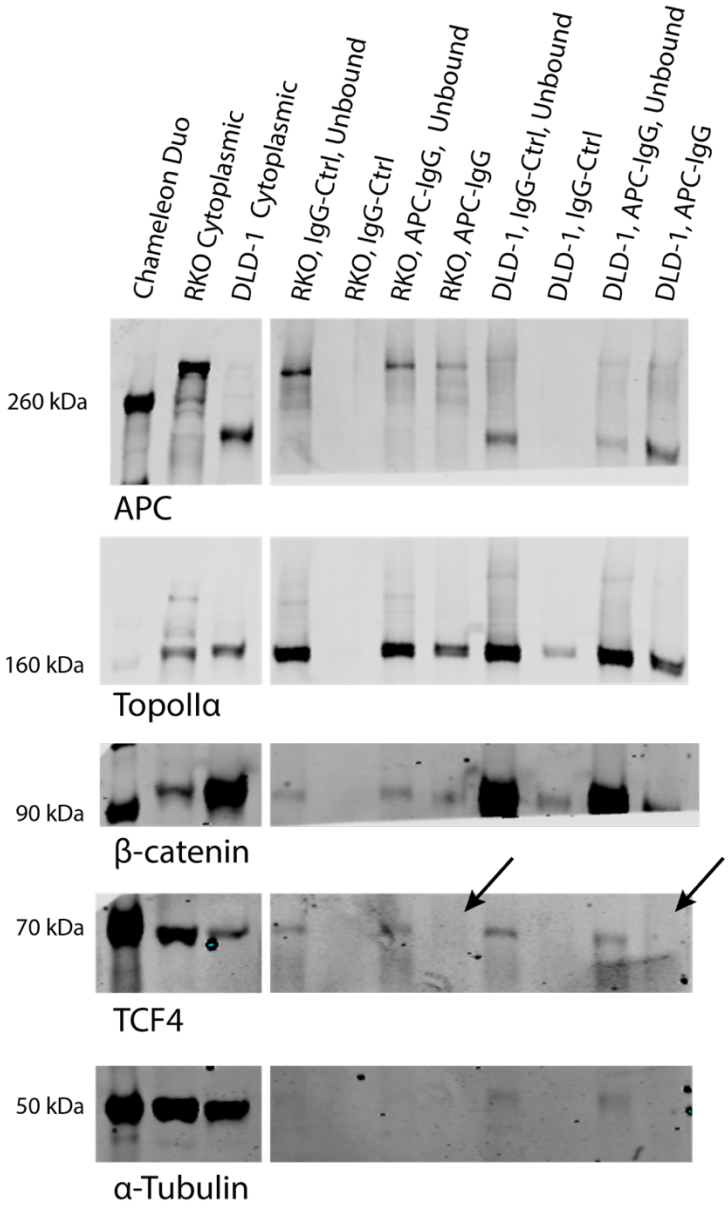

Figure 4.3 Immunoprecipitation of APC Nuclear extracts of RKO (APC wild type) or DLD-1 (APC mutant) cells were incubated with Dynabeads conjugated with anti-APC antibodies. Proteins pulled down analyzed by Western blot. Left two columns show cytoplasmic fractions from nuclear extract. IgG controls show no non-specific binding for RKO cells, with some non-specific binding for DLD-1 cells. Black arrows indicate absence of bands for TCF4, indicating APC is not in a complex with TCF4 in the nucleus.

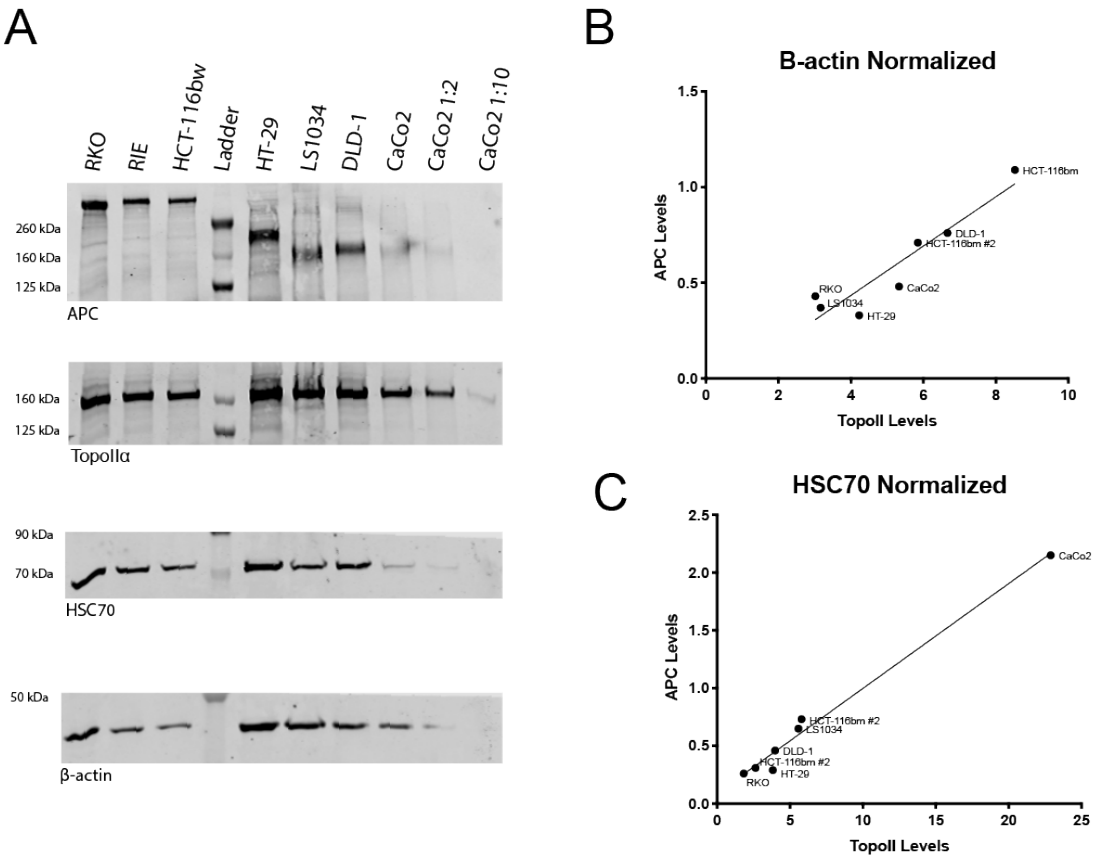

Figure 4.4 Protein Levels of APC and TopoIIα A) Western blot of APC and TopoIIα, with HSC70 and β-actin as loading controls. Far right two lanes representative of signal linearity test for accurate quantification. B) Levels of APC plotted against levels of TopoIIα. Strong correlation observed when normalized to β-actin. C) Levels of APC plotted against levels of TopoIIα. Strong correlation observed when normalized to HSC70.

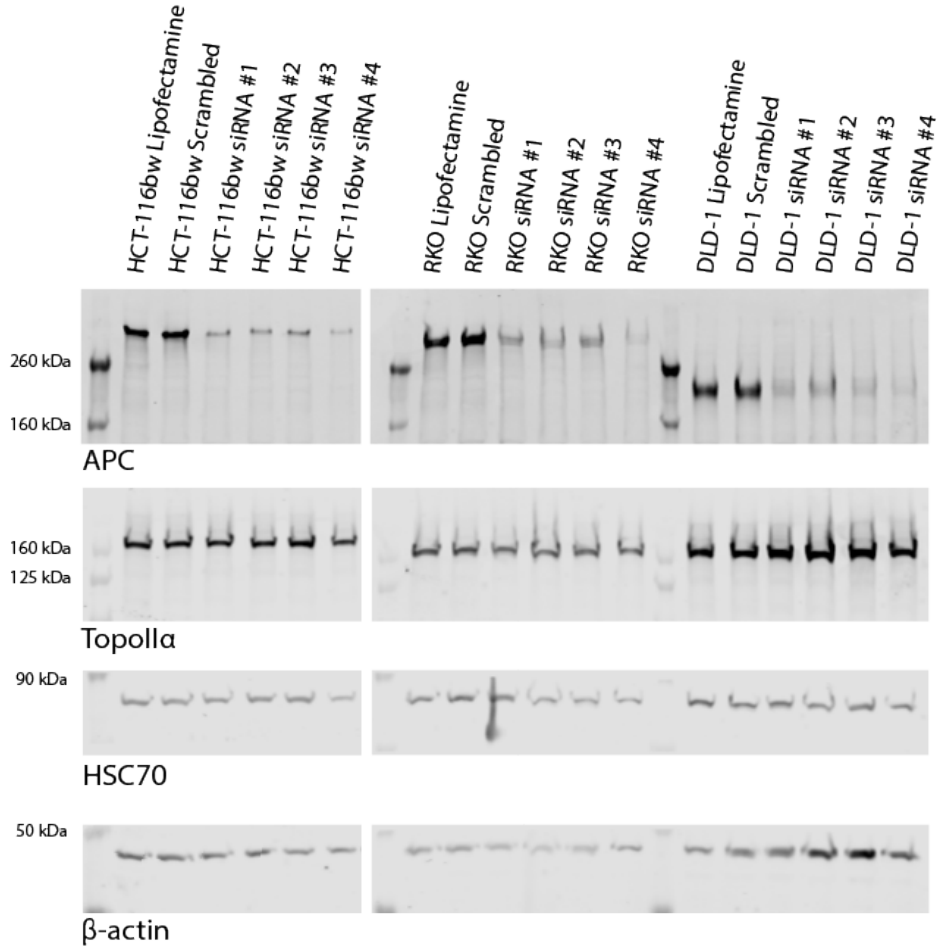

Figure 4.5 siRNA mediated APC depletion does not alter TopoIIα level. Four different RNA's tested, to account for possible off-target effects. Lipofectamine only used as control. Topoisomerase IIα levels were similar in siRNA treated cells and control cells.

increase in our *APC*-mutant cell lines, interestingly, we did observe a correlation between total levels of TopoIIα and APC regardless of APC mutation status.

To determine if our observed correlation of protein levels was a result of TopoIIα regulation by APC, we used siRNA to reduce endogenous APC protein levels. Western blots were quantified as before. Figure 4.5 shows that upon APC depletion, TopoIIα levels remained unchanged, indicating that APC does not directly control the cellular levels of TopoIIα.

TopoIIα shows higher catalytic activity in APC mutant or null cells

Previous work in the Neufeld lab revealed that fragments of APC could alter the catalytic activity of TopoIIα *in vitro*[9,10]. Additionally, it was found that TopoIIα activity was severely diminished in nuclear extracts from HCT116-βw cells expressing exogenous fragments of APC containing the 15-aa repeat region (APC-M2) or the 20-aa repeat region (APC-M3) (unpublished data). HCT116-βw cells express wild-type APC, so this effect could be a dominant negative function of the APC fragments. To investigate this further, nuclei were extracted from a panel of colon cancer cell lines expressing wild type, mutant, or no APC. Nuclear extracts were then assayed for TopoIIα to determine the TopoIIα catalytic efficiency of endogenous WT- and mutant APC. Figure 4.6 shows that TopoIIα activity is 30-40% higher in cells that are either APC-null or cells expressing mutant APC.

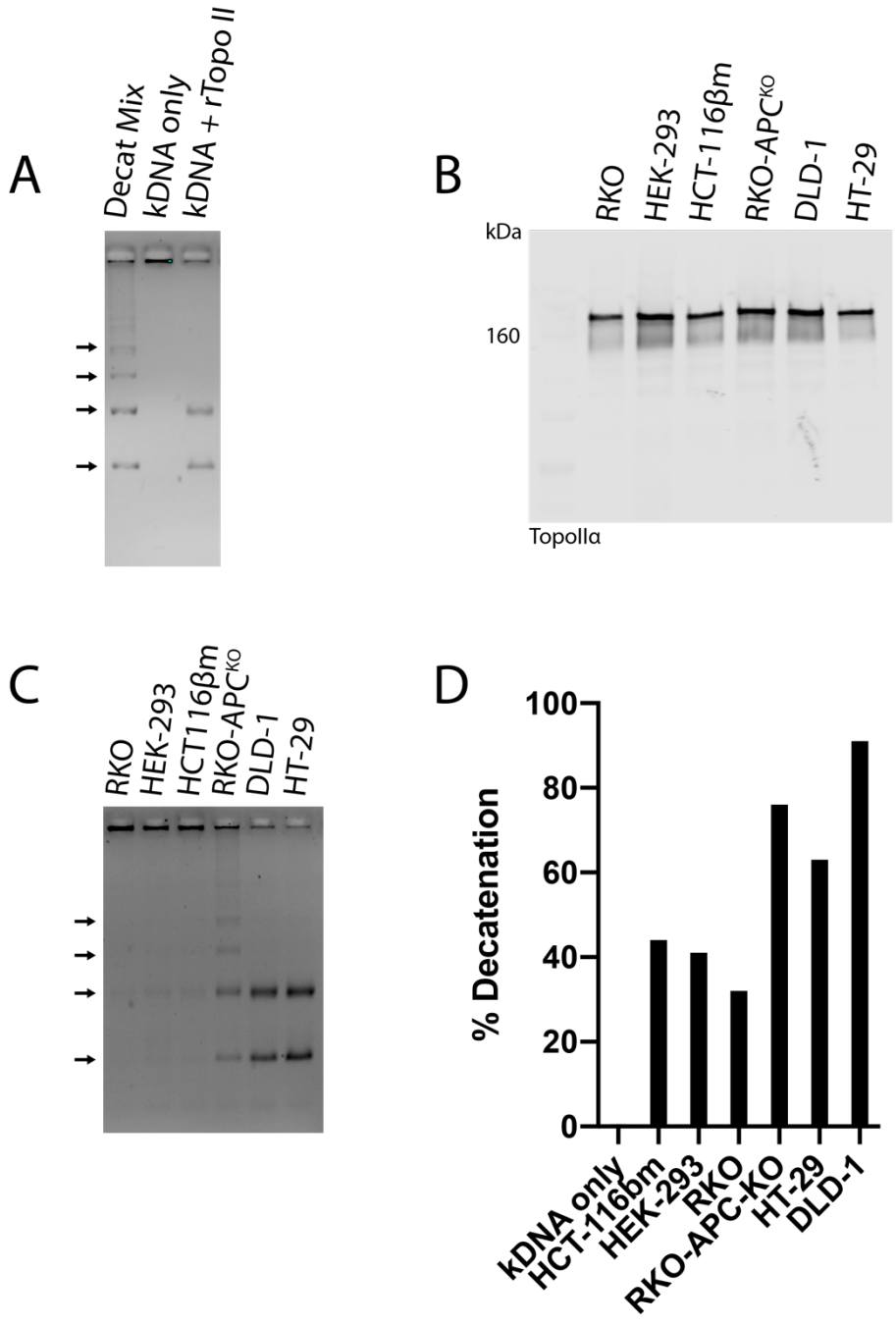

Figure 4.6 TopoIIα Catalytic Activity Assay A) Positive control for assay, recombinant TopoIIα (TopoGen) showing efficient decatenation of catenated kDNA (TopoGen). Catenated DNA is unable to migrate out of the well. Decatenated DNA marked by arrows. B) Western blot of nuclear extracts used as source of TopoIIα for decatenation assay. Used to normalize for

TopoIIα levels in assay. C) Decatenation assay with a panel of colon cancer cells expressing wild-type APC (RKO, HEK-293, HCT115βm), null APC (RKO-APC^{KO}), or mutant APC (DLD-1, HT-29). Catenated DNA is unable to migrate out of the well. Decatenated DNA marked by arrows. D) Plot of decatenation assay, normalized for TopoIIα levels from Western blot. Plot shows cells with wild-type APC have decreased TopoIIα decatenation activity compared to APC null or APC mutant cells.

Discussion

Cancer is a highly heterogenous disease, which varies greatly from person to person and tissue to tissue. Mechanisms of resistance to cancer therapeutics can be derived intrinsically (i.e. before therapy is applied) or can be acquired by selective pressure by the therapy itself[28]. Polytherapy or combination therapy is an approach to treatment that attempts to hit multiple molecular targets at once[28–30]. Targeting the mechanisms of resistance is one strategy of combination therapy that aims to re-sensitize a cancer cell to first-line treatments designed to induce cell death. For this approach to be effective, mechanisms of resistance must be well-understood and characterized. In the context of colorectal cancer, understanding molecular mechanisms of resistance to TopoIIα-targeting compounds remains a gap in the knowledge.

To begin to address this gap, we hypothesized that there was a connection between TopoIIα-targeting compounds and APC status. To test this hypothesis, we mined data from the Genomics of Drug Sensitivity in Cancer database. This database is an ongoing project containing (as of June 2020) 446,146 dose-response curves for 518 compounds across 1000 cell lines, with 693 genetic features, including *APC* mutation[31]. From this analysis, we observed that cells with *APC* mutation had an increased resistance to topoisomerase-targeting compounds compared to other chemotherapeutic compounds. As a note, one must carefully interpret results from this screen, as several IC50s fall outside the maximum screening conditions (see supplemental data provided). However, I believe the trends observed are important and that the resistance observed indicates that APC may be playing a mechanistic role in colon cancer chemotherapeutic resistance. Additionally, I propose that screening for APC mutation could be an important step in deciding which treatment options to use for CRC and cancers of other organs. In the case of

colorectal cancer, 20% do not contain mutation to *APC*[1]. This smaller subset of cancers may be responsive to topoisomerase-targeting drugs such as etoposide.

We next hypothesized that cells expressing mutated *APC* would have decreased levels of TopoIIα, as down-regulation of TopoIIα has been proposed as a mechanism of resistance[32,33]. However, we did not observe TopoIIα to be down- or up-regulated dependent on APC status. We did observe a correlation to total cellular levels between APC and TopoIIα, however depletion of cellular APC had no effect on overall TopoIIα levels. Whether the noted correlation was simply due to a relatively small sample size or if this association is physiologically relevant will need to be studied further.

We next sought to determine if APC might associate with TopoIIα along with β-catenin and TCF4, as it has been reported that TopoIIα is a part of the β-catenin transcriptional complex[24]. While we were able to co-immunoprecipitate TopoIIα and β-catenin using antibodies raised against APC, we were unable to detect TCF4. β-catenin binds to APC and TCF4 using the same armadillo groove, a binding event that has been reported to be mutually exclusive[34]. Therefore, we attribute the presence of APC in this complex to an association through TopoIIα. Our data indicates that the nuclear pool of APC bound to β-catenin and/or TopoIIα is independent from the β-catenin transcriptional complex.

Previous data from our lab indicated that fragments of APC could alter the catalytic activity of TopoIIα *in vitro*. We hypothesized that truncation mutants of APC would also alter the catalytic activity of TopoIIα. To test this idea, we extracted the nuclei from a panel of colon cancer cell lines and analyzed protein extracts for TopoIIα activity. Surprisingly, TopoIIα activity was increased in cells with mutant APC and a cell line with no APC when compared to cells with wild type APC. We had expected the catalytic activity of TopoIIα to weaken in the

presence of mutant APC, as was observed during *in vitro* assays using recombinant protein. This discrepancy is likely due to all other proteins of the nucleus being present in the extract, as opposed to only TopoIIα and APC fragments in the assays with recombinant protein. APC's ability to bind multiple proteins at once and scaffold complexes almost certainly means that while it may be able to associate with TopoIIα, other unidentified proteins are likely present as well. If TopoIIα catalytic activity was increased only in APC-mutant cells, a dominant-negative effect could be occurring. However, the increased activity in the APC-null RKO-APC^{KO} cells complicates this theory. It would appear that wild type APC, or more specifically the C-terminal domain of APC, functions to restrict the catalytic activity of TopoIIα. It will be interesting to probe the effects of the C-terminal domain of APC on the catalytic activity of TopoIIα. Understanding how mutant APC is contributing to TopoIIα activity and resistance to TopoIIα targeting compounds will be important for expanding treatment options for colorectal cancer.

Materials and Methods

Generation of anti-APC-M2 Chicken IgY Antibody

The central region of APC (amino acids 1001-1326, "APC-M2") was cloned and ligated into the pET28b (Novagen) expression vector, which contains an N-terminal 6X-His tag. Sequence-verified plasmids were transformed into BL21-CodonPlus-(DE3)-RIPL *E. coli* cells (NEB) for expression. Cells were grown in standard LB broth containing 50 μg/mL kanamycin at 37°C with shaking (225 rpm) and induced with 0.2 mM isopropyl-β-D-thiogalactopyranoside (IPTG) for protein expression when an OD of 0.4-0.6 was reached. Cells were allowed to express induced protein product for 3-4 hours at 37°C with shaking before harvested by centrifugation at 4,000 rpm, 15 min, 4°C. Cellular pellets were resuspended in a buffer containing 50 mM Tris pH

8.0, 50 mM NaCl, 50 mM imidazole, 10% glycerol, and HALT protease cocktail (Thermo). Cells were lysed by a French pressure cell (35,000 psi), and the insoluble cellular debris was removed by centrifugation at 16,000 x g for 45 min, 4°C. Supernatant was applied to a chelating sepharose fast-flow column (Amersham Biosciences) charged with nickel chloride and pre-equilibrated in resuspension buffer. Protein retained on the column was washed with a 3 column volumes (C.V.) salt gradient (50 mM potassium phosphate pH 8.0, 500 mM NaCl, 50 mM imidazole, 10% glycerol). Protein was eluted with an imidazole buffer gradient (50 mM Tris pH 8.0, 500 mM NaCl, 500 mM imidazole, 10% glycerol). Fractions containing recombinant protein were pooled and applied to a Superdex 200 size-exclusion column (Amersham Biosciences) pre-equilibrated with 50 mM Tris, pH 8.0, 150 mM NaCl, and 10% glycerol, 1 mM DTT, and 1 mM octyl β-D-gluctopyranoside. Fractions containing recombinant protein were pooled and concentrated with Amicon Ultra centrifugal filters (Millipore).

Recombinant APC antigen was shipped to Gallus Immunotech Inc. (now Exalpha Biologicals, Inc.) for injection into hens, and extraction of IgY-containing yolk extract. The anti-APC IgY was purified from the returned yolk extracts by affinity chromatography. Briefly, NHS-Sepharose (GE Healthcare) was conjugated with APC-M2 antigen, purified as described above. 1M Tris (pH 8.0) and Tween-20 were added to the yolk extracts, to final concentrations of 10 mM and 0.2%, respectively. Buffered yolk extract was incubated with prepared APC-M2-conjugated NHS-Sepharose overnight at 4°C. Columns were washed with multiple column volumes of PBS and PBS-T buffers. Anti-APC-M2 IgY was eluted from the column in 0.2M glycine, pH 2.0. Fractions containing eluted anti-APC-M2 IgY were dialyzed into a buffer containing PBS at pH 7.4, 5% glycerol, and 0.01% sodium azide.

Western Blotting and Quantification

All cells were harvested at 60-80% confluency. Cells were first briefly washed in phosphate buffered saline (PBS). Cells were directly lysed in a high-salt sample lysis buffer (20% glycerol, 2% SDS, 30% 5X PBS, 2.5% β-mercaptoethanol) heated to 95°C. Cells were scraped from the wells and transferred to Eppendorf tubes and heated at 95°C for 1 min. Lysate was then pulled through an insulin syringe three times to lyse DNA, and heated again for 3 min. Samples were separated on 7.5% SDS-PAGE (Bio-Rad, TGX FastCast Acrylamide Kit) using Tris-Glycine running buffer and transferred to a nitrocellulose membrane (GE) with a 0.45-μm pore size. Antibodies were diluted in Odyssey Blocking Buffer TBS (LI-COR) as follows: anti-APC-M2 Chicken pAb (1:2,000), anti-TopoIIα rabbit pAb (1:4,000), anti-β-actin mouse mAb (Sigma, 1:2,000), anti-TCF4 rabbit mAb (Abcam, 1:500), anti-HSC70 rat mAb (Abcam, 1:1000) and IRDye 680LT and 800CW anti-rabbit, anti-mouse, anti-rat, or anti-chicken secondary antibodies (1:15,0000). Immunoblots were imaged on a Li-Cor Odyssey CLx imaging system and quantified using Image Studio software (Li-Cor).

APC Knockdown and Immunoprecipitation

Human cell lines were cultured in Dulbecco's Modified Eagle Medium (DMEM) supplemented with 10% fetal bovine serum. For knockdown of APC, cells were transfected with siRNAs targeting APC (Dharmacon) using Lipofectamine 3000 (Invitrogen) according to manufacturer's protocol. For the immunoprecipitations, cells were first harvested at 60-80% confluency. Cells were washed with cold PBS, gently scraped into PBS, and spun for 3 minutes, 1000 x G, 4°C. The cell pellet was resuspended in hypotonic lysis buffer (10 mm HEPES, pH 7.5, 1.5 mm $MgCl_2$, 10 mM KCl) with HALT protease inhibitor (Thermo) and incubated for 15 min at 4°C with rotation. Cell membranes were lysed by drawing solution through a 26-gauge syringe 7-10

times. Lysate was spun for 5 min, 1000 x G, 4°C to give a pellet containing insoluble material and intact nuclei. Supernatant contained the soluble cytoplasmic fraction, and was removed for analysis. The nuclear pellet was rinsed with hypotonic buffer, then re-suspended and incubated in a low-salt buffer (10 mM Tris, pH 7.4, 2 mM $MgCl_2$, 1% Triton-X100) with HALT protease inhibitor for 25 min at 4°C. Following incubation in low-salt buffer to lyse nuclear membrane, nuclear extracts were sonicated for 2 minutes using a Covaris S220 with the following settings: PIP = 140, Duty Factor = 5%, CPB = 200. After sonication, nuclear extracts were spun for 5 min, 1000 x G, 4°C. Supernatant was then pre-cleared by incubation with Protein G beads (Thermo) and 100 mM NaCl. Protein G beads were removed, and Dynabeads (Thermo) conjugated with our rabbit APC-M2 antibody were added to the nuclear extract, and incubated overnight at 4°C. Beads were washed with TBS and TBS-T before elution in sample lysis buffer. Protein samples were separated by SDS-PAGE and analyzed by Western blot.

Nuclear Extractions

Cells were grown in 10 cm dishes in DMEM supplemented with 10% fetal bovine serum. Cells were harvested at ~80% confluency. Cells were washed with cold PBS, gently scraped into PBS, and spun for 45 seconds, 2000 x G, 4°C. PBS was removed, and cell pellet was resuspended in hypotonic lysis buffer (10 mm HEPES, pH 7.5, 1.5 mm $MgCl_2$, 10 mM KCl) with HALT protease inhibitor (Thermo) and incubated for 15 min at 4°C with rotation. Cell membranes were lysed by drawing solution through a 26-gauge syringe 7-10 times. Lysate was spun for 45 seconds, 21,000 x G, 4°C producing a crude nuclear pellet. Supernatant was removed as the cytoplasmic fraction. The nuclear pellet was resuspended in a high-salt buffer (20 mM HEPES, 420 mM NaCl, 1.5 mM $MgCl_2$, 0.2 mM EDTA, 25% glycerol, pH 7.5) and incubated for 30 min

at 4°C with rotation, with vortexing every ~5 min. Nuclear lysate was spun for 5 min, 21,000 x G, 4°C. Supernatant was removed as the nuclear extract. Nuclear extract was dialyzed against a buffer containing 20 mM HEPES, 100 mM KCl, 0.2 mM EDTA, 20% glycerol, pH 7.5 to lower the concentration of salt. Dialyzed extract aliquots were frozen in liquid nitrogen until use.

Decatenation Assays

Decatenation assays (TopoGen) were performed according to manufacturer's protocols. Briefly, frozen nuclear extracts were thawed, and total protein concentration determined by Bradford assay. Nuclear extracts were diluted so that each reaction received the same volume of nuclear extract, owing to concerns that different amounts of extract buffer skewed TopoIIα activity. kDNA substrate (TopoGen) was combined with reaction buffer and nuclear extracts for 30 min, 37°C. Stop solution was added to reaction before resolution on a 1.0% agarose gel and imaging. Bands were quantified using Image Studio (Li-Cor).

Supplemental Materials

Raw data from the Genomics of Drug Sensitivity in Cancer[15]. Brown lines on graphs denote screening maximum and minimum. For scatter plots, compound and mutation are indicated. _mut = mutant

Pan-Cancer Raw Data, Accessed July 13, 2020

		Teniposide		Etoposide		Mitoxantrone		Doxorubicin	
Topoisomerase II		APC Mutant	APC WT	APC Mutant	APC WT	APC Mutant	APC WT	APC Mutant	APC WT
	Number of Cell Lines	54	643	47	806	54	643	46	798
	Median	4.0210	1.5509	11.615	4.143	6.3676	1.6259	0.23723	0.14783
	Geometric Mean	3.7125	1.5120	8.4351	4.6329	5.0707	1.5458	0.27943	0.16791
	Fold Change (Mean)	2.4554		1.8207		3.2803		1.6642	
	Dataset	GDSC2		GDSC1		GDSC2		GDSC1	

		Topotecan		SN-38		Camptothecin		Irinotecan	
Topoisomerase I		APC Mutant	APC WT	APC Mutant	APC WT	APC Mutant	APC WT	APC Mutant	APC WT
	Number of Cell Lines	54	643	55	837	55	721	55	714
	Median	3.0777	1.0067	0.039818	0.014804	0.16809	0.080773	29.535	12.484
	Geometric Mean	2.5767	1.0569	0.034043	0.012373	0.18091	0.1064	29.401	13.428
	Fold Change (Mean)	2.4380		2.7514		1.7003		2.1895	
	Dataset	GDSC2		GDSC1		GDSC2		GDSC2	

		CHIR-99021		Wnt-C59		MN-64		LGK-974	
Wnt		APC Mutant	APC WT	APC Mutant	APC WT	APC Mutant	APC WT	APC Mutant	APC WT
	Number of Cell Lines	47	805	53	826	54	643	51	826
	Median	24.8770	23.5080	17.396	12.986	139.09	104.51	18.175	13.873
	Geometric Mean	21.9390	19.4000	15.866	12.294	136.46	110.58	18.392	13.278
	Fold Change (Mean)	1.1309		1.2905		1.2340		1.3851	
	Dataset	GDSC1		GDSC1		GDSC2		GDSC1	

		XAV939		SB216763		WIKI4	
Wnt		APC Mutant	APC WT	APC Mutant	APC WT	APC Mutant	APC WT
	Number of Cell Lines	55	642	49	773	51	669
	Median	110.1500	74.1150	102.25	85.064	39.685	38.436
	Geometric Mean	113.7000	81.2090	96.468	73.685	48.444	41.974
	Fold Change (Mean)	1.4001		1.3092		1.1541	
	Dataset	GDSC2		GDSC1		GDSC2	

		5-FU		Oxaliplatin		Cetuximab	
CRC		APC Mutant	APC WT	APC Mutant	APC WT	APC Mutant	APC WT
	Number of Cell Lines	53	826	55	715	51	794
	Median	28.0200	39.9480	22.291	44.38	518.74	491.75
	Geometric Mean	35.9100	36.2050	32.766	42.355	358.73	399.47
	Fold Change (Mean)	0.9919		0.7736		0.8980	
	Dataset	GDSC1		GDSC2		GDSC1	

Pan-Cancer Raw Data, Accessed July 13, 2020

		KRAS Mutant	KRAS WT	p53 Mutant	p53 WT	SMAD4 Mutant	SMAD4 WT
Etoposide	Number of Cell Lines	109	744	582	271	36	817
	Median	3.5830	4.3612	4.389	4.0011	4.0554	4.284
	Geometric Mean	5.5674	4.6839	5.0869	4.2053	5.8238	4.7473
	Fold Change (Mean)	1.1886		1.2096		1.2268	
	Dataset	GDSC1		GDSC1		GDSC1	
		KRAS Mutant	KRAS WT	p53 Mutant	p53 WT	SMAD4 Mutant	SMAD4 WT
Doxorubicin	Number of Cell Lines	11054	734	575	269	36	808
	Median	0.1237	0.1507	0.15296	0.14325	0.10867	0.15061
	Geometric Mean	0.1747	0.1723	0.1825	0.15331	0.1874	0.17201
	Fold Change (Mean)	1.0139		1.1904		1.0895	
	Dataset	GDSC1		GDSC1		GDSC1	
		KRAS Mutant	KRAS WT	p53 Mutant	p53 WT	SMAD4 Mutant	SMAD4 WT
Mitoxantrone	Number of Cell Lines	105	592	474	223	34	663
	Median	2.5239	1.6765	2.2382	1.2472	5.2012	1.6679
	Geometric Mean	3.0551	1.5267	2.1121	1.0616	4.6011	1.6102
	Fold Change (Mean)	2.0011		1.9895		2.8575	
	Dataset	GDSC2		GDSC2		GDSC2	
		KRAS Mutant	KRAS WT	p53 Mutant	p53 WT	SMAD4 Mutant	SMAD4 WT
Teniposide	Number of Cell Lines	105	592	474	223	34	663
	Median	2.2778	1.4690	1.7449	1.4062	3.3177	1.5273
	Geometric Mean	2.6795	1.4827	1.8302	1.2523	3.3402	1.562
	Fold Change (Mean)	1.8072		1.4615		2.1384	
	Dataset	GDSC2		GDSC2		GDSC2	

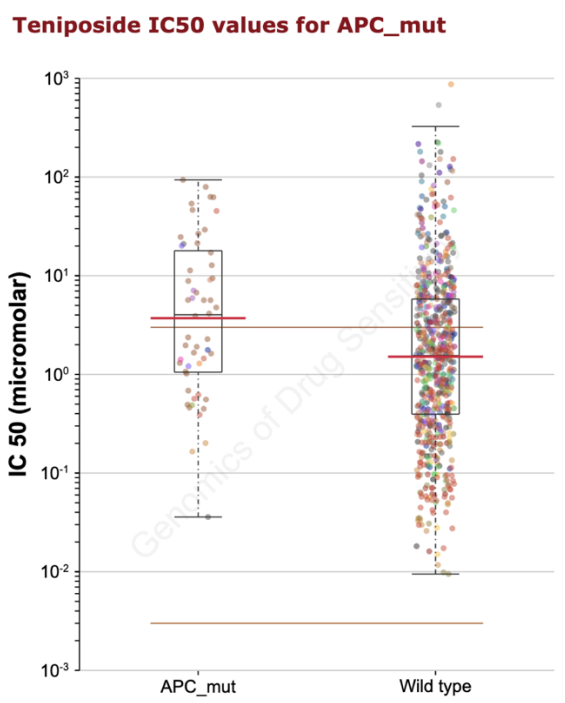
Teniposide IC50 values for APC_mut
IC 50 (micromolar)
APC_mut
Wild type

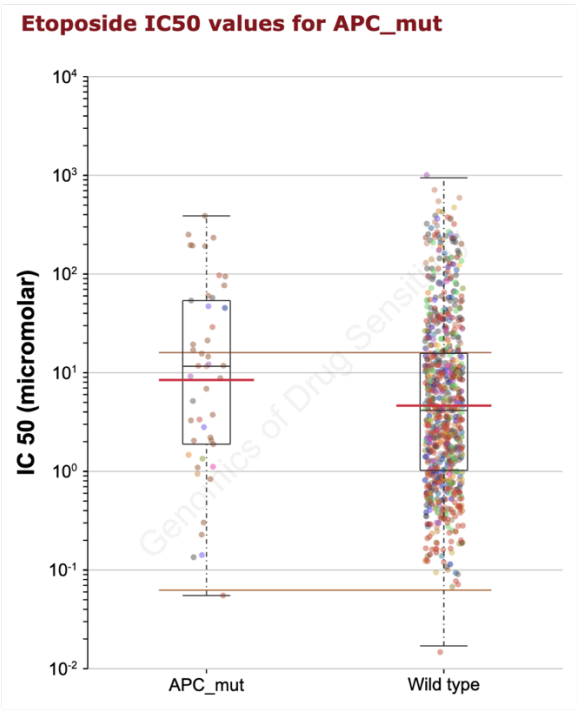
Etoposide IC50 values for APC_mut
IC 50 (micromolar)
APC_mut
Wild type

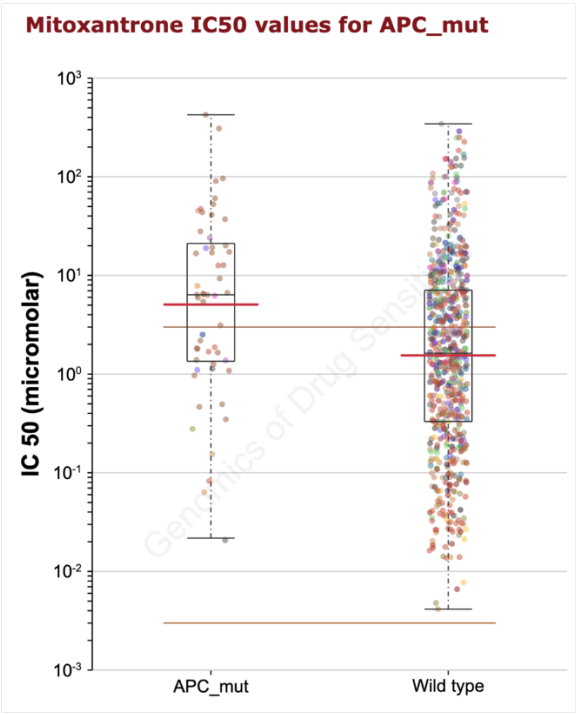
Mitoxantrone IC50 values for APC_mut
IC 50 (micromolar)
APC_mut
Wild type

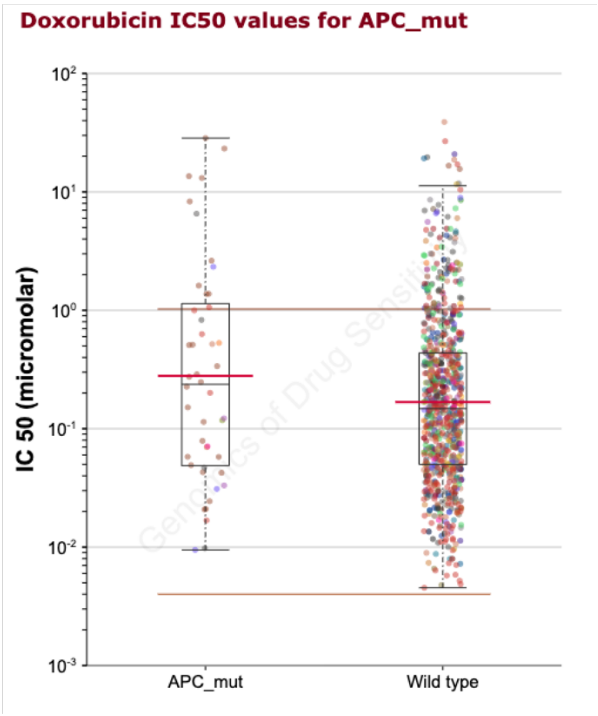
Doxorubicin IC50 values for APC_mut
IC 50 (micromolar)
APC_mut
Wild type

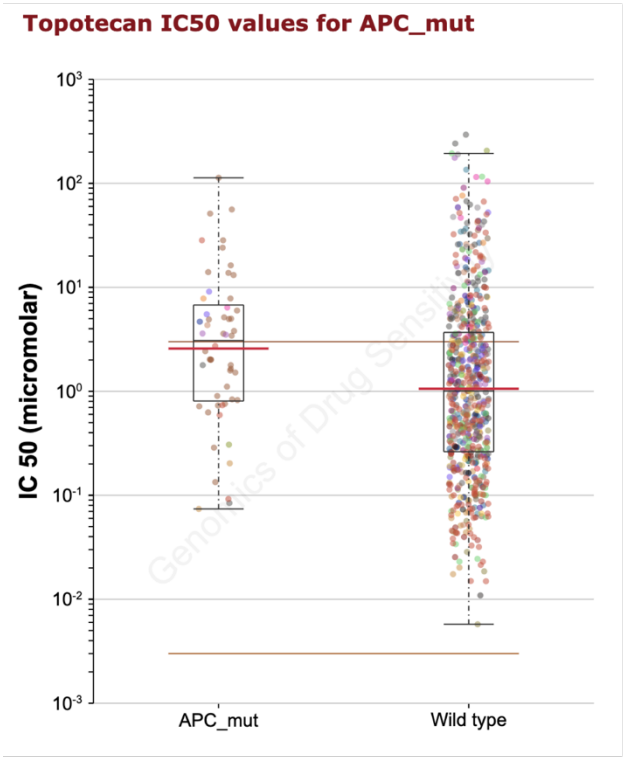
Topotecan IC50 values for APC_mut
IC 50 (micromolar)
APC_mut
Wild type

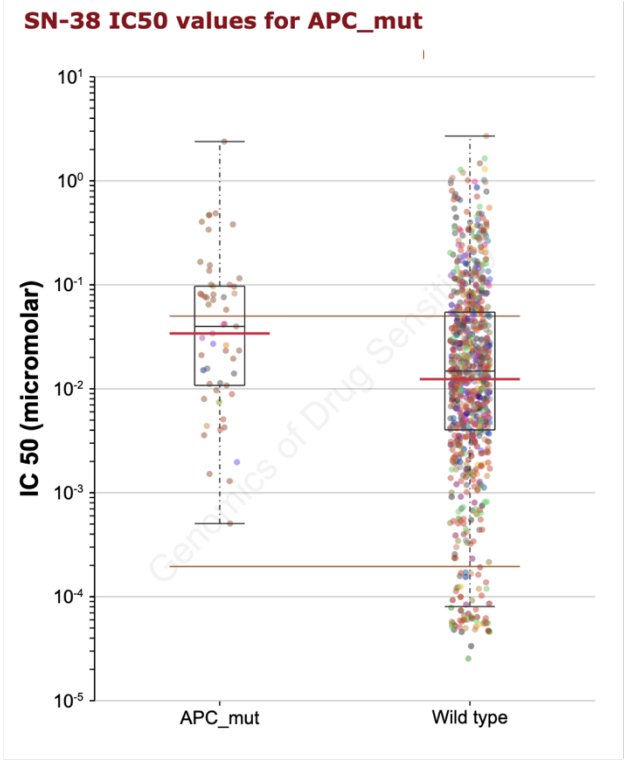
SN-38 IC50 values for APC_mut
IC 50 (micromolar)
APC_mut
Wild type

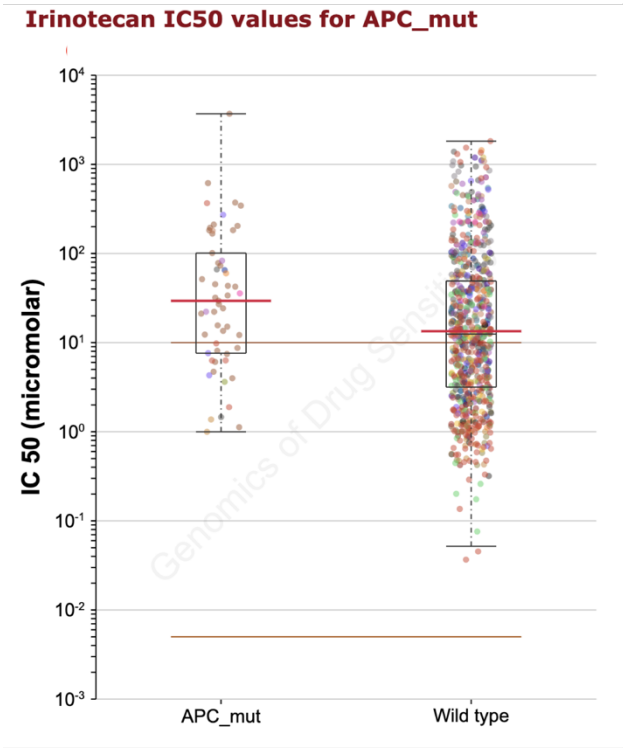
Irinotecan IC50 values for APC_mut
IC 50 (micromolar)
APC_mut
Wild type

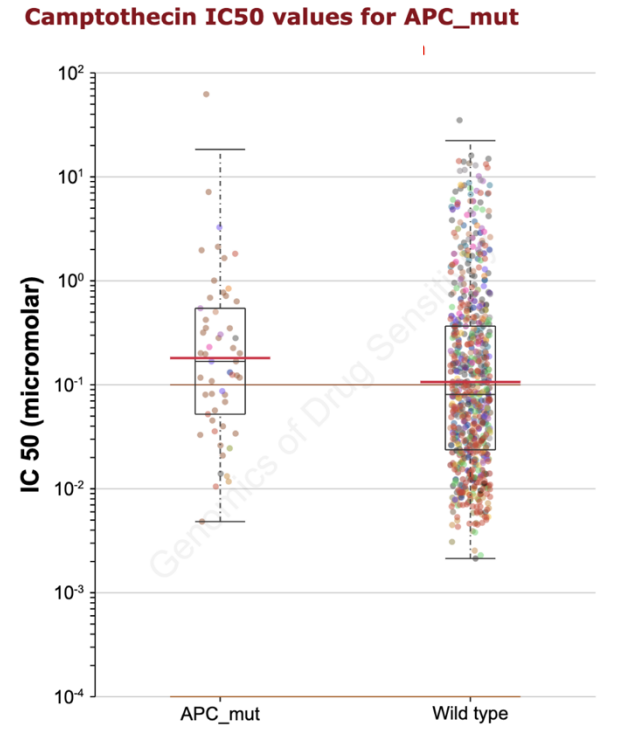
Camptothecin IC50 values for APC_mut
IC 50 (micromolar)
APC_mut
Wild type

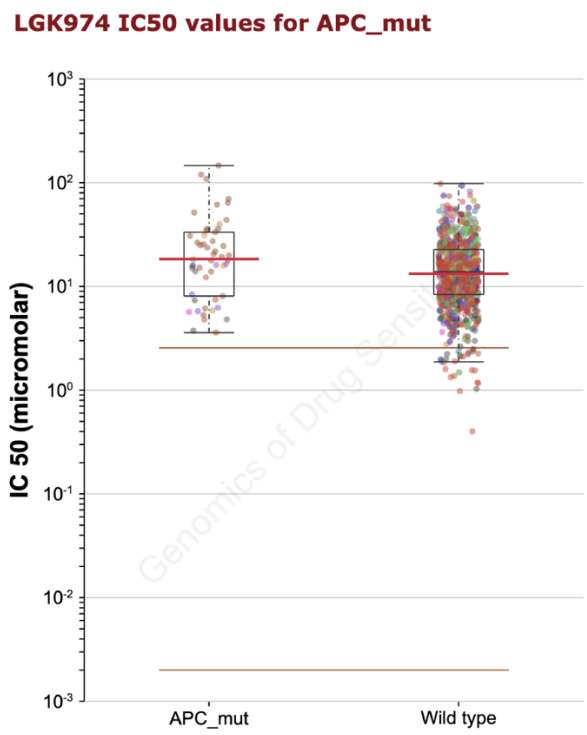
LGK974 IC50 values for APC_mut
IC 50 (micromolar)
APC_mut
Wild type

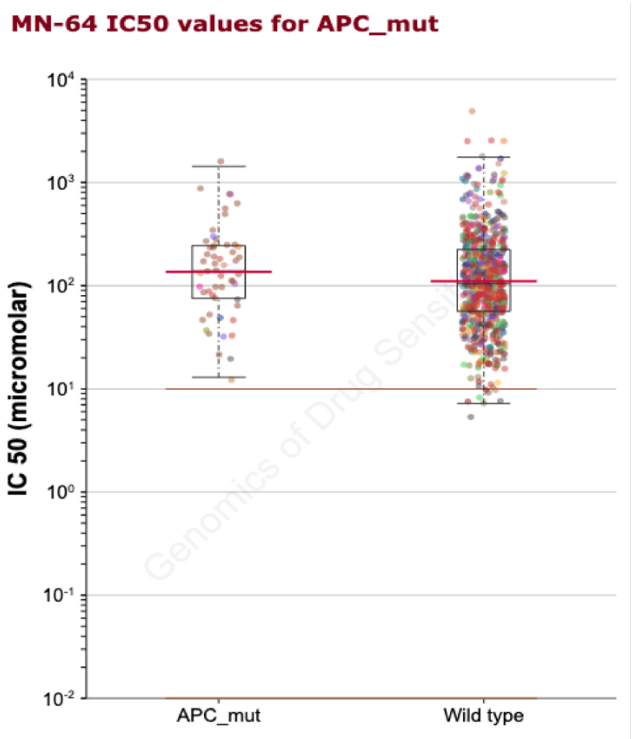
MN-64 IC50 values for APC_mut
IC 50 (micromolar)
APC_mut
Wild type

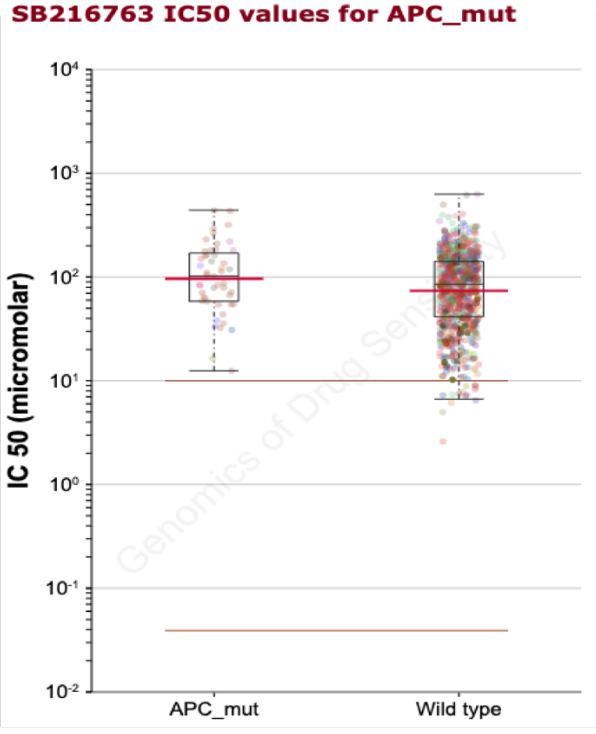
SB216763 IC50 values for APC_mut
IC 50 (micromolar)
APC_mut
Wild type

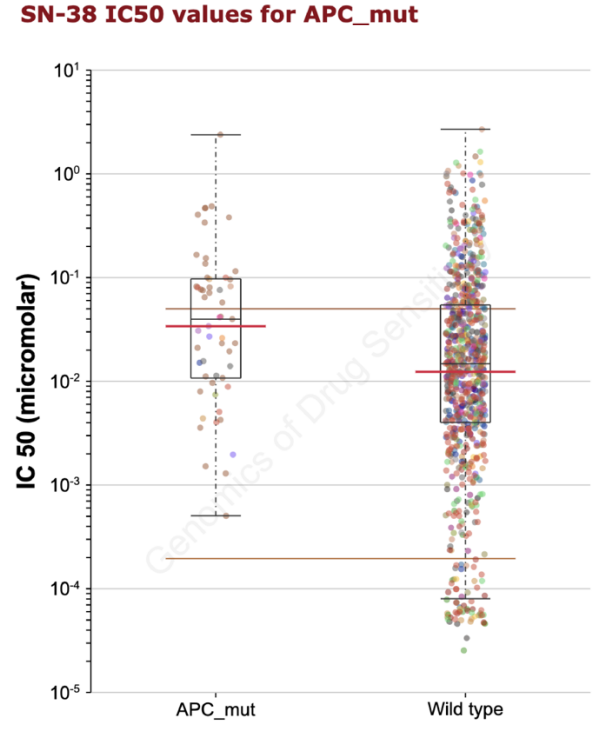
SN-38 IC50 values for APC_mut
IC 50 (micromolar)
APC_mut
Wild type

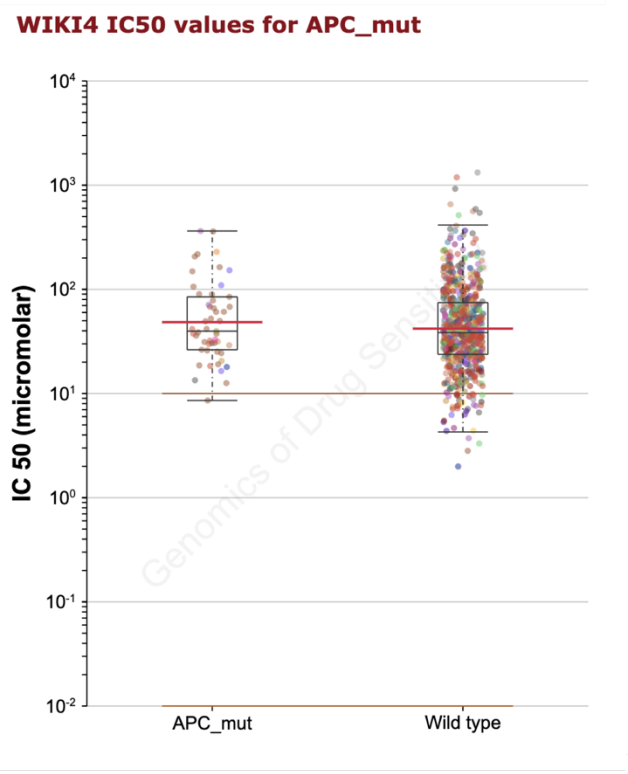
WIKI4 IC50 values for APC_mut
IC 50 (micromolar)
APC_mut
Wild type
Genomics of Drug Sensitivity

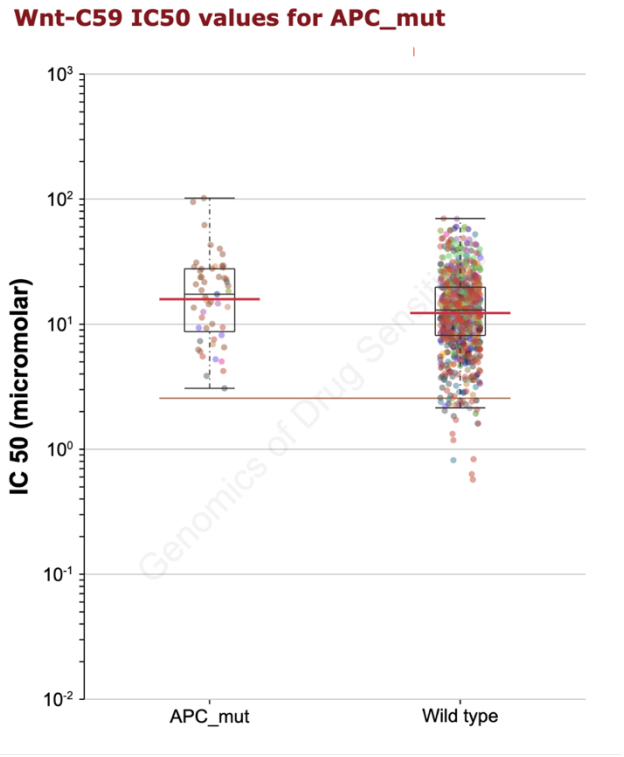
Wnt-C59 IC50 values for APC_mut
IC 50 (micromolar)
APC_mut
Wild type
Genomics of Drug Sensitivity

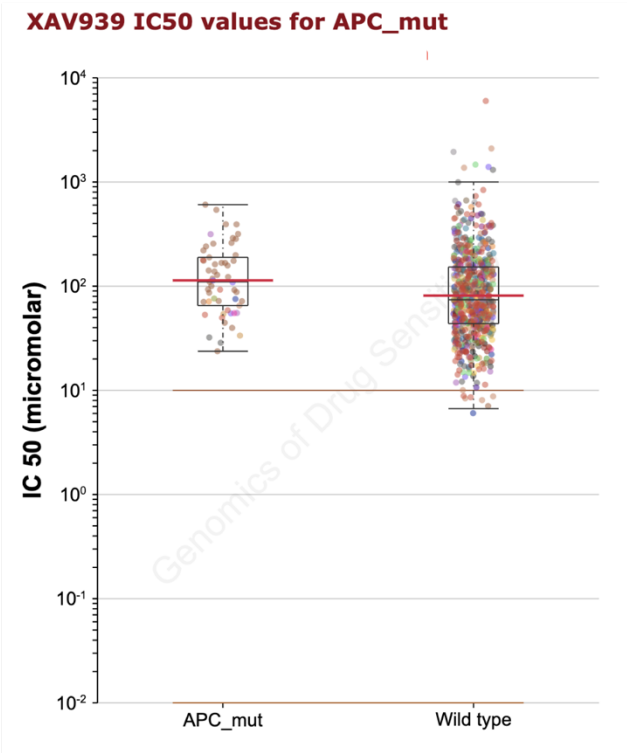
XAV939 IC50 values for APC_mut
IC 50 (micromolar)
APC_mut
Wild type
Genomics of Drug Sensitivity

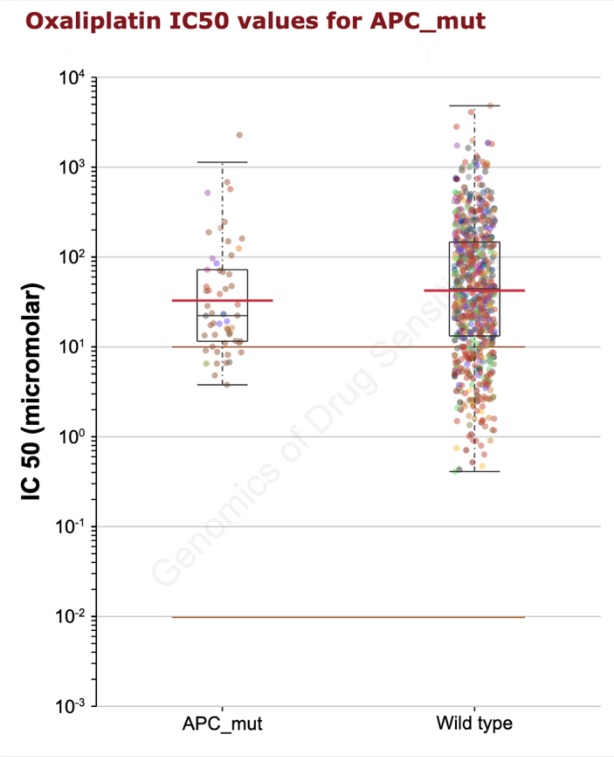
Oxaliplatin IC50 values for APC_mut
IC 50 (micromolar)
APC_mut
Wild type

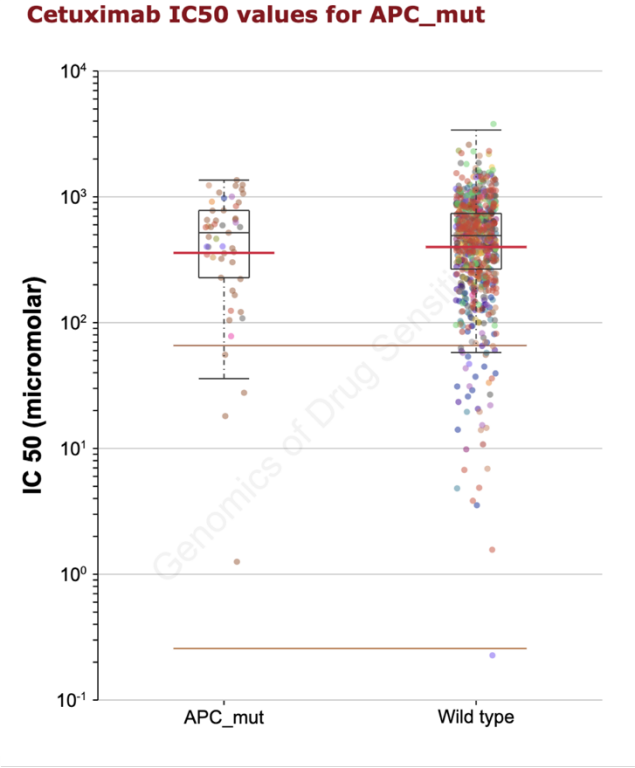
Cetuximab IC50 values for APC_mut
IC 50 (micromolar)
APC_mut
Wild type

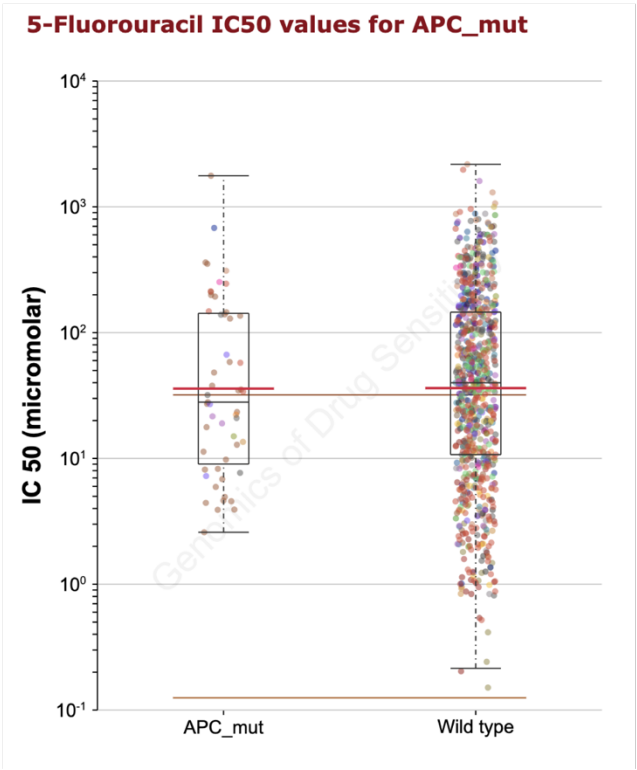
5-Fluorouracil IC50 values for APC_mut
IC 50 (micromolar)
APC_mut
Wild type

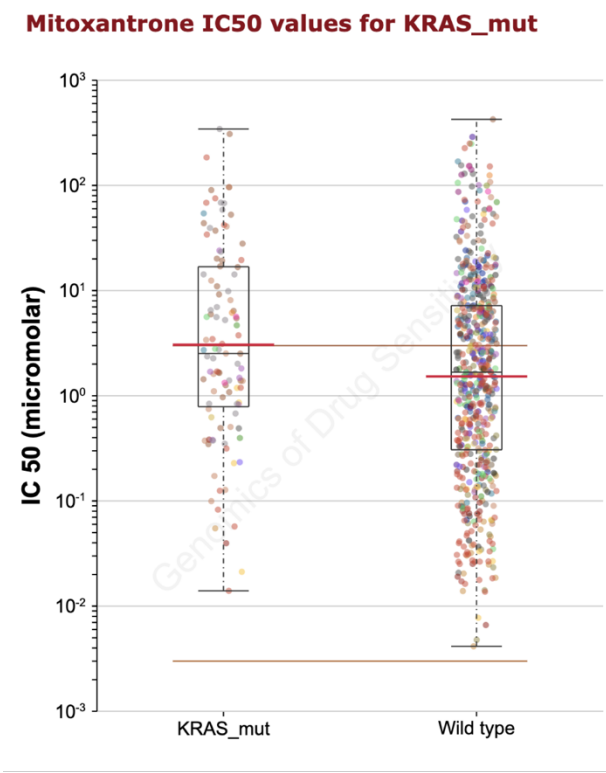
Mitoxantrone IC50 values for KRAS_mut
IC 50 (micromolar)
10^{3}
10^{2}
10^{1}
10^{0}
10^{-1}
10^{-2}
10^{-3}
KRAS_mut
Wild type

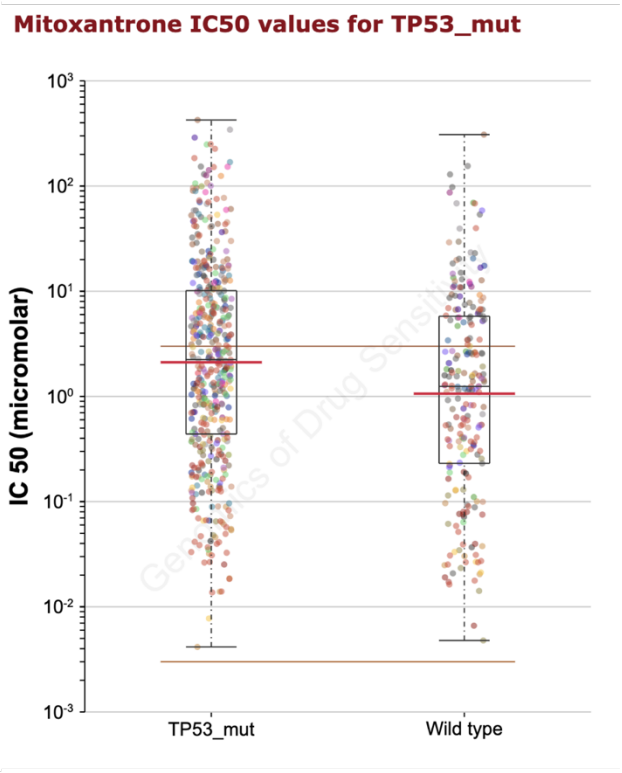
Mitoxantrone IC50 values for TP53_mut
IC 50 (micromolar)
10^{3}
10^{2}
10^{1}
10^{0}
10^{-1}
10^{-2}
10^{-3}
TP53_mut
Wild type

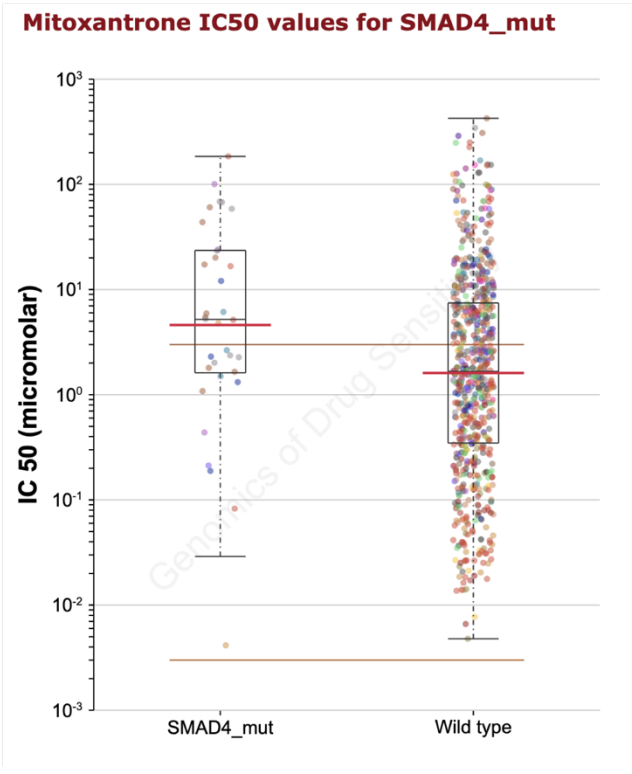
Mitoxantrone IC50 values for SMAD4_mut
IC 50 (micromolar)
10^{3}
10^{2}
10^{1}
10^{0}
10^{-1}
10^{-2}
10^{-3}
SMAD4_mut
Wild type

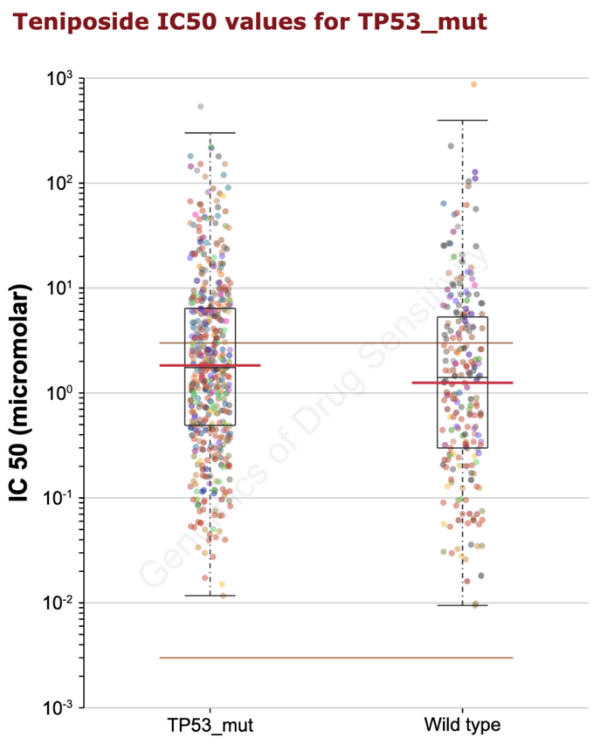
Teniposide IC50 values for TP53_mut
IC 50 (micromolar)
TP53_mut
Wild type

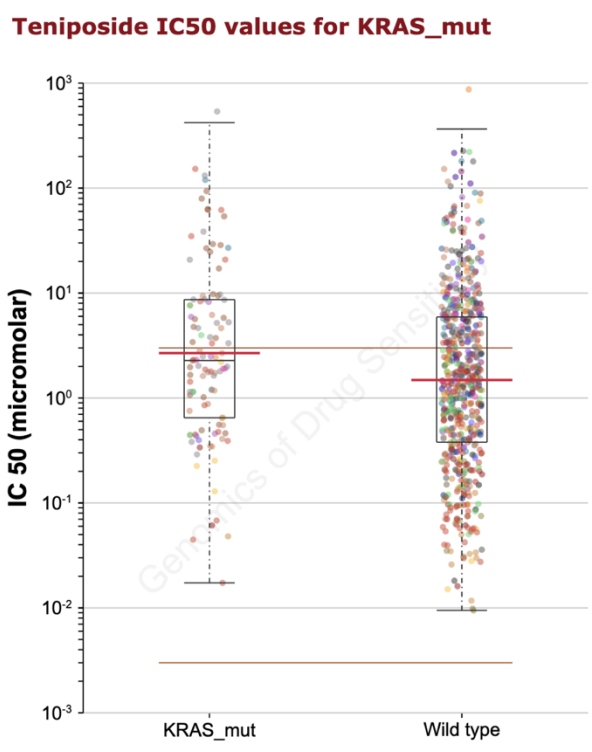
Teniposide IC50 values for KRAS_mut
IC 50 (micromolar)
KRAS_mut
Wild type

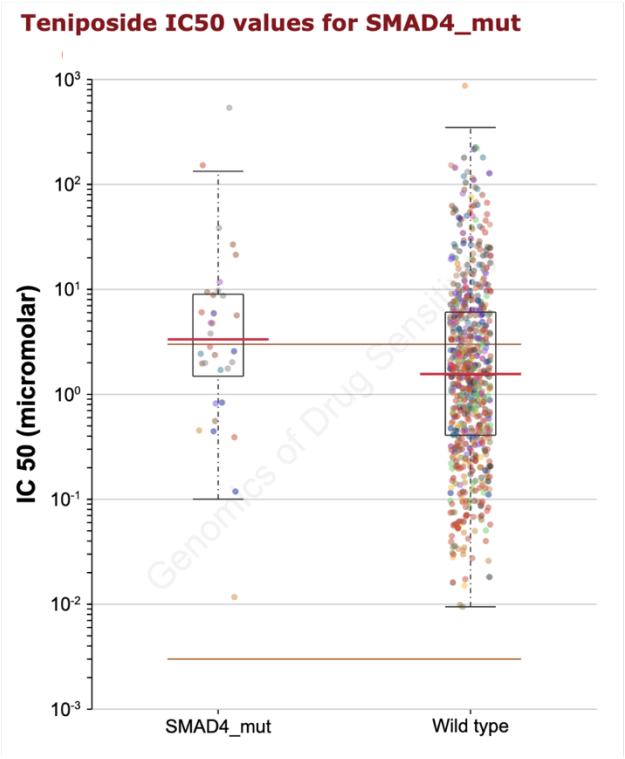
Teniposide IC50 values for SMAD4_mut
IC 50 (micromolar)
SMAD4_mut
Wild type

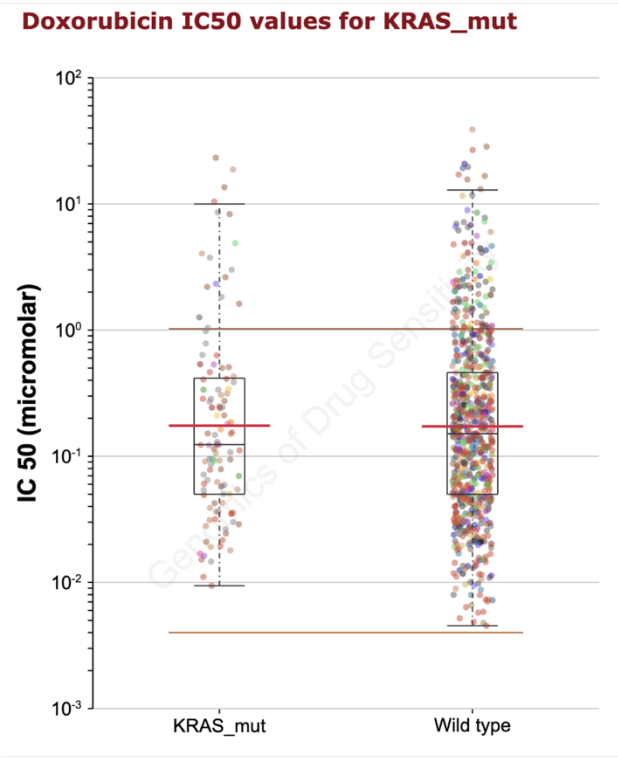
Doxorubicin IC50 values for KRAS_mut
IC 50 (micromolar)
KRAS_mut
Wild type

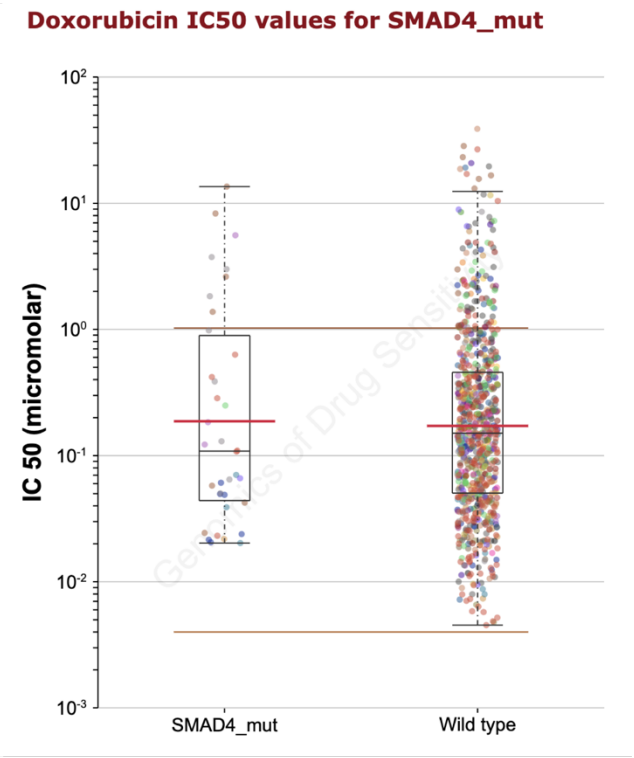
Doxorubicin IC50 values for SMAD4_mut
IC 50 (micromolar)
SMAD4_mut
Wild type

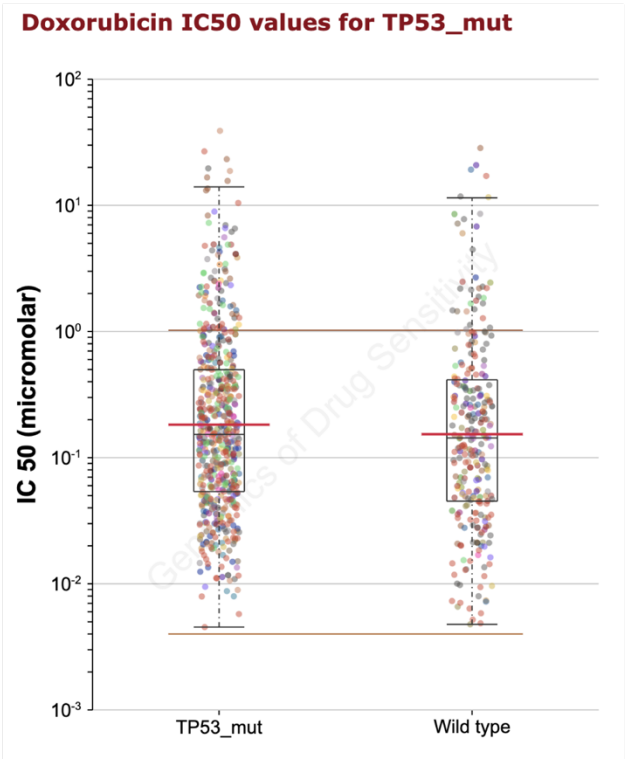
Doxorubicin IC50 values for TP53_mut
IC 50 (micromolar)
TP53_mut
Wild type

References

(1) Kinzler, K. W.; Vogelstein, B. Lessons from Hereditary Colorectal Cancer. *Cell* **1996**, *87* (2), 159–170. https://doi.org/10.1016/S0092-8674(00)81333-1.
(2) Green, R. A.; Wollman, R.; Kaplan, K. B. APC and EB1 Function Together in Mitosis to Regulate Spindle Dynamics and Chromosome Alignment. *Mol Biol Cell* **2005**, *16* (10), 4609–4622. https://doi.org/10.1091/mbc.E05-03-0259.
(3) Bahmanyar, S.; Nelson, W. J.; Barth, A. I. M. Role of APC and Its Binding Partners in Regulating Microtubules in Mitosis. *Adv Exp Med Biol* **2009**, *656*, 65–74.
(4) Kaplan, K. B.; Burds, A. A.; Swedlow, J. R.; Bekir, S. S.; Sorger, P. K.; Näthke, I. S. A Role for the Adenomatous Polyposis Coli Protein in Chromosome Segregation. *Nat Cell Biol* **2001**, *3* (4), 429–432. https://doi.org/10.1038/35070123.
(5) Lui, C.; Ashton, C.; Sharma, M.; Brocardo, M. G.; Henderson, B. R. APC Functions at the Centrosome to Stimulate Microtubule Growth. *Int. J. Biochem. Cell Biol.* **2016**, *70*, 39–47. https://doi.org/10.1016/j.biocel.2015.10.028.
(6) Musacchio, A. The Molecular Biology of Spindle Assembly Checkpoint Signaling Dynamics. *Current Biology* **2015**, *25* (20), R1002–R1018. https://doi.org/10.1016/j.cub.2015.08.051.
(7) Damelin, M.; Bestor, T. H. The Decatenation Checkpoint. *Br J Cancer* **2007**, *96* (2), 201–205. https://doi.org/10.1038/sj.bjc.6603537.
(8) Downes, C. S.; Clarke, D. J.; Mullinger, A. M.; Giménez-Abián, J. F.; Creighton, A. M.; Johnson, R. T. A Topoisomerase II-Dependent G2 Cycle Checkpoint in Mammalian Cells. *Nature* **1994**, *372* (6505), 467–470. https://doi.org/10.1038/372467a0.
(9) Wang, Y.; Azuma, Y.; Moore, D.; Osheroff, N.; Neufeld, K. L. Interaction between Tumor Suppressor Adenomatous Polyposis Coli and Topoisomerase IIα: Implication for the G2/M Transition. *Mol Biol Cell* **2008**, *19* (10), 4076–4085. https://doi.org/10.1091/mbc.E07-12-1296.
(10) Wang, Y.; Coffey, R. J.; Osheroff, N.; Neufeld, K. L. Topoisomerase IIα Binding Domains of Adenomatous Polyposis Coli Influence Cell Cycle Progression and Aneuploidy. *PLoS One* **2010**, *5* (4). https://doi.org/10.1371/journal.pone.0009994.
(11) Hande, K. R. Etoposide: Four Decades of Development of a Topoisomerase II Inhibitor. *European Journal of Cancer* **1998**, *34* (10), 1514–1521. https://doi.org/10.1016/S0959-8049(98)00228-7.
(12) Reyhanoglu, G.; Tadi, P. Etoposide. In *StatPearls*; StatPearls Publishing: Treasure Island (FL), 2020.
(13) Houghton, J. A.; Cheshire, P. J.; Hallman, J. D.; Lutz, L.; Luo, X.; Li, Y.; Houghton, P. J. Evaluation of Irinotecan in Combination with 5-Fluorouracil or Etoposide in Xenograft Models of Colon Adenocarcinoma and Rhabdomyosarcoma. *Clin. Cancer Res.* **1996**, *2* (1), 107–118.
(14) Sinkule, J. A. Etoposide: A Semisynthetic Epipodophyllotoxin Chemistry, Pharmacology, Pharmacokinetics, Adverse Effects and Use as an Antineoplastic Agent. *Pharmacotherapy: The Journal of Human Pharmacology and Drug Therapy* **1984**, *4* (2), 61–71. https://doi.org/10.1002/j.1875-9114.1984.tb03318.x.
(15) Yang, W.; Soares, J.; Greninger, P.; Edelman, E. J.; Lightfoot, H.; Forbes, S.; Bindal, N.; Beare, D.; Smith, J. A.; Thompson, I. R.; Ramaswamy, S.; Futreal, P. A.; Haber, D. A.; Stratton, M. R.; Benes, C.; McDermott, U.; Garnett, M. J. Genomics of Drug Sensitivity in Cancer

(GDSC): A Resource for Therapeutic Biomarker Discovery in Cancer Cells. *Nucleic Acids Res* **2013**, *41* (D1), D955–D961. https://doi.org/10.1093/nar/gks1111.
(16) Garnett, M. J.; Edelman, E. J.; Heidorn, S. J.; Greenman, C. D.; Dastur, A.; Lau, K. W.; Greninger, P.; Thompson, I. R.; Luo, X.; Soares, J.; Liu, Q.; Iorio, F.; Surdez, D.; Chen, L.; Milano, R. J.; Bignell, G. R.; Tam, A. T.; Davies, H.; Stevenson, J. A.; Barthorpe, S.; Lutz, S. R.; Kogera, F.; Lawrence, K.; McLaren-Douglas, A.; Mitropoulos, X.; Mironenko, T.; Thi, H.; Richardson, L.; Zhou, W.; Jewitt, F.; Zhang, T.; O'Brien, P.; Boisvert, J. L.; Price, S.; Hur, W.; Yang, W.; Deng, X.; Butler, A.; Choi, H. G.; Chang, J. W.; Baselga, J.; Stamenkovic, I.; Engelman, J. A.; Sharma, S. V.; Delattre, O.; Saez-Rodriguez, J.; Gray, N. S.; Settleman, J.; Futreal, P. A.; Haber, D. A.; Stratton, M. R.; Ramaswamy, S.; McDermott, U.; Benes, C. H. Systematic Identification of Genomic Markers of Drug Sensitivity in Cancer Cells. *Nature* **2012**, *483* (7391), 570–575. https://doi.org/10.1038/nature11005.
(17) Iorio, F.; Knijnenburg, T. A.; Vis, D. J.; Bignell, G. R.; Menden, M. P.; Schubert, M.; Aben, N.; Gonçalves, E.; Barthorpe, S.; Lightfoot, H.; Cokelaer, T.; Greninger, P.; van Dyk, E.; Chang, H.; de Silva, H.; Heyn, H.; Deng, X.; Egan, R. K.; Liu, Q.; Mironenko, T.; Mitropoulos, X.; Richardson, L.; Wang, J.; Zhang, T.; Moran, S.; Sayols, S.; Soleimani, M.; Tamborero, D.; Lopez-Bigas, N.; Ross-Macdonald, P.; Esteller, M.; Gray, N. S.; Haber, D. A.; Stratton, M. R.; Benes, C. H.; Wessels, L. F. A.; Saez-Rodriguez, J.; McDermott, U.; Garnett, M. J. A Landscape of Pharmacogenomic Interactions in Cancer. *Cell* **2016**, *166* (3), 740–754. https://doi.org/10.1016/j.cell.2016.06.017.
(18) Brocardo, M.; Näthke, I. S.; Henderson, B. R. Redefining the Subcellular Location and Transport of APC: New Insights Using a Panel of Antibodies. *EMBO Rep.* **2005**, *6* (2), 184–190. https://doi.org/10.1038/sj.embor.7400329.
(19) Davies, M. L.; Roberts, G. T.; Stuart, N.; Wakeman, J. A. Analysis of a Panel of Antibodies to APC Reveals Consistent Activity towards an Unidentified Protein. *British Journal of Cancer* **2007**, *97* (3), 384–390. https://doi.org/10.1038/sj.bjc.6603873.
(20) Wang, Y.; Azuma, Y.; Friedman, D. B.; Coffey, R. J.; Neufeld, K. L. Novel Association of APC with Intermediate Filaments Identified Using a New Versatile APC Antibody. *BMC Cell Biol* **2009**, *10*, 75. https://doi.org/10.1186/1471-2121-10-75.
(21) Ryu, H.; Azuma, Y. Rod/Zw10 Complex Is Required for PIASy-Dependent Centromeric SUMOylation. *J Biol Chem* **2010**, *285* (42), 32576–32585. https://doi.org/10.1074/jbc.M110.153817.
(22) Korinek, V.; Barker, N.; Morin, P. J.; van Wichen, D.; de Weger, R.; Kinzler, K. W.; Vogelstein, B.; Clevers, H. Constitutive Transcriptional Activation by a Beta-Catenin-Tcf Complex in APC-/- Colon Carcinoma. *Science* **1997**, *275* (5307), 1784–1787. https://doi.org/10.1126/science.275.5307.1784.
(23) Poy, F.; Lepourcelet, M.; Shivdasani, R. A.; Eck, M. J. Structure of a Human Tcf4-Beta-Catenin Complex. *Nat. Struct. Biol.* **2001**, *8* (12), 1053–1057. https://doi.org/10.1038/nsb720.
(24) Huang, L.; Shitashige, M.; Satow, R.; Honda, K.; Ono, M.; Yun, J.; Tomida, A.; Tsuruo, T.; Hirohashi, S.; Yamada, T. Functional Interaction of DNA Topoisomerase II␣ With the ␤-Catenin and T-Cell Factor-4 Complex. **2007**, *133* (5), 10.
(25) Sato, S.; Idogawa, M.; Honda, K.; Fujii, G.; Kawashima, H.; Takekuma, K.; Hoshika, A.; Hirohashi, S.; Yamada, T. β-Catenin Interacts With the FUS Proto-Oncogene Product and Regulates Pre-MRNA Splicing. *Gastroenterology* **2005**, *129* (4), 1225–1236. https://doi.org/10.1053/j.gastro.2005.07.025.

(26) Coss, A.; Tosetto, M.; Fox, E. J.; Sapetto-Rebow, B.; Gorman, S.; Kennedy, B. N.; Lloyd, A. T.; Hyland, J. M.; O'Donoghue, D. P.; Sheahan, K.; Leahy, D. T.; Mulcahy, H. E.; O'Sullivan, J. N. Increased Topoisomerase IIalpha Expression in Colorectal Cancer Is Associated with Advanced Disease and Chemotherapeutic Resistance via Inhibition of Apoptosis. *Cancer Lett.* **2009**, *276* (2), 228–238. https://doi.org/10.1016/j.canlet.2008.11.018.
(27) Tsavaris, N.; Lazaris, A.; Kosmas, C.; Gouveris, P.; Kavantzas, N.; Kopterides, P.; Papathomas, T.; Arapogiannis, G.; Zorzos, H.; Kyriakou, V.; Patsouris, E. Topoisomerase I and IIα Protein Expression in Primary Colorectal Cancer and Recurrences Following 5-Fluorouracil-Based Adjuvant Chemotherapy. *Cancer Chemother Pharmacol* **2009**, *64* (2), 391–398. https://doi.org/10.1007/s00280-008-0886-4.
(28) Chatterjee, N.; Bivona, T. G. Polytherapy and Targeted Cancer Drug Resistance. *Trends in Cancer* **2019**, *5* (3), 170–182. https://doi.org/10.1016/j.trecan.2019.02.003.
(29) Neel, D. S.; Bivona, T. G. Resistance Is Futile: Overcoming Resistance to Targeted Therapies in Lung Adenocarcinoma. *npj Precision Oncology* **2017**, *1* (1), 1–6. https://doi.org/10.1038/s41698-017-0007-0.
(30) Lim, Z.-F.; Ma, P. C. Emerging Insights of Tumor Heterogeneity and Drug Resistance Mechanisms in Lung Cancer Targeted Therapy. *Journal of Hematology & Oncology* **2019**, *12* (1), 134. https://doi.org/10.1186/s13045-019-0818-2.
(31) Home page - Cancerrxgene - Genomics of Drug Sensitivity in Cancer https://www.cancerrxgene.org/ (accessed Jun 25, 2020).
(32) Mo, Y.-Y.; Wang, Q.; Beck, W. T. Down-Regulation of Topoisomerase IIα in CEM Cells Selected for Merbarone Resistance Is Associated with Reduced Expression of Sp3. *Cancer Res* **1997**, *57* (22), 5004–5008.
(33) Wang, J.; Song, Y.; Xu, S.; Zhang, Q.; Li, Y.; Tang, D.; Jin, S. Down-Regulation of ICBP90 Contributes to Doxorubicin Resistance. *Eur. J. Pharmacol.* **2011**, *656* (1–3), 33–38. https://doi.org/10.1016/j.ejphar.2011.01.042.
(34) Omer, C. A.; Miller, P. J.; Diehl, R. E.; Kral, A. M. Identification of Tcf4 Residues Involved in High-Affinity Beta-Catenin Binding. *Biochem. Biophys. Res. Commun.* **1999**, *256* (3), 584–590. https://doi.org/10.1006/bbrc.1999.0379.

CHAPTER 5

DISCUSSION, CONCLUSIONS, AND FUTURE DIRECTIONS

Disrupting what is "just-right" to kill mutant cells

The β-catenin destruction complex as a whole contains a relatively high degree of intrinsic disorder, from almost complete disorder in the scaffolds Axin and APC to the disordered N- and C-terminal tails of β-catenin and kinases GSK3β and CK1[1]. This disorder has long stood as an obstacle to understanding the precise mechanisms of how β-catenin is cycled and regulated. APC's role specifically within the complex is also debated, with evidence for β-catenin binding activity of APC to be both essential[2,3], and not required[4] for β-catenin degradation in cell culture models. Ha and colleagues propose that the reason APC contains both high affinity 20-aa and lower affinity 15-aa repeats is so that β-catenin can be more precisely controlled in both Wnt-on and Wnt-off circumstances[5]. In this scenario, the 15-aa repeats are utilized more when there is high cellular levels of β-catenin, such as when a cell is winding down from a Wnt signal and returning to a Wnt-off state. The 15-aa repeats would be important for sequestering excess β-catenin while the 20-aa repeats function in the actual down-regulation. We observe that the 15-aa repeat region of APC binds increasing amounts of β-catenin as the concentration rises, which would make sense for a "mopping up" type of role. As has been mentioned, mutations of *APC* tend to cluster in a central "mutation cluster region". However, this region itself spans several hundred residues. We were not able to detect a specific binding site for β-catenin in our binding analysis, which suggests that the binding of β-catenin to APC is heterogenous. This observation could explain why observed mutations to APC are more spread out, as β-catenin can adjust how it binds to APC depending on the context of the truncating mutation. In this way, more *APC* mutations are tolerated that are still able to retain a "just-right" level of β-catenin control.

It has also been proposed that the 15-aa repeats do not simply hold on to excess β-catenin, but that they are essential to the downstream ubiquitination and degradation of β-

catenin[6]. In that same study, APC homologue APCL (APC2) which lacks the 15-aa repeats was observed to require the 15-aa repeats of APC in order to down-regulate β-catenin. When the high affinity β-catenin-binding domain of E-cadherin was added to APCL, β-catenin degradation was compromised. The flexibility we observe with APC both in the bound and unbound states increases the accessibility to β-catenin, but also likely allows for fast protein exchange critical for effective β-catenin degradation and protein partner turnover.

Truncated APC that retains the 15-aa repeat region is positively selected in colon cancer cells. Therefore, some ability of APC to bind β-catenin may be required for cancer cell survival. Our finding that APC remains disordered upon β-catenin binding likely reflects another key aspect of this interaction. The 15-aa repeats do not need to be phosphorylated to bind β-catenin, unlike the 20-aa repeats which are lost in a majority of mutation events[5,7]. This lack of phosphorylation requirement of the 15aa repeats, the intrinsic disorder present before binding, and the disorder that remains after binding allow APC to retain a specific level of control over β-catenin. Additional evidence for the "just right" hypothesis comes not only from the location of APC truncations which retain some β-catenin binding capacity, but also from the second allelic mutational event. If the initial *APC* mutation happens around codon 1300 in the middle of the 20-aa repeats, then most often the second allele of *APC* is completely lost in a process called loss of heterozygosity (LOH)[89]. However, if mutations happen outside of this region, then the second *APC* "hit" tends to be a truncating mutation within the MCR[8,9]. This suggests that APC needs to maintain a certain level of control over β-catenin for there to be a selective advantage in a tumor. Therapeutics targeting this region and disrupting the specific association of β-cat to the 15-aa repeats might be effective in causing a cancer cell to lose all remaining regulatory control of β-catenin, thus triggering cell death pathway activation.

TopoIIα-targeting therapeutics in APC mutant tumors

Our lab's discovery of the ability of APC to bind TopoIIα added a new dimension to the role of APC in the cell-cycle. APC presence in the nucleus has been established[10], yet its role is unclear (reviewed here[11]). Nuclear APC is implicated in binding to DNA[12], may be involved in base excision repair[13], and binds the transcriptional co-repressor C-terminal binding protein (CtBP)[14]. Whether the association of APC to transcription machinery is independent of β-catenin binding activity in the nucleus remains to be determined. My dissertation project has attempted to gain more insight into the effects of APC's association with the DNA topology modifying enzyme TopoIIα. We have shown that APC mutation increases a cell's resistance to TopoIIα-targeted therapeutics. One possible explanation of this observation is that upon mutation of *APC*, truncated APC is able to bind to TopoIIα and restrict the ability of drugs to effectively bind to TopoIIα. This could be due to APC blocking docking sites, or allosterically modifying TopoIIα so that it is not responsive to inhibitors/poisons. In this scenario, TopoIIα must still retain native catalytic activity, otherwise the decatenation checkpoint will be activated. Our studies showing that the presence of wild-type APC results in lower catalytic activity of TopoIIα compared to mutant or no *APC* supports the notions that APC can modify TopoIIα catalytic activity in such a way that it would respond differently to inhibitors. *In vitro* studies focusing on catalytic TopoIIα in the presence of different inhibitors using various APC mutants are needed to test this hypothesis. It should be noted that *APC* mutation is not confined to cancers of the colon and rectum, and is observed in cancers that are actively treated with TopoIIα poisons such as lung cancer[15]. In such cases, screening for *APC* mutation would be pertinent, as patients with *APC* mutant tumors would not benefit from TopoIIα targeting therapeutics.

Conclusions and Significance

This work contains the first biochemical analysis of β-catenin binding to the complete 15-aa repeat region of APC. Our findings demonstrate that the 15-aa repeat region of APC can bind more than one β-catenin molecule and that APC does not undergo structural transitions to a folded-like state upon this binding. These results can guide future studies aimed to establish the dynamics and architecture of the β-catenin destruction complex. Computational models and analysis of stoichiometry and β-catenin sequestration/turnover will also benefit from the work presented here. Our peak assignment of the NMR backbone fingerprint for the 15-aa repeat region of APC will enable sophisticated NMR techniques to probe the biophysical properties of APC and its binding partners, and will facilitate finer detailing of APC's contribution to β-catenin regulation and tumorigenesis. Our deposition of the backbone assignment of APC15R-BCD represents a significant contribution to the Biological Magnetic Resonance Databank (BMRB) for APC, as to our knowledge, the only other peak chemical shift assignments made for APC comprise a C-terminal fragment of 12 residues[16] and a 19 residue fragment comprising the first SAMP repeat[17].

We show here that mutation of *APC* seems to result in an increased resistance to chemotherapeutics targeting topoisomerase, and propose that screening for APC mutation could help oncologists determine more effective treatment strategies. We also show that APC is likely not present in the β-catenin transcriptional complex, but confirm it associates with TopoIIα and β-catenin in the nucleus. Finally, we show that *APC* mutation seems to increase the catalytic activity of TopoIIα in a decatenation assay. These data will be essential to understanding the effect of TopoIIα binding to APC, and what cellular pathways are altered as a result.

Future Directions

Moving forward, determining the kinetics of the binding of β-catenin to the 15-aa repeat region of APC will be an important step in understanding how the complex assembles. Liu and colleagues used isothermal titration calorimetry to estimate that two binding sites of an APC fragment similar to APC15R-BCD had K_d's of 800(±180) and 110(±8.1)[7]. It will be interesting to see if this 8-fold difference in apparent binding is consistent when using the full 15-aa repeat region of APC, as it has been hypothesized that Repeat A (not included in the study by Liu et al.) is the highest affinity site[2]. Hydrogen-deuterium exchange could provide more insight into how β-catenin interacts with APC by revealing amide backbone hydrogens that are more protected from solvent exchange when bound. Cryo-EM could also be a valuable tool in looking at how the β-catenin complex assembles and identifying approximate stoichiometries in a heterogeneous sample mixture. Ultimately, the question that most needs to be addressed, is "Can the binding of APC to β-catenin at the 15-aa repeats be disrupted by small molecules, and if so, would that disruption be enough to either cause cells to die, or make them more susceptible to other treatments?" This question will be very important for development of therapeutics that specifically target mutant-APC cells, which represent 80% of all colorectal tumors.

Many questions remain for how and why APC interacts with and alters the catalytic activity of TopoIIα. Experiments knocking down and overexpressing wild type APC, as well as mutant forms of APC will be important for working out the details of what domains of APC are required to activate/inhibit TopoIIα. Whether APC can bind directly to TopoIIα is an important outstanding question. Our studies indicate that the C-terminal domain of TopoIIα is critical to the association, as TopoIIβ (homologous to TopoIIα except for divergent C-terminal domain) does not co-immunoprecipitate with APC. Finally, experiments knocking down, overexpressing, or

inducing expression of truncated APC protein in cells to compare IC50s of various TopoIIα poisons or inhibitors would be an excellent method to test the observations from Figure 4.1. These experiments will be necessary to define the role that APC is playing in the resistance of colorectal cancers to chemotherapeutics targeting topoisomerase.

References

(1) Xue, B.; Dunker, A. K.; Uversky, V. N. The Roles of Intrinsic Disorder in Orchestrating the Wnt-Pathway. *J. Biomol. Struct. Dyn.* **2012**, *29* (5), 843–861. https://doi.org/10.1080/073911012010525024.

(2) Kohler, E. M.; Brauburger, K.; Behrens, J.; Schneikert, J. Contribution of the 15 Amino Acid Repeats of Truncated APC to β-Catenin Degradation and Selection of APC Mutations in Colorectal Tumours from FAP Patients. *Oncogene* **2010**, *29* (11), 1663–1671. https://doi.org/10.1038/onc.2009.447.

(3) Schneikert, J.; Behrens, J. Truncated APC Is Required for Cell Proliferation and DNA Replication. *Int. J. Cancer* **2006**, *119* (1), 74–79. https://doi.org/10.1002/ijc.21826.

(4) Yamulla, R. J.; Kane, E. G.; Moody, A. E.; Politi, K. A.; Lock, N. E.; Foley, A. V. A.; Roberts, D. M. Testing Models of the APC Tumor Suppressor/β-Catenin Interaction Reshapes Our View of the Destruction Complex in Wnt Signaling. *Genetics* **2014**, *197* (4), 1285–1302. https://doi.org/10.1534/genetics.114.166496.

(5) Ha, N.-C.; Tonozuka, T.; Stamos, J. L.; Choi, H.-J.; Weis, W. I. Mechanism of Phosphorylation-Dependent Binding of APC to Beta-Catenin and Its Role in Beta-Catenin Degradation. *Mol. Cell* **2004**, *15* (4), 511–521. https://doi.org/10.1016/j.molcel.2004.08.010.

(6) Schneikert, J.; Chandra, S. H. V.; Ruppert, J. G.; Ray, S.; Wenzel, E. M.; Behrens, J. Functional Comparison of Human Adenomatous Polyposis Coli (APC) and APC-Like in Targeting Beta-Catenin for Degradation. *PLOS ONE* **2013**, *8* (7), e68072. https://doi.org/10.1371/journal.pone.0068072.

(7) Liu, J.; Xing, Y.; Hinds, T. R.; Zheng, J.; Xu, W. The Third 20 Amino Acid Repeat Is the Tightest Binding Site of APC for Beta-Catenin. *J. Mol. Biol.* **2006**, *360* (1), 133–144. https://doi.org/10.1016/j.jmb.2006.04.064.

(8) Lamlum, H.; Ilyas, M.; Rowan, A.; Clark, S.; Johnson, V.; Bell, J.; Frayling, I.; Efstathiou, J.; Pack, K.; Payne, S.; Roylance, R.; Gorman, P.; Sheer, D.; Neale, K.; Phillips, R.; Talbot, I.; Bodmer, W.; Tomlinson, I. The Type of Somatic Mutation at APC in Familial Adenomatous Polyposis Is Determined by the Site of the Germline Mutation: A New Facet to Knudson's "two-Hit" Hypothesis. *Nat. Med.* **1999**, *5* (9), 1071–1075. https://doi.org/10.1038/12511.

(9) Albuquerque, C.; Breukel, C.; van der Luijt, R.; Fidalgo, P.; Lage, P.; Slors, F. J. M.; Leitão, C. N.; Fodde, R.; Smits, R. The "just-Right" Signaling Model: APC Somatic Mutations Are Selected Based on a Specific Level of Activation of the Beta-Catenin Signaling Cascade. *Hum. Mol. Genet.* **2002**, *11* (13), 1549–1560. https://doi.org/10.1093/hmg/11.13.1549.

(10) Neufeld, K. L.; Nix, D. A.; Bogerd, H.; Kang, Y.; Beckerle, M. C.; Cullen, B. R.; White, R. L. Adenomatous Polyposis Coli Protein Contains Two Nuclear Export Signals and Shuttles between the Nucleus and Cytoplasm. *PNAS* **2000**, *97* (22), 12085–12090. https://doi.org/10.1073/pnas.220401797.
(11) Neufeld, K. L. Nuclear APC. *Adv Exp Med Biol* **2009**, *656*, 13–29.
(12) Deka, J.; Herter, P.; Sprenger-Haussels, M.; Koosch, S.; Franz, D.; Müller, K. M.; Kuhnen, C.; Hoffmann, I.; Müller, O. The APC Protein Binds to A/T Rich DNA Sequences. *Oncogene* **1999**, *18* (41), 5654–5661. https://doi.org/10.1038/sj.onc.1202944.
(13) Narayan, S.; Jaiswal, A. S.; Balusu, R. Tumor Suppressor APC Blocks DNA Polymerase Beta-Dependent Strand Displacement Synthesis during Long Patch but Not Short Patch Base Excision Repair and Increases Sensitivity to Methylmethane Sulfonate. *J. Biol. Chem.* **2005**, *280* (8), 6942–6949. https://doi.org/10.1074/jbc.M409200200.
(14) Hamada, F.; Bienz, M. The APC Tumor Suppressor Binds to C-Terminal Binding Protein to Divert Nuclear Beta-Catenin from TCF. *Dev. Cell* **2004**, *7* (5), 677–685. https://doi.org/10.1016/j.devcel.2004.08.022.
(15) Ohgaki, H.; Kros, J. M.; Okamoto, Y.; Gaspert, A.; Huang, H.; Kurrer, M. O. APC Mutations Are Infrequent but Present in Human Lung Cancer. *Cancer Lett.* **2004**, *207* (2), 197–203. https://doi.org/10.1016/j.canlet.2003.10.020.
(16) Walma, T.; Aelen, J.; Nabuurs, S. B.; Oostendorp, M.; van den Berk, L.; Hendriks, W.; Vuister, G. W. A Closed Binding Pocket and Global Destabilization Modify the Binding Properties of an Alternatively Spliced Form of the Second PDZ Domain of PTP-BL. *Structure* **2004**, *12* (1), 11–20. https://doi.org/10.1016/j.str.2003.11.023.
(17) Kaieda, S.; Matsui, C.; Mimori-Kiyosue, Y.; Ikegami, T. Structural Basis of the Recognition of the SAMP Motif of Adenomatous Polyposis Coli by the Src-Homology 3 Domain. *Biochemistry* **2010**, *49* (25), 5143–5153. https://doi.org/10.1021/bi100563z.